UNIVERSITY OF TEXAS ARLINGTON | DEPARTMENT OF COMPUTER SCIENCE AND ENGINEERING

Optimizing the Demand and Distribution of Power in Smart Grids

By

Saifullah Khalid

DISSERTATION

Submitted in partial fulfillment of the requirements

for the degree of Doctor of Philosophy at

The University of Texas at Arlington

August, 2021

Arlington, Texas

Supervising Committee:

Dr. Ishfaq Ahmad, Supervising Professor

Dr. Hao Che

Dr. Manfred Huber

Dr. Ramez Elmasri

Acknowledgments

I am very grateful to my supervisor Dr. Ishfaq Ahmad for his support and guidance throughout my doctoral research. This dissertation would not have been possible without his dedicated mentoring and exceptional supervision. I would also thank my dissertation committee members, Dr. Ramez Elmasri, Dr. Manfred Huber, and Dr. Hao Che, for reviewing my dissertation, sparing time, and always being supportive and accommodating. I also enjoyed great support and help from all the technical and support staff at CSE, UTA. In particular, I would like to thank Pam Mcbride, Sherri Gotcher, and Bito Irie for all of their help and efforts. Furthermore, I thank my father, Sardar Khan, whom I lost during my Ph.D. in 2019, and my mother, Sakeena Bibi, who always supported me in whatever I chose to do in my life. Finally, I would like to express my gratitude to my wife Saadia and my four sons Zaid, Hamza, Umer, and Usman, to fill my life with happiness and create joy and laughter even during stressful times. Most of all, I thank Almighty Allah for giving me the opportunity, strength, and ability to work on my dissertation and for showering his countless blessings on me.

August 03, 2021

To my parents

Optimizing the Demand and Distribution of Power in Smart Grids

Saifullah Khalid, Ph.D.

Supervisor: Dr. Ishfaq Ahmad

Abstract

The electricity is generated in bulk power plants and transported to the end-user through the transmission and distribution networks. The process incurs heavy losses adding to the operational costs. Secondly, fossil fuels dominate energy generation and are a major source of greenhouse gases. Thirdly, the power grid is vulnerable to natural disasters. The smart grid addresses these challenges by integrating distributed energy resources (DERs) in the distribution system closer to the load and with greater penetration of renewable energy. Renewable energy is key to cutting carbon emissions due to fossil fuel-based electricity generation and reducing operating costs. It can also effectively help speedier localized service restoration before the main supply becomes available after a disaster. However, renewable energy sources, such as solar and wind, bring in a new challenge of intermittent generation which can destabilize the power grid. As a result, to incentivize the user to do demand-side management, the power grid employs dynamic electricity pricing.

In this context, this dissertation focuses on optimizing the demand and distribution of power in a smart grid. In the first case, we investigate profit maximization in geo-distributed data centers by optimizing power consumption through request routing and optimal resource allocation. Next, we extend this work by proposing a cooperative strategy where data centers incorporate grid stability into the optimization process. It enables the data centers to utilize lower power tariffs while minimizing geographic load balancing overheads. It also facilitates the grid to increase renewable penetration without catering to additional reserves. In the second case, this dissertation investigates the use of DERs to mitigate disaster effects through energy donation. Our approach simultaneously prioritizes

critical load and provides relief to those in dire need while complying with resources and network constraints. Finally, this dissertation includes a blockchain approach to enable energy sharing for restoration in the aftermath of a disaster. The technique utilizes a consortium formulation mechanism and a light-weight consensus protocol for optimizing the blockchain operations' energy cost. The winner block selected through the proposed consensus mechanism intrinsically preserves network stability while conforming to resource and stability constraints.

We adopted evolutionary optimization techniques as a solution approach to address multi-objective problems and provide system managers with trade-off solutions to meet requirements posed by various operational scenarios.

Contents

Abstract **v**

List of Figures **ix**

List of Tables **xi**

List of Symbols **xii**

1 Introduction **1**
1.1 Problem Description 1
1.2 Literature Review 3
1.2.1 Data Center Profit Optimization 3
1.2.2 Energy Donation 4
1.3 Dissertation organiztion 5
1.3.1 Chapter 2 —Dual Optimization of Data Center Revenue and Expense in a Smart Grid using an Evolutionary Approach 5
1.3.2 Chapter 3 - QoS and Power Network Stability Aware Simultaneous Optimization of Data Center Revenue and Expenses 6
1.3.3 Chapter 4 - Optimizing Energy Donation in a Smart Grid during Crisis 6
1.3.4 Chapter 5 - Energy Sharing for Service Restoration using a Consortium Blockchain Approach in a Smart Grid 7

2 Dual Optimization of Revenue and Expense in Geo-Distributed Data Centers using the Smart Grid **8**
2.1 Introduction 8
2.2 Related work 11
2.3 Problem Formulation 12
2.3.1 Preliminaries 12
2.3.2 Electricity Pricing 13
2.3.3 Cloud Power Consumption 14
2.3.4 Objective Function 17

2.4 Proposed Solution 18
2.4.1 Constraints Handling 19
2.5 Performance Evaluation 28
2.5.1 Simulation Setup 28
2.5.2 Performance Measures 30
2.6 Conclusion 33

3 QoS and Power Network Stability Aware Simultaneous Optimization of Data Center Revenue and expenses 35
3.1 Introduction 35
3.2 Related work 37
3.3 Problem Formulation 39
3.3.1 Data Center Power Consumption 41
3.3.2 Power Network Stability 42
3.3.3 Objective Function 43
3.4 Proposed Solution 44
3.4.1 Constraints Handling 45
3.4.2 Initial Population 46
3.4.3 Environmental Selection 46
3.4.4 Genetic Operations 47
3.4.5 Solution Selection 47
3.5 Performance Evaluation 47
3.5.1 Performance Comparison 48
3.5.2 Voltage Stability 49
3.5.3 Voltage Profile 50
3.6 Conclusion 51

4 Optimizing Energy Donation for Service Restoration in a Power Distribution System 52
4.1 Introduction 52
4.2 Problem Formulation 55
4.2.1 Network Model 55
4.2.2 Commodity Valuation and User Contribution 56
4.2.3 Energy Allocation 57
4.2.4 Social Welfare 59
4.2.5 Power Flow 61
4.2.6 Distribution Losses 62
4.2.7 Voltage Stability 62
4.2.8 Optimization Objectives 64
4.3 Proposed Solution 64

4.3.1 Constraints Handling . . . 66
4.3.2 Initial Population . . . 66
4.3.3 Genetic Operations . . . 68
4.3.4 Repair Operator . . . 68
4.4 Performance Measures . . . 69
4.4.1 Demand, Priority, and Phase 1 Allocation . . . 69
4.4.2 Phase 1 vs. Final Allocation . . . 70
4.4.3 Welfare and Loss . . . 72
4.4.4 Load Priority vs. Allocation . . . 72
4.4.5 Demand vs. Allocation . . . 72
4.4.6 Contribution vs. Allocation . . . 73
4.4.7 Impact of Crossover and Mutation Probabilities . . . 74
4.4.8 Voltage Stability Index . . . 75
4.4.9 Bus Voltage Profile . . . 76
4.5 Conclusion . . . 77

5 Energy Sharing for Service Restoration using a Consortium Blockchain Approach in a Power Distribution System 79
5.1 Introduction . . . 79
5.2 Problem Formulation . . . 83
5.2.1 Network Model . . . 85
5.2.2 Energy Allocation Model . . . 85
5.2.3 Optimization Problem . . . 87
5.3 Blockchain System Model . . . 88
5.3.1 System Infrastructure . . . 88
5.3.2 Node Reputation . . . 89
5.3.3 Consortium Formulation . . . 89
5.3.4 Consensus Mechanism . . . 90
5.4 Service Restoration Framework . . . 93
5.5 Evaluation and Assessment . . . 94
5.5.1 Security Analysis . . . 94
5.5.2 Performance Results . . . 95
5.6 Conclusion . . . 99

6 Conclusion and Future Work 101

A List of Publications 103

Bibliography 104

List of Figures

2.1 System model for profit maximization problem. 13
2.2 Evolutionary algorithm based optimization approach 20
2.3 Test scenarios: initial population. 23
2.4 Chromosome formulation and composition of initial population. 23
2.5 Impact of initial population selection. 24
2.6 Evolution process: chromosomes for the current and elite populations . . . 25
2.7 Impact of combining recombination operation. 27
2.8 Impact of crossover and mutation probabilities. 27
2.9 Pareto fronts 28
2.10 Impact of system utilization. 30
2.11 Impact of dynamic pricing on data center expense 31
2.12 Comparison of normalized profit of proposed and baseline approaches in the small cloud. 32
2.13 Comparison of normalized profit of proposed and baseline approaches in the medium cloud. 32
2.14 Comparison of normalized profit of proposed and baseline approaches in the large cloud. 32
2.15 Meeting revenue target or an expense constraint. 33
3.1 Geo distributed data centers and power grid infrastructure. 40
3.2 Evolutionary algorithm based higher level optimization approach 45
3.3 Pareto fronts for two phases of algorithm 48
3.4 Comparison of normalized expense of the proposed and baseline approaches under low, medium, and high load conditions 49
3.5 Comparison of normalized profit of the proposed and baseline approaches under low, medium, and high load conditions 50
3.6 Voltage stability index (VSI) 50
3.7 Voltage profile 51

4.1 Energy donation network model. 56
4.2 Energy allocation 59
4.3 Single line and phasor diagram of two bus system 60
4.4 Evolutionary technique based optimization algorithm. 67
4.5 Polynomial curve fitted on demand, priority, and phase 1 allocation data. 70
4.6 Phase 1 and final energy allocations 71
4.7 Welfare and loss plot 72
4.8 Impact of load priority on allocation 73
4.9 Impact of demand on allocation 74
4.10 Impact of contribution on allocation 75
4.11 Impact of crossover and mutation probabilities on unmet-demand. 76
4.12 Pareto front 76
4.13 Voltage stability index 77
4.14 Voltage profile 77

5.1 Blockchain model for service restoration 83
5.2 Evolutionary algorithm based consensus mechanism 92
5.3 Blockchain enabled service restoration approach 93
5.4 Proof of welfare (PoWel) 96
5.5 Welfare and loss plot 97
5.6 Stability index (SI) 33-bus system 98
5.7 Stability index (SI) 69-bus system 98
5.8 Bus voltage profile 33-bus system 99
5.9 Bus voltage profile 69-bus system 99

List of Tables

2.1 System Parameters 29

3.1 Simulation Parameters 48

4.1 Chromosome - energy allocation vectors 66
4.2 Microgrids with surplus supply 70

5.1 Blockchain System Key Elements Defined 84
5.2 Simulation Parameters 96

List of Symbols

$\mathcal{R}_i$	A nodes' reputation
$\bar{P}^s$	Maximum static consumption of a server
$\mathcal{C}_i^l$	Unit price of electricity on ith power node or bus
$\mathcal{C}_b$	Base price in region or node
$\mathcal{L}$	Power load on node
$\mathcal{S}_g$	Power generation at node
$\mathcal{S}_{in}$	Power injection at a node
E_j^{net}	Net amount of energy in jth operation window
Ed_j	Energy available through donation process
Et_j	Energy available through trade process
m	Price gradient
P_j^c	Server power consumption vector for machines in same cabinet
P_{dc}^{cool}	Cooling related power consumption in a data center
P_{dc}	Server computing related power consumption in data center
R^t	System response time
T_{in}	Server inlet temperature
T_{max}	Maximum temperature limit inside data center
$U_i(E_i)$	Utility achieved by ith user with allocated energy E_i
v_d	Energy value in case of a donation

v_t	Energy value in case of a trade
x_{ij}	Probability of request assignment to server j in ith data center
CoP_{dc}	CRAC coefficient of performance
α	Type of energy transaction—trade, donation, or borrowing
$\bar{E}^m$	Average energy consumption by nodes on mining across the network
$\bar{P}^d$	Maximum dynamic consumption of a server
$\bar{P}^d$	Maximum dynamic power consumption of a server
$\bar{P}^s$	Maximum static power consumption of a server
$\boldsymbol{E}$	Power cost on servicing requests
$\boldsymbol{f}$	SLA based cloud revenue
$\boldsymbol{r}$	Server resource allocation configuration
$\boldsymbol{x}$	Vector of request dispatch probabilities
δ^p	Angle variation between two nodes
Γ_{ij}	A binary variable: true if a node successfully mines a block and false otherwise
λ	Mean request arrival rate in cloud
λ	Mean request arrival rate in a cloud
$\mathcal{V}_j^{rat}$	Rationalized energy value for jth operation slot
ψ	Allocation basis —priority, contribution, or combination
ψ	Controls allocation or rationing basis
$\mathcal{N}$	Number of geographically distributed data centers
$\mathcal{N}$	Number of geo-distributed cloud data centers
$\mathcal{N}$	Number of microgrids in the system
$\mathcal{R}^{con}$	Nodes' mining eligibility threshold
$\mathcal{R}_i$	Rationing index
$\mathcal{T}$	Systems' operation horizon

$\mathcal{V}_j$ Energy value in a given slot

$\mathcal{W}_i$ The weight assigned to individual MGs' demand

$\mathcal{D}$ Cross-interference coefficients matrix

$\mathcal{N}$ Number of microgrids

$\mu,\ \mu_{ij}$ Processing capacity of a server in a data center

μ_{ij} Processing capacity of server j in ith data center

Ω_{ij} Effective line resistance between nodes i & j

θ Impedance angle

$\vec{\mathcal{D}}$ A vector of energy demand of microgrids

$\vec{C}$ MGs' historical contribution $\vec{C} := \{c_i\}\ \forall i \in \mathcal{N}$

$\vec{D}$ MGs' demands $\vec{D} := \{d_i\}\ \forall i \in \mathcal{N}$

$\vec{P}$ MGs' service priorities $\vec{P} := \{p_i\}\ \forall i \in \mathcal{N}$

$\zeta,\ \delta$ Utility function parameters

$\zeta,\ \delta$ Cloud utility function constants

C_i^l Electricity unit price on ith power bus

c_i Contribution of ith microgrid to donation framework

$C_{b,i}$ Base price of electricity on ith power bus

CoP_{dc} Co-efficient of performance of a CRAC unit

D^{sla} Response time deadlines vector as per users' SLA

d_i Demand of ith microgrid

$D_{dc,i}$ Thermal cross interference matrix

E_i^s A nodes' energy state; True when node has sufficient energy for mining and consensus operations

E^p Net available energy pledged by MGs in a given slot as donation and trade

e_i^w Energy allocation in first step through weighted gains rationing

E_i Energy allocation to ith microgrid

f^w Weighted gains rationing function

h Server consumption due to base hardware

h Technology server power model constant

h_i Hybrid allocation basis; a function of service priority and contribution

L_i Power loss on ith link connecting two peer MGs

m Price gradient — rate of change of electricity

$P^c_{dc,i}$ Data center computing related power consumption

P^d_j Dynamic consumption of a server

P^s_j Static consumption of a server

P^{ac}_{dc} Data center cooling related power consumption

P^d Dynamic power consumption of a server

P^s Static power consumption of a server

p_c Crossover probability

P_G Power generation or compensation at a node

P_i Real power at sending node

p_i, c_i, d_i Service priority, contribution, and demand of ith MG

P_L Power load at a node

p_m Mutation probability

P_o Load on a bus other than data center

P_r Renewable power generation on a bus

$P_{dc,i}$ Power consumed in ith data center

$P_{g,i}$ Power generation on ith bus

P_{nr} Non-renewable power generation on a bus

Q_i Reactive power at sending node

R	Mean response time of a server, a function of x_{ij}&r_{ij}
$r,\ r_{ij}$	Resources allocated to service requests by a server in data center
r_{ij}	The resources allocated by server j in ith data center to service a request
SI	Power stability index
T_i	Temperature of ith server in a data center
T_{in}	Server inlet temperature
T_{max}	Data center temperature safe threshold
V_i	Sending end node voltage
V_{max}	Maximum node voltage
V_{min}	Minimum node voltage
$x,\ x_{ij}$	Probability of request assignment to a server in a data center
E_i	Net energy allocation to ith MG
e_i^o	Energy allocation in second step by optimization algorithm considering a multi-objective criterion
CRAC	Computer room air conditioner
K	Number of servers in a data centers

Chapter 1

Introduction

1.1 Problem Description

Traditionally, electricity is generated centrally in bulk power plants and delivered through transmission and distribution networks. The delivery process incurs heavy losses resulting in increased operating costs. Most importantly, the power grid failed to keep pace with modern technological developments leaving the whole system inefficient, vulnerable to interruptions, and lacking reliability [1]. Power demand depicts inherent variability [2,3] with the peak demand be orders of magnitude higher than the off-peak load. Therefore, the grid maintains fossil fuel-based costly generation reserves to provide uninterrupted supply, increasing operating costs. Apart from the higher operating cost, the power losses and reliance on fossil fuels for electricity generation have critical environmental implications. For example, in the United States, electricity generation is the second largest contributor to greenhouse gases with a share of 28% [4]. The smart grid addresses these challenges by integrating distributed energy resources (DERs) in the distribution system closer to the load and with greater penetration of renewable energy. Renewable energy is key to cutting carbon emissions due to fossil fuel-based electricity generation and reducing operating costs. It can also be effectively used for speedier localized service restoration after a disaster before the main supply becomes available.

However, the assimilation of renewable energy sources, e.g., solar and wind, because of their dependence on environmental factors brings in a new challenge of intermittent generation. Therefore, to incentivize the user to do demand-side management, the power grid employs dynamic pricing of electricity where prices vary depending on real time demand, generation, and network conditions. The energy prices change from one region to another, across grid nodes, and time intervals. For example, if the grid is overloaded in a region, it may increase the prices to promote demand-side management [5]. Similarly, it can lower tariffs if excess power is available to incentivize users to consume more, thus helping it avoid stability issues.

In the new power grid paradigm, users actively participate in demand management by curtailing their power consumption during the peak demand period when the energy prices are high. Thus, it benefits both the user and the grid. For example, geo distributed data centers can utilize lower power tariffs by routing computing traffic to areas with minimum electricity costs [6–8]. Similarly, the grid can benefit by using them as dispatchable loads, i.e., data centers reduce demand by deferring or shifting computing tasks to regions with lower prices allowing their use as an alternative to fossil fuel-based reserves. However, changes in the data center load can destabilize the power grid and stimulate major voltage collapses. In such circumstances, the power grid raises energy prices to incentivize users to do demand-side management. As a result, the data center may have to reroute traffic, thus stimulating a chain reaction or counteracting the objective of availing lower power prices. This mutual interaction of demand, cost, and price paradoxically continues to create a vicious cycle [9]. Therefore, a cooperative approach is imperative to look after the interests of all actors. For example, by embedding power stability in the optimization process, the data center can utilize lower power tariffs, minimize geographic load balancing overheads, and fulfill social responsibilities towards a greener future.

Over the years, the research community has contributed remarkably towards optimizing power grid processes, including generation, transmission, distribution, and demand. The researchers have utilized different computational optimization techniques. The solution approaches include game-theoretic approaches, convex optimization, heuristics, evolutionary, and genetic algorithms. However, the impact of geo-distributed data centers on the power grid is not a very well explored area of research. Though some studies have focused on the interaction of a data center with a power grid [9–14] yet the impact of dynamic changes in data center load on power system stability has received little attention. At best, some of these researches have tried to curtail power grid load imbalances and consequent instability through indirect performance measures [11,12]. Similarly, the use of DERs for distribution system service restoration despite its tremendous potential is another area requiring increased focus. Restoration during major power disruptions presents additional challenges because of limited supply, unstable network, the requirement of prioritizing critical load while providing relief to those in dire need. In this context, many contemporary works have overlooked critical aspects. For example, [15, 16] ignored distribution systems' operational constraints so their solution may destabilize distribution system. Furthermore, neither works used a pricing mechanism, so all transactions carry the same value irrespective of supply-demand conditions. It adversely affects the fairness and thus lowers the incentive for the participants. DER-based restoration manifests exchanges from distributed sources to the loads either directly or through aggregators. In both cases, efficient accounting and integrity of transactions are essential. Despite a widely sought research area, few approaches currently exist that utilize blockchain for DER-based energy sharing for restoration [17–21].

In this context, this dissertation focuses on optimizing the demand and distribution of power in a smart grid. The first problem addressed falls in the category of demand optimization. More specifically, we investigated profit maximization in geo-distributed data centers by optimizing power consumption through request routing and optimal resource allocation. Next, we extended this work by proposing a cooperative strategy where data centers incorporate grid stability into the optimization process. This is an emerging approach where data centers instead of selfish profit maximization cooperate with the grid by embedding power system stability in the optimization process. The approach benefits both the data centers as they can utilize lower power tariffs, minimize geographic load balancing overheads, and fulfill social responsibilities towards a greener future. Whereas the grid can increase renewable penetration without catering to additional reserves and still provide a stable power supply to its users.

The second problem which we explored falls in the domain of power distribution system optimization. We propose an alternate energy supply strategy for service restoration in the aftermath of a disaster. The proposed approached uses energy crowdsourced through donation and trade to restore service. It simultaneously prioritizes critical load and provides relief to those in dire need while complying with resources and network constraints. Finally, this dissertation includes a blockchain-based energy sharing approach for service restoration. The scheme is designed for limited supply scenarios. The technique utilizes microgrids' supply situation and reputation as consortium admission criteria for optimizing the blockchain operations' energy cost. The winner block selected through proposed consensus mechanism intrinsically preserves network stability while conforming to resource and stability constraints.

We adopted evolutionary optimization techniques as a solution approach to address multi-objective problems and provide system managers with trade-off solutions to meet requirements posed by various operational scenarios.

1.2 Literature Review

In this section, we review the related research from data center profit maximization and the distribution system optimization domains.

1.2.1 Data Center Profit Optimization

The research for data center profit maximization has progressed into two main directions. The first category tries to reduce energy consumption for a data center by optimally dispatching service requests and allocating resources. Salient works in this category include [22–27]. In the second category, researchers consider spatio-temporal variations of electricity prices in deregulated energy market to minimize electric expenditure. These

works have additionally relied on optimization of request routing and resource allocation. Salient works from this category include [13, 28–34]. In summary, irrespective of the class of research, the key objective is always to reduce the power bill of the data center either by reducing the consumption or shifting load to areas where lesser cost electricity is available or using them in combination.

The contemporary works have sought to address the problem generally from the data centers' perspective making the benefits flow unidirectional [9]. Most solutions seek to maximize data center revenues, reduce the cost of operation, and maintain a higher availability of data center [35]. However, analysis of the impact of dynamic changes in data center load on power grid stability is critical for reliability and sustainability of power grid. Only a handful of these studies have explored the interaction of a data center with a power grid [9–14]. In general, these works have not evaluated the impact of dynamic changes in data center load on power system stability. At best, some of these researches have tried to curtail power grid load imbalances and consequent instability through indirect performance measures. For example, [11, 12] use electric load imbalance index —the ratio of demand to system capacity. Therefore, research into an integrative strategy that balances interests of both data centers and the power is required. So far, to the best of our knowledge, no contemporary work has directly incorporated power networks' operational constraints especially voltage stability into the data center optimization process.

1.2.2 Energy Donation

In a smart grid, energy sharing or trading takes place directly among peers —users, houses, MGs. For example, [15,36–38] proposed direct energy sharing among multi-microgrids, [39] studied peer-to-peer energy trading among users within a microgrid, and [40–42] explored sharing of energy among neighbouring homes. In other cases, the sharing or trading are facilitated by a central entity, e.g., a DSO [15, 43]. Here, the controller manages energy allocation and transactions from DERs to loads thereby avoiding problem caused by uncoordinated energy exchanges [44]. However, many contemporary works have overlooked critical aspects of restoration in both scenarios, particularly when supply is limited. For example, [15] ignored distribution systems' operational constraints so their solution may destabilize distribution system. Furthermore, neither works used a pricing mechanism, so all transactions carry the same value irrespective of supply-demand conditions. It adversely affects the fairness and thus lowers the incentive for the participants. In contrast, Kim *et al.* [36] handled power balance and network constraints but did not address prioritized allocation. Another issue across these schemes is their sole focus on the participants' benefit rather than the collective interest of the community affected by a disaster. For example, in [40–42] houses participate in trading as long as the payoff is significant; otherwise, they defect.

Similarly, traditional restoration approaches become ineffective when supply from the

central generation is not available [45]. So, a body of research exists that have studied DER-based restoration after a high impact event [45–50]. For example, Xu *et al.* [46] utilized microgrids' resources to restore critical loads when utility power is interrupted. They form a minimum length restoration tree rooted at the closest MG that can provide sufficient energy to restore a load group. Similarly, [47] adopted a two-level restoration approach in that they establish restoration paths followed by restoration through solving a linear program. An identical approach in [48] used a spanning tree to divide the distribution system into microgrids and restore the critical loads utilizing locally available combined heat and power units.

1.3 Dissertation organiztion

The dissertation comprises four main chapter after the introduction. This section includes brief summary of each chapter.

1.3.1 Chapter 2 —Dual Optimization of Data Center Revenue and Expense in a Smart Grid using an Evolutionary Approach

Energy expenses can overwhelm data center operating costs and cripple its profits. In a smart grid environment, electricity prices change dynamically across geo-regions, time-of-use, and in relation to real-time demand. A data center, if equipped with the capability to shift load to other data centers and flexible resource allocation, can benefit from the variable prices and grow its profit by curtailing expenditures. In this chapter, we provide an overview of research approaches for modeling the profit maximization problem. Next, we present an evolutionary approach for the simultaneous optimization of data center revenue and expense objectives. The proposed approach utilizes the Strength Pareto Evolutionary Algorithm (SPEA-II) as the base framework and adapts it to devise an algorithm. The algorithm considers real-time electric price variations while taking request routing decisions. The proposed scheme is suitable for data centers with heterogeneous and homogeneous servers, is temperature aware, and considers both cooling and computing power consumption. The scheme provides trade-off solutions for system managers for use in varied operational scenarios.

1.3.2 Chapter 3 - QoS and Power Network Stability Aware Simultaneous Optimization of Data Center Revenue and Expenses

Data center profit maximization research have sought to address the problem generally from the data centers' perspective making the benefits flow unidirectional [9]. Most solutions seek to maximize data center revenues, reduce the cost of operation, and maintain a higher availability of data center [35]. However, analysis of the impact of dynamic changes in data center load on power grid stability is critical for reliability and sustainability of power grid. Only a handful of these studies have explored the interaction of a data center with a power grid [9–14]. In general, these works have not evaluated the impact of dynamic changes in data center load on power system stability. At best, some of these researches have tried to curtail power grid load imbalances and consequent instability through indirect performance measures. For example, [11, 12] uses electric load imbalance index —the ratio of demand to system capacity.

In this chapter, we propose an integrative strategy that balances the interests of both data centers and the power is required. So far, to the best of our knowledge, no contemporary work has directly incorporated power networks' operational constraints, especially voltage stability, into the data center optimization process. Thus, this research is most suited to futuristic integrated power systems and data centers.

1.3.3 Chapter 4 - Optimizing Energy Donation in a Smart Grid during Crisis

Energy donation is an attractive mechanism to mitigate the effects of the power crisis resulting from weather or human-made interruptions. Tapping enhanced philanthropic sentiment during the crisis and encouraging the trade of user-owned surplus capacity, the grid can restore critical loads and provide a degree of relief to the affected users.

In this chapter, we propose a novel framework to mitigate the effects of crisis through energy donation. The approach envisages a microgrid (MG) based distribution network where MGs with surplus supply provide energy to those in need. The energy is allocated to MGs based on the criticality of the load they serve and their historical contribution. This research employs an evolutionary optimization technique to maximize social welfare that is to achieve maximum coverage while keeping losses minimum so as to distribute limited energy resource optimally.

1.3.4 Chapter 5 - Energy Sharing for Service Restoration using a Consortium Blockchain Approach in a Smart Grid

Power network disruptions triggered by weather events or otherwise leave devastating effects on communities. Microgrids with distributed energy resources can help swift localized restoration following the interruption of utility power. However, because of microgrids' limited generation and storage capacity, service restoration would require prioritizing critical load and optimality of operations for rendering relief to those in dire need. Moreover, fair energy allocation, trust-free energy exchanges, and the integrity of transactions are crucial.

This chapter proposes a blockchain-based energy sharing approach for service restoration using energy crowdsourced through donation or trade. The proposed framework utilizes microgrids' supply situation and reputation as consortium admission criteria for optimizing the blockchain operations' energy cost. In addition, the proposed approach uses a measure called proof of welfare (PoWel) which solves the rationing problem to produce an energy allocation block accordingly by utilizing weighted rationing for prioritizing critical load restoration and an evolutionary optimization algorithm for maximizing social welfare and minimizing power losses. The winner block selected through consensus intrinsically preserves network stability while conforming to resource and stability constraints.

Chapter 2

Dual Optimization of Revenue and Expense in Geo-Distributed Data Centers using the Smart Grid

Exorbitant energy expenses can supersede data center profits. Electricity prices often vary across the geographic regions, caused by gaps in the supply-demand, time of use, and production cost factors. Geo-distributed cloud data centers facilitated by a smart grid and enabled by cloud computing can potentially utilize the spatiotemporal diversity of energy prices to reduce operational expenditure and maximize profit. In this chapter, we solve the data center profit by formulating it as a constrained multi-objective optimization problem. The proposed solution utilizes an evolutionary algorithm-based higher-level heuristic that optimizes data center revenue and expense objectives simultaneously. The proposed technique provides system managers with trade-off solutions suited to varied operational scenarios. Ours is a multi-step approach, utilizing the optimization scheme to obtain Pareto optimal solutions for the request dispatch and resource allocation problem. When broadly evaluated against a comparative resource optimization scheme, our technique increases revenue while lowering expense and collectively yields a higher profit. It exhibits such performance over a broad range of price changes regardless of the data center's size and utilization level. The extensive simulation results ascertain the effectiveness of the proposed approach across a myriad of system parameters.

2.1 Introduction

Data centers incur massive power consumption, devouring billions of kilowatts each year. Their power consumption, despite improvements in server technologies, has exhibited steady growth in the past decade [51]. In 2014 alone, US data centers consumed 70 billion kilowatt-hours, equivalent to an estimated 1.8% of the total energy demand of the entire

United States [52]. Apart from its economic pitfalls, power consumption has severe repercussions for global warming. The fossil fuel required to power the worlds' data centers releases an amount of carbon dioxide equal to that of the entire airline traffic [53]. As our communities and industries move forward to embrace massive data storage and communication, data centers will continue to expand with steady growth in their power demand. Cloud data traffic exhibits a large amount of temporal variability, with peak volume orders of magnitude higher than the nominal value. As a result, the data centers build excess capacity to meet quality-of-service (QoS) requirements specified in the user service level agreement (SLA), even for the busiest period. This overprovisioning of data centers leads to excessive power-related operational expenditure (OPEX). In this backdrop, carefully designed algorithms are required for optimizing data center resource allocation to reduce OPEX while still meeting the SLA provisions. In addition, the smart grid with its information infrastructure and deregulated energy market offers additional avenues for OPEX reduction.

Power grid revitalization through the assimilation of renewable energy sources brings in a new challenge of intermittent generation. Therefore, to provide an uninterrupted and stable supply, the grid maintains fossil fuel-based dispatchable generation reserves. In addition, it takes measures, e.g., dynamic energy pricing, to incentivize the users to do demand-side management. Under this paradigm, the electricity prices vary across geographic regions and the time of the day depending on the availability of renewable power, realtime demand, and state of the power grid. For example, if the grid is overloaded in a region, it may increase the prices to promote demand-side management [5]. Similarly, it can lower prices if excess power is available to incentivize users to consume more, thus helping it avoid stability issues. Data centers under the realm of cloud computing can effectively utilize this spatiotemporal diversity at energy prices.

Research in data center profit maximization has progressed into two primary directions. In first case, researchers strive to improve data center energy efficiency by optimizing request routing and resource allocation [22–24, 26, 27, 54]. The goal here is to maximize resource utilization by consolidating tasks to fewer servers and putting remaining into low power modes or switching them off altogether. These works also utilize advanced CPU features like low power modes, dynamic voltage frequency scaling (DVFS), and temperature control for further reducing power consumption. While these measures effectively minimize consumption on computing, they also have related pitfalls. For example, switching off servers create QoS issues, while consolidation may lead to the creation of hotspots within the data center, adversely affecting equipment safety and increasing expenses on environmental control [55]. Therefore, to address the issue, some researchers have investigated the optimization of both computing and cooling-related power consumption simultaneously [56–58].

In second case, researchers additionally tap the spatiotemporal price diversity offered

by bulk power systems [13, 28–34, 59, 60]. The key idea is to route service requests to data centers in geographic regions with cheaper electricity to minimize power expense. However, this leads to sudden changes in the data center load which may destabilize the power grid, forcing it to increase power prices to stabilize the situation [5, 61]. These spot prices may be orders of magnitude higher and can cripple data center profit. Therefore, the data center needs to consider real-time energy price variations caused by changes in demand in the optimization process. However, despite it importance, only a handful of existing works have investigated this critical aspect [5, 13, 61, 62].

Furthermore, the data center profit depends on two factors, the revenue and expense. Although both originate from the same financial domain, their simultaneous optimization provides a better control to cloud managers. It does so by facilitating each component's analysis separately and providing multiple Pareto optimal configurations, thereby allowing system managers to choose from what is commensurate with their resources. For example, a data center may operate to achieve a revenue target, given an expense budget. Alternatively, a data center may operate to achieve the optimal value of the expense, given a revenue target. However, to the best of our knowledge, no known scheme provides simultaneous trade-off solutions for revenue and expense objectives, while considering computing and cooling-related expenses, and utilizing diversity at power prices available to data centers operating in a cloud setting under a smart grid.

In this context, this chapter formulates the data center profit maximization involving geo-distributed cloud data centers as a multi-objective constrained optimization problem. It then proposes a higher-level heuristic that uses evolutionary technique to solve it. Our proposed technique utilizes the Strength Pareto Evolutionary Algorithm (SPEA-II) [63] as the base framework and adapt it to devise an algorithm. As opposed to using a straight SPEA-II based algorithm, the proposed technique is "hyper-evolutionary" in the sense that it formulates a high-level algorithm in which the evolutionary component is invoked multiple times. The technique finds Pareto optimal solutions for data center request dispatch and resource allocation in a bulk power system operation.

The proposed technique considers spatiotemporal diversity and real-time electricity price variations with net demand and simultaneously minimizes OPEX on computing and cooling. Specifically, the contributions are as follows: First, we propose an effective algorithm that uses the evolutionary technique as a basic component to obtain Pareto-optimal solutions. Second, the proposed technique considers real-time electric price variations due to load and renewable power availability while assigning requests to data centers. Third, our scheme is suitable for data centers with heterogeneous and homogeneous architectures. Fourth, the scheme is temperature aware, considers the cost of electricity consumed in computing as well as cooling, and to the best of our knowledge, is the first scheme to utilize multi-objective constrained evolutionary optimization technique for simultaneous optimization of data center revenue and expense. The algorithm achieves higher revenue

and lower expense than the comparative resource optimization approach. Our technique maintains its higher profit over a broad range of price changes regardless of the data center's size and utilization levels. The chapter includes extensive simulation results that ascertain the effectiveness of the proposed approach.

The rest of the chapter is organized as follows: Section II presents the related work, summarizing and highlighting the differences with our work. Section III elaborates the problem formulation. Section IV explains the design of the proposed optimization scheme and its operation. Section V presents the performance evaluation and analysis of results. Section VI concludes the chapter by providing some highlights of the future work directions.

2.2 Related work

A broad range of work has been done in achieving data center energy efficiency by optimizing service requests assignment, resource utilization, and environmental control [22–24, 26, 27, 54, 64]. For example, Ardagna *et al.* [22, 23], in order to reduce consumption, studied adaptive control of data centers' computing resources using short and long term resource management measures. They considered DVFS, server power state tuning, load balancing, VM allocation, and adjusting active servers with varying user demand as short-term measures. Approaches using switching servers and moving VMs for the next control slot aimed for long-term optimization. The work reported in [24] explored optimal cloud configuration and proposed a double renting-based resource provisioning approach. Song *et al.*, [27] proposed a two-tiered on-demand resource allocation framework considering demand and QoS needs of the applications. They reduced consumption by optimizing resource allocation at the server and data center levels.

As opposed to the proposed approach, contemporary works have notable limitations effecting their efficacy. For example, many of them [22–24, 27] have focused on computing-related power optimization only leaving out environment control that may account upto 50% of data center consumption [65]. The others are only applicable to homogeneous data center architecture [24]. In comparison, the proposed approach optimizes both cooling and computing-related power and is equally applicable to homogeneous and heterogeneous DC architectures.

In the second category, researchers have explored smart grid and data interactions, specifically diversity of electricity prices with time and across geographic regions and its impact on the profit of geo-distributed data centers [12, 28–30, 66, 67]. For instance, Wang *et al.* formulated the electricity network and data center interactions as a two-stage problem. In stage-1, the smart grid tries load balancing by providing incentives to users (data centers) to shift computing load to areas with cheaper electricity, and in stage-2, a data center optimizes its profit by using its load-shifting capabilities. Besides, [30] investigated the effects of the choice of energy options, i.e., retail market, day-ahead, local renewable

generation, or using spatiotemporal variations of prices on data center profit.

There has been a body of research that has used spatiotemporal diversity of energy prices in a deregulated market for data center profit maximization [13, 31–34, 60]. For example, Ghamkhari *et al.* [31], modeled data center profit maximization problem when green energy was available behind the meter and otherwise. Similarly, [32] used an SLA-based approach for the profit maximization problem considering deregulated power prices. The authors divided the data center workload into green and brown categories for servicing on servers powered with green and brown energy, respectively. Besides, [33] focused on data center resizing and DVFS to conserve energy. It schedules service tasks considering spatiotemporal price diversity to reduce electricity expenses. Similarly, [68,69] investigated the workload placement methodologies to reduce the energy cost of geo-distributed data centers. In another work, Wang *et al.* [13] modeled the interaction system of the bulk power system and cloud as a Stackelberg game with two players. They used convex optimization and simulated annealing techniques for solving the problem.

While all fore mentioned works are related and comparable, the proposed approach differs in several ways. For example, [31] tried to maximize profit just by optimizing resource allocation that too within a lone data center setting, whereas we consider both resource and request routing optimization in a cloud environment. Secondly, both [31, 32] optimized profit as a composite objective; in contrast, our work optimizes revenue and expense objectives simultaneously, which is more flexible from the application point of view. It facilitates each component's analysis separately and provides multiple Pareto optimal configurations for system managers to choose from what commensurate with their resources. Similarly, [33] did not cover the demand-driven dynamic pricing scenario. Therefore, a derived solution may overload the smart grid in a particular data center area, stimulate a price hike and thwart the cost reduction goal. Finally, in contrast to our approach, [13] did not consider cooling-related energy, thereby ignoring a major component of data center power expenses.

2.3 Problem Formulation

2.3.1 Preliminaries

We consider a cloud consisting of $\mathcal{N}$ geo-distributed data centers powered by a smart grid that has distributed generation. A representative network setup is shown in Fig. 2.1. The data centers comprise heterogeneous servers with varying computational capacities. Cloud service requests arrive at front-end portals and are assigned to servers in the data centers considering the price of electricity in a given region.

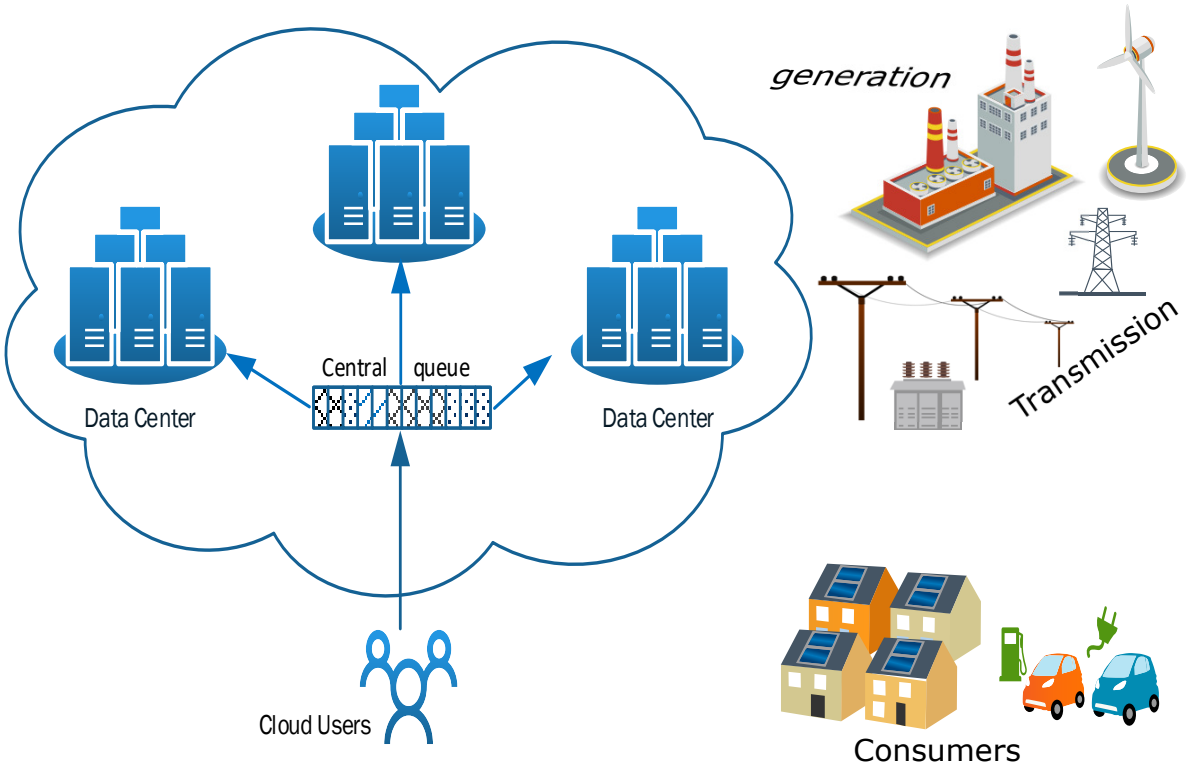

Figure 2.1: System model for profit maximization problem.

2.3.2 Electricity Pricing

Electricity prices vary across the geographic regions depending upon the production cost factors, the gap in the supply-demand, network congestion, and losses. The prices may also change with time of use, day-to-day, and in real-time. Typically, the deregulated electricity market considers two dynamic pricing scenarios. In first, Day-Ahead pricing, the price of electricity is settled the day before the operating day. The clearing of prices ahead of time allows the users to adjust their consumption by postponing the loads to the time when the cost of electricity is less. The second case is the Real-Time pricing, where the real-time energy demand and the actual generation determine the price. So, if the demand is more prices rise to balance the supply-demand gap; otherwise, the rates drop. The prices in the spot market can vary significantly, thus affecting users' power expenses. In this chapter, we investigate data center profit under Real-Time pricing. The key objective of dynamic pricing is to promote demand-side management and mitigate the requirement of building costly generation reserves. For this, to enable demand response, the grid controller generates a price signal for users to indicate a tariff change. Based on real-time power grid load conditions, assumed to be known to cloud controller, the controller runs power price forecasting algorithms and migrates its computing workload to the data centers with the lowest cost of energy. We further assume that the other load lack computational intelligence and thus knowledge about price signal beforehand, so they

are not able to alter their demand. Therefore, during the one-time slot, the load from the other consumers remain constant.

For this work, we set the price of electricity proportional to the gap in supply and demand. So, the unit price on ith power node (bus) is as follow:

$$C_i^l = \begin{cases} C_{b,i} - mP_{in,i} & \forall \ P_{in,i} < 0 \\ C_{b,i} & \text{Otherwise} \end{cases} \tag{2.1}$$

where $P_{in,i} = P_{g,i} - L_i$ is the gap in the supply and load on a power node. In addition, m is price gradient — rate of change of price by grid, $P_{g,i}$ is available supply, and L_i is load on ith node (bus) as given below.

$$P_{g,i} = P_{r,i} + P_{nr,i} \tag{2.2}$$

$$L_i = P_{dc,i} + P_{o,i} \tag{2.3}$$

where $P_{r,i}$ and $P_{nr,i}$ are the power generation from renewable and non-renewable sources respectively. $P_{dc,i}$ is the power consumed by data center connected to ith bus and is specified later in Section 2.3.3 whereas $P_{o,i}$ is the load from devices other than the data center. The pricing scheme (2.1) enables demand response and embeds the location-dependent price variations. The scheme is similar to [70, 71], with a base price $C_{b,i}$ that varies according to a geographic location and the dynamic component that incorporates the demand and supply factors. In (2.1), if $P_{in,i} \geq 0$ i.e., supply is abundant or demand is less, the energy price is set to $C_{b,i}$ otherwise, the price rises above the base value. The factor m controls the rate of a price increase to incentivize users to do load management but is subject to load-balancing requirements of the grid.

2.3.3 Cloud Power Consumption

Data center power consumption comprises two major components that are the energy used to carry out computing tasks and environmental control. Most of the energy consumed dissipates as heat that requires effective management for the safe and efficient operation of the data center. Typically, data centers follow a hot-aisle and cold-aisle arrangement to minimize the mixing of hot-air and cold-air, thereby minimizing the creation of hotspots. The cooling cost may account for up to 50% of the net energy expenses [65]. In this section, we specify the data center energy consumption on cooling, referred to as Cooling Power and computing tasks referred to as Computing Power.

Cooling Power

The power consumption on cooling depends on three factors: First, the maximum temperature allowed inside a data center T_{max}. For safe operation, the temperature of a machine should not exceed T_{max}, which has an optimum range of $18 - 27$ degrees Celsius [72]. Second, a server inlet temperature T_{in} that is the temperature of the air supplied by computer room air conditioner (CRAC). Third, the coefficient of performance (CoP) of the CRAC units. The CoP is the ratio of the amount of heat removed to the power required by CRAC for that work. Moore *et al.* [58] used CoP to model efficiency of the CRAC unit as a function of the temperature of the supplied air T_{in} as given in (2.4). The CoP is a super-linear function, and CRAC efficiency increases with a rise in the temperature of the air supplied. So, a unit with higher CoP consumes less power to remove a specific amount of heat.

$$CoP_{dc}(T_{in}) = 0.0068T_{in}^2 + 0.0008T_{in} + 0.458 \tag{2.4}$$

Most of the power consumed by servers in a data center dissipates as heat that needs removal to control the temperature inside the data center. The CoP establishes the relationship between computing and cooling power P_{dc}^{ac} which is given as:

$$P_{dc}^{ac}(T_{max}, T_{in}) = P_{dc}/CoP_{dc}(T_{in}) \tag{2.5}$$

where P_{dc} is the computing power and CoP_{dc} is the CoP of the CRAC unit. To cut down the cooling cost, a data center requires to maximize the temperature of the air supplied by CRAC units by scheduling computing tasks in a manner that machine temperatures T_i do not rise beyond the safe threshold T_{max}. The machine temperature, using abstract heat model of a data center [73], in terms of consumed power, and the supply temperature can be written as:

$$T_i = T_{in} + max(\boldsymbol{D}\overrightarrow{\boldsymbol{P_j^c}}) \tag{2.6}$$

where T_{in} is the inlet temperature, $\overrightarrow{\boldsymbol{P_j^c}} = \{p_1^c, p_2^c, \ldots, p_n^c\}$ is the power consumption vector of machines. The consumed power in a machine dissipates as heat and affects itself as well as other machines since a part of the exhaust hot-air may recirculate within a cabinet or a data center. The effect is called cross-interference and is represented in matrix $\boldsymbol{D}$— the heat distribution matrix. Each element of the matrix $d_{ij} \in \boldsymbol{D}$ shows an increase in the temperature of machine i due to the consumption of machine j. The matrix $\boldsymbol{D}$ is used to transform the server power consumption into the temperature domain. Moreover, for a data center, the elements of $\boldsymbol{D}$ depends on the pattern of air movement, which is usually fixed for a given data center configuration and physical layout [74].

Cross-interference profiling to create a thermal map of the data center is widely researched. The techniques fall in three main categories, the analytical approaches based on

basic heat transfer models, predictive approaches based on machine learning and neural networks, and computation fluid dynamics (CFD) based approaches. These techniques have varying degrees of complexity and accuracy. For an algorithm that makes scheduling decisions based on the thermal map of a data center, the complexity of the profiling approach is very critical. Though the CFD approaches are most accurate yet their complexity makes them unsuitable for thermal-aware task scheduling scenarios [73].

For the data centers, where cold-air is supplied through raised floors, the machines located away from floor tend to have higher temperatures compared to the counterparts lower in the racks. This is because the heat produced by machines located at lower levels affects temperatures of the upper level but not the other way around [73]. For thermal profiling, we consider the model as in [57]. The model has two assumptions: First, it considers the interference from the servers located in the same rack. Second, the heat from the servers that are below a machine in the same cabinet affects its temperature. The second assumption builds on the fact that hot air always flows upwards, and the heat energy falls off exponentially with distance. The elements of heat distribution matrix are expressed as $\boldsymbol{d_{ij}} = \{k^{|i-j|^{-1}}\}$, where k is a constant > 1.

Computing Power

A server power consumption has two components: the dynamic part that is proportional to the server utilization and the static component that depends on its hardware configuration and the idling time. The static consumption accounts for 60% of server power demand [75], beyond that, the dynamic part changes linearly with the load. As the data centers have low utilization in the range of 20 - 30 % [75] and are over-provisioned, the static consumption is a major source of energy wastage. To optimize energy usage, many researchers propose to consolidate servers to maximum capacity and shutting down the unused ones [54]. However, this leads to QoS issues and increased algorithmic complexity.

We assume that the request generation in a cloud follows a Poisson distribution with the average arrival rate of λ [76]. The requests gather in a central queue, and the cloud controller then assigns them to servers in different data centers. The probability of assignment of a request to a server is x. We consider the data centers comprising heterogeneous servers with varying request processing capabilities given by μ. The controller allocates adequate computing resources r to service requests in line with user SLA requirements. Now, using queuing theoretic approach [13, 29, 77] to model server power consumption, the dynamic and static consumption components can be written as (2.7) and (2.8) respectively.

$$P^d = \frac{x\lambda}{\mu}\bar{P}^d \tag{2.7}$$

$$P^s = h + r(\bar{P}^s - h) \tag{2.8}$$

where h is a constant and $\bar{P}^d$ & $\bar{P}^s$ are the maximum dynamic and static power consumption respectively. Based on these computing power consumption P^c_{dc} of a data center with K number of servers is given as

$$P^c_{dc} = \sum_{j \in K} (P^d_j + P^s_j) \tag{2.9}$$

where P^d_j is dynamic and P^s_j static power consumption of jth server.

Given a cloud with $\mathcal{N}$ data centers the net power consumption in terms of computing $\overrightarrow{\boldsymbol{P^c_{dc}}}(r, x) = \{P^c_{dc,1}, P^c_{dc,2}, \ldots, P^c_{dc,\mathcal{N}}\}$ and cooling $\overrightarrow{\boldsymbol{P^{ac}_{dc}}}(T_{max}, T_{in}) = \{P^{ac}_{dc,1}, P^{ac}_{dc,2}, \ldots, P^{ac}_{dc,\mathcal{N}}\}$ power consumption is given as

$$P_{cloud} = \sum_{i \in \mathcal{N}} \left(1 + \frac{1}{CoP_i(T_{in})}\right) P^c_{dc,i} \tag{2.10}$$

2.3.4 Objective Function

In a cloud, the request arrival in central pool follows a Poisson process with an average arrival rate of λ [76]. As the requests are assigned to individual servers the system can still be modeled as M/M/1 queuing system. The response time R of the system with the request processing rate u_{ij} is given as

$$R = \begin{cases} (r_{ij}\mu_{ij} - x_{ij}\lambda)^{-1} & \text{if } x_{ij} > 0 \\ 0 & \text{Otherwise} \end{cases} \tag{2.11}$$

A cloud earns revenue by servicing requests according to SLA and gets penalized if a request misses a response time deadline. Typically cloud computing systems' income is represented as a utility function [13, 22, 34]. In this work, we use a linear non-increasing utility function, $U = \zeta - \delta R$ to model cloud revenue. Also, we assume that the system allocates sufficient resources, as in (2.15), to meet response time requirements specified in SLA and thus it effectively avoids penalties. The system profit depends on the number of requests serviced according to SLA, and the cost of power consumed. The income and expense functions for the cloud computing system are as per (2.12) and (2.13) respectively.

$$\boldsymbol{f} = \lambda(\zeta - \delta \sum_{i \in \mathcal{N}} \sum_{j \in K} \frac{x_{ij}}{r_{ij}\mu_{ij} - x_{ij}\lambda}) \tag{2.12}$$

$$\boldsymbol{E} = \sum_{i \in \mathcal{N}} C^l_i P_{dc,i} \tag{2.13}$$

Given the income and expense functions, the objective, i.e., profit is as follows

$$\max_{x,r} \ \boldsymbol{f} - \boldsymbol{E} \tag{2.14}$$

Subject to:

$$
\begin{aligned}
& 0 \leq r_{ij} \leq 1 && \forall i \in \mathcal{N}, j \in K \\
& 0 \leq x_{ij} \leq 1 && \forall i \in \mathcal{N}, j \in K \\
& \sum_{i \in \mathcal{N}} \sum_{j \in K} x_{ij} = 1 && \\
& x_{ij}\lambda < r_{ij}\mu_{ij} && \forall i \in \mathcal{N}, j \in K \\
& max\{D_{dc,i} \times P^{c}_{dc,i}\} + T_{in} < T_{max} &&
\end{aligned}
\tag{2.15}
$$

The cloud controller tries to maximize the objective (2.14) which is a non-linear function and is neither convex nor concave on decision variables $\boldsymbol{r} := \{r_{ij}\}$ and $\boldsymbol{x} := \{x_{ij}\}$ $\forall i \in \mathcal{N}, j \in K$. Equation (2.15) describes the constraints on the optimization problem. The first two specify the domains of the decision variables, whereas the third ensures that all requests received in the cloud are serviced. The fourth constraint caters for the allocation of sufficient resources to meet response time requirements specified in SLA. The last one is the temperature constraint. It ensures that while optimizing request dispatch and resources, the system does not overload a machine so that its temperature rises beyond the safe threshold. This constraint helps to achieve maximum equipment efficiency and minimize cooling costs.

2.4 Proposed Solution

The optimization problem (2.14) with conflicting objectives forms a case of multi-objective-constrained optimization, which in its generic form is given as follows

$$
\begin{aligned}
& \min\ f_i(x) = f_i(x_1, x_2, ..., x_n) \quad \forall i = 1, 2, ..., p \\
& \text{subject to:} \\
& g_j(x) = g_j(x_1, x_2, ..., x_n) \leq 0 \quad \forall j = 1, 2, ..., q \\
& h_j(x) = h_j(x_1, x_2, ..., x_n) = 0 \quad \forall j = q+1, 2, ..., m \\
& x_k^{min} \leq x_k \leq x_k^{max} \qquad k = 1, ..., n
\end{aligned}
\tag{2.16}
$$

The formulation involves p objective functions, $f_i(x)$, defined over an n dimensional search space R^n with upper and lower bounds given by x_k^{min} and x_k^{max}. The objectives are simultaneously optimized subject to q inequality and $m-q$ equality constraints. When we have multiple conflicting objectives, the optimization transforms into Pareto optimality defined based on the dominance relationship between feasible solutions. For solutions x_i and x_j in

a feasible design space S, the dominance relationship is as follow:

$$\begin{aligned} & x_i \preceq x_j \text{ iff} \\ & f_i(x_i) \leq f_i(x_j) \quad \text{for } i \in 1, 2, ..., p \\ & f_i(x_i) < f_i(x_j) \quad \text{for at least one } i \in 1, 2, ..., p \end{aligned} \tag{2.17}$$

So, solution x_i is said to dominate solution x_j if x_i is no worst than x_j in all objectives and solution x_i is better than x_j in at least one objective. Such non-dominated solutions in a feasible space are called Pareto optimal. In other words, for x_i to be Pareto optimal point, no other point exists in the feasible design space S that improves at least one objective function while keeping others unchanged. The non-dominated solutions evolve in the form of Pareto fronts (PF).

We propose an evolutionary algorithm based upon a higher-level heuristic, as shown in Fig. 2.2 to solve data center profit maximization problem. The algorithm alternatively optimizes the request dispatch and resource allocation until the incremental increase in the profit stays above a given threshold ($\boldsymbol{\epsilon}$). The basis of the proposed algorithm is built on the principles of a multi-objective evolutionary optimization algorithm called SPEA-II [63]. It operates on a set of initial candidate solutions iteratively applying natural selection based on fitness, removing weak members, and introducing randomness through mutation, thus resulting in gradual evolution. The selection operation is guided by fitness assignment function, and the genetic operations are used to produce new offspring. The base framework of SPEA-II, including initial population selection, the fitness assignment, and the genetic operations, are required to be adapted according to the nature of the problem. More importantly, the framework does not have a constraint handling mechanism in place, but for most practical problems, constraint handling is fundamental. Proposed algorithm is not a direct SPEA-based technique. Instead, it is a higher-level algorithm that systematically employs SPEA-II to determine optimized solutions. Besides, the SPEA-II component, its parameters and evolution process, is designed with several problem-specific steps including constraints handling, techniques for determining the initial population, and genetic operators specific to this problem. We describe main algorithmic components in the following sections.

2.4.1 Constraints Handling

This work uses a problem specific hybrid constraint handling that comprises constraint dominance [78] and self-adaptive penalty function approaches [79]. The resource allocation phase of the algorithm just has the inequality constraints whereas the request dispatch additionally involve an equality constraint. The equality constraints are relatively hard to satisfy requiring a robust constraint handling method. Therefore, based on the nature of the constraints, the Algorithm in Fig. 2.2 invokes constraint dominance [78] in resource allocation phase to achieve a performance boost and self-adaptive penalty function approach

Algorithm: Optimization Approach

Require: Initial guess: $\boldsymbol{x} := \{x_{ij}\}$, $\boldsymbol{r} := \{r_{ij}\}$ and the system parameters
Ensure: Pareto optimal request routing schedule ($\boldsymbol{x}$) and resource allocation configuration ($\boldsymbol{r}$)

1: **while** Profit increase $> \epsilon$ **do**
2: **Phase 1: Request dispatch:** Optimize $\boldsymbol{x} \mid \boldsymbol{r}$
3: Execute CORE BLOCK ▷ Steps {9 - 20}
4: $\boldsymbol{x} :=$ PF member with maximum net profit
5: **Phase 2: Resource allocation:** Optimize $\boldsymbol{r} \mid \boldsymbol{x}$
6: Execute CORE BLOCK ▷ Steps {9 - 20}
7: $\boldsymbol{r} :=$ PF member with maximum net profit
8: **end while**

9: **procedure Core Block**
10: Generate initial population —$\boldsymbol{x}^1$ or $\boldsymbol{r}^2$
11: **for all** $i \in$ *generations* **do**
12: Apply hybrid constraint handling method
13: Assign fitness values
14: $\hat{P} := |\hat{P}|$ (Non-dominated solutions)[3]
15: Binary tournament selection
16: Apply hybrid recombination operation
17: Apply mutation
18: **end for**
19: Return Pareto front
20: **end procedure**

[1] Decision variable in request dispatch. [2] Decision variable for resource allocation. [3] If non-dominated solutions are less than the size of the elite set ($|\hat{P}|$), the best dominated solutions are used to fill remaining members.

Figure 2.2: Evolutionary algorithm based optimization approach

for the request dispatch optimization [79]. We describe this technique as hybrid constraint handling approach. The approach is suitable for problems that have disjoint or very small feasible regions as is the case here with both equality and inequality constraints. The two approaches are described next.

Constrained Dominance

The technique uses a constrained binary tournament to select a solution based on its dominance status, i.e., a solution s_i is said to constraint dominate solution s_j if any of the following conditions are true: first, s_i is feasible and s_j is not, second, both solutions are infeasible, but s_i has smaller constraints violation. Third, both are feasible, but s_i dominates s_j.

Self-Adaptive Penalty Function Approach

In the request routing phase, we use the adaptive penalty function technique [79]. The technique is suitable for problems with hard constraints and disjoint feasible regions. It allows infeasible solutions with better objective values to evolve along with the feasible solutions during its operation. Thus, the algorithm searches for optimal solutions from both sides of the constraint boundary, converges quickly, and avoids being stuck in a local optimum. The technique uses a modified objective function to rank solutions across the population. The objective is modified based on the constraint violation and objective performance. The modified objective has two components, i.e., distance measure and adaptive penalty. The algorithm operates in the following steps:

- Step 1: For each member x of the population, normalize the values of the objectives and constraints.

$$\hat{f}_i(x) = \frac{f_i(x) - \underline{f_i}(x)}{\overline{f_i}(x) - \underline{f_i}(x)} \quad \forall i \in p \tag{2.18}$$

  where $\overline{f_i}(x)$, $\underline{f_i}(x)$ are the maximum and the minimum values of the ith objective. The mean normalized constraint violation $\hat{v}(x)$ is as follow

$$\hat{v}(x) = \frac{1}{m} \sum_{j}^{m} \frac{c_j(x)}{\overline{c_j}(x)} \tag{2.19}$$

$$\text{where} \qquad c_j(x) = \begin{cases} \max(0, g_j(x)) \ \forall j = 1, 2, .., q \\ \max(0, |h_j(x)| - \eta) \ \forall j = q+1, .., m \end{cases}$$

  and $\overline{c_j}(x) = \max_x c_j(x)$, η is the tolerance value used for relaxing equality constraint.
- Step 2: Next, compute the distance (2.20) for each solution. The parameter α is a ratio of available feasible solutions to the population size. During the evolution, when no feasible solution exists, i.e., $\alpha = 0$, the distance depends on the constraint violation only. Later, with $\alpha > 0$, the distance comprise both the violation and the objective magnitudes. The dependence of the distance on feasible solutions first

drives the search to the feasible region and later, by considering the violation and the objective, forces the algorithm to look for better solutions.

$$d(x) = \begin{cases} \hat{v}(x) & \text{if } \alpha = 0 \\ \sqrt{\hat{f}_i(x)^2 + \hat{v}(x)^2} & \text{if } \alpha > 0 \end{cases} \tag{2.20}$$

- Step 3: In this step, the algorithm applies two additional penalties basing on the constraint violation and objective value while α balances the degree of penalty.

$$p_i(x) = (1-\alpha)X_i(x) + \alpha Y_i(x) \tag{2.21}$$

$$X_i(x) = \begin{cases} 0 & \text{No feasible solution} \\ \hat{v}(x) & \text{Otherwise} \end{cases} \tag{2.22}$$

$$Y_i(x) = \begin{cases} 0 & \text{if } x \text{ is feasible} \\ \hat{f}_i(x) & \text{otherwise} \end{cases} \tag{2.23}$$

- Step 4: Finally, modified objective function is given as

$$\omega(x) = d(x) + (1-\alpha)X_i(x) + \alpha Y_i(x) \tag{2.24}$$

Overall, the penalty varies with the availability of feasible solutions. First, when no feasible solution exists, the algorithm penalizes infeasible solutions. Otherwise, when their number is small, more penalty is applied to solutions with a higher violation. Finally, as the feasible population grows, the algorithm exerts more pressure on solutions with poor objective value.

Initial Population Selection

The initial population impacts the convergence of an algorithm and the quality of evolved solutions. Initialization with the feasible population is often essential for constrained optimization problems with hard constraints and broken or smaller feasible regions. However, initializing with all feasible can affect the quality of solutions from the diversity point of view [80]. The size of the initial population is another important factor; it is a user-defined parameter and depends upon the required number of solutions in the Pareto front.

For this work, the initial population includes 10% infeasible solutions. The reaming population comprises two equal-size groups of feasible individuals. The solutions in the first group produce better revenue, i.e., their bias is toward the first objective. The second group is biased towards the second objective, i.e., they provide higher expenses. The initialization scheme aims at building diversity and thus evolving to better solutions. A snapshot of chromosome composition is shown in Fig. 2.4.

To investigate the efficacy of the initialization methodology, we tested six scenarios. All samples contain $N/10$ random individuals, whereas, for the remaining feasible population,

we vary the size and biasing across subsets. Fig. 2.3 illustrates the composition of test sets, whereas the results of the study are in Fig. 2.5. The test set 2, containing the same number of solutions biased toward the two objectives, produces the highest profit across the full spectrum of price gradient.

Fitness Assignment

At the start of each iteration, the algorithm evaluates the members of the initial and elite populations assigning objective values. The values determine the fitness of a solution that drives the evolution process. The fitness has two components: domination strength or frailty and solution density. The frailty is defined to be the number of individuals dominated by the members that dominate the solution under consideration. The other component, solution density, is the distance of a solution in objective space from its kth nearest neighbor. This fitness assignment approach is particularly effective for higher-dimensional problems [63]. The fitness of ith solution in population is given as

$$fitness_i = (frailty_i + density_i)^{-1} \tag{2.25}$$

Test Set	Feasible Population size			Infeasible Population size
	Biased towards objective 1	Biased towards objective 2	Unbiased	
1 (30_30_30)	0.3 N	0.3 N	0.3 N	0.1 N
2 (45_45)	0.45 N	0.45 N	0	0.1 N
3 (60_30)	0.60 N	0.30 N	0	0.1 N
4 (70_10)	0.7 N	0.20 N	0	0.1 N
5 (80_10)	0.80 N	0.10 N	0	0.1 N
6 (90_10)	0.90 N	0	0	0.1 N

Figure 2.3: Test scenarios: initial population.

Type	1	2	3		n-2	n-1	n	1	2	3		n-2	n-1	n
Infeasible 0.1 N	0.6716	0.9872	0.1201	...	0.9578	0.9873	0.4529	0.9281	0.2719	0.8459		0.7270	0.4619	0.4993
	.	.	.		.	.	.	.	.	.		.	.	.
Feasible – Obj 1 0.45 N	0.6009	0.2983	0.7143	...	0.7639	0.8685	0.7733	0.0137	0.0232	0.0385	...	0.0182	0.0154	0.0245
	0.9141	0.7628	0.6561	...	0.6696	0.4674	0.5173	0.0139	0.0235	0.0389	...	0.0185	0.0156	0.0248
	.	.	.		.	.	.	.	.	.		.	.	.
Feasible – Obj 2 0.45 N	0.2660	0.9366	0.5010	...	0.2686	0.8578	0.4416	0.0138	0.0233	0.0386	...	0.0183	0.0155	0.0246
	0.2660	0.8865	0.7173	...	0.2760	0.4543	0.8498	0.0232	0.0112	0.0181	...	0.0032	0.0198	0.0159
	.	.	.		.	.	.	.	.	.		.	.	.
Phase	Resource Allocation							Request Dispatch						

Figure 2.4: Chromosome formulation and composition of initial population.

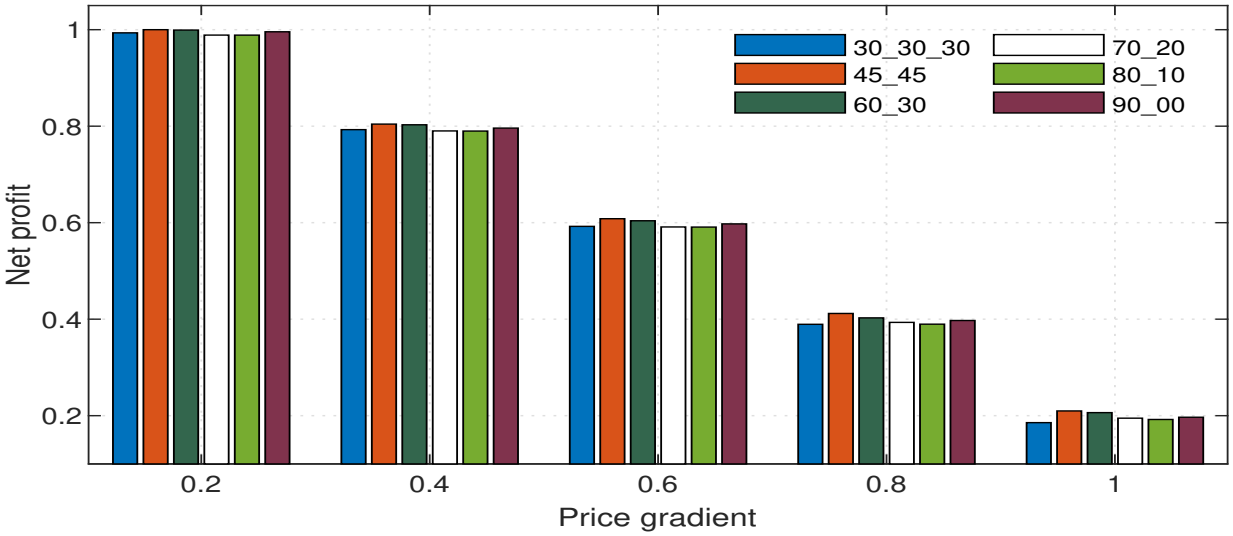

Figure 2.5: Impact of initial population selection.

Environmental and Mating Selection

The algorithm maintains two sets of population, current P, and elite $\hat{P}$, which has no members in the beginning. After assigning fitness, the algorithm copies $|\hat{P}|$ non-dominated members of P, with the highest fitness, to the elite set. If the non-dominated members fall short, the best dominated solutions fill the remaining space. As the evolution advances, $\hat{P}$ is updated with the best non-dominated solutions from the set $P \cup \hat{P}$. During this update, if the size of $\hat{P}$ exceeds $|\hat{P}|$, the truncation operator removes excess weak individuals based on the density of the region where they are located. The solutions from denser regions are removed first to enhance diversity in the Pareto front.

The selection of mating pairs for next-generation happens using the binary tournament. The tournament involves a pair of solutions randomly drawn from the elite pool. A competitor with the best fitness wins the match. An elite pool member participates in a tournament with a probability of $1/\omega$ where $\omega := |\hat{P}|$ is the cardinality of the elite set. After ω matches, we get as many best solutions, which undergo three genetic operations to create offspring. Figure 2.6 illustrates the evolution process showing the chromosomes for the current and elite populations, values for both objective functions, i.e., f and E, and the fitness. The highlighted solutions show an update across two generations, where one at the top of the updated elite pool is newly moved from the current population.

Genetic Operations

Based on the crossover and mutation probabilities, a selected set of solutions under three genetic operations in each iteration. The operations include two recombinations, single point crossover [81] and simulated binary crossover [82], applied sequentially one after the other and a mutation operation. We use multiple recombination operations to ensure a better evolution [83]. Next, we describe the genetic operations and the selection of

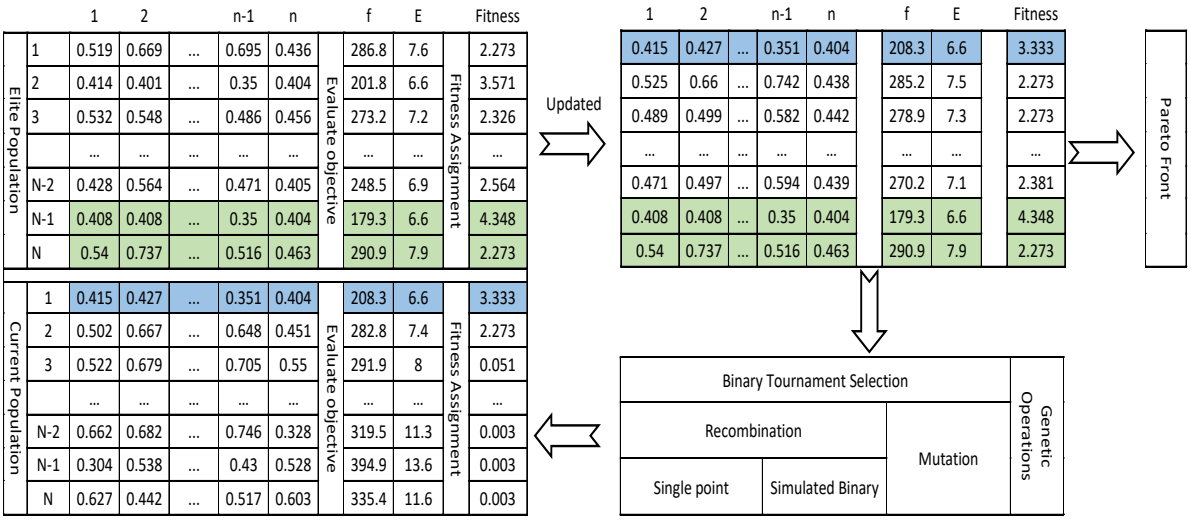

Figure 2.6: Evolution process: illustration of chromosomes for the current and elite populations, both objective functions, i.e., f and E, and the fitness. The highlighted solutions show an update across two generations.

corresponding probabilities.

In single point crossover, a random starting index is selected from where each pair swaps its decision variable values to the end of the chromosome. The process creates two child solutions. The operation of single point crossover on a mating pair p_1 and p_2 each with n features is as follow:

$$\begin{aligned} p_1 &= x_1(1), ..., x_1(m), x_1(m+1), ..., x_1(n) \\ p_2 &= x_2(1), ..., x_2(m), x_2(m+1), ..., x_2(n) \end{aligned} \tag{2.26}$$

where $x_1(m)$ and $x_2(m)$ are the mth features of the p_1 and p_2 respectively. The crossover produces the child solutions given as follow by swapping parents features starting from $m+1$

$$\begin{aligned} c_1 &= x_1(1), ..., , x_1(m), x_2(m+1), ..., x_2(n) \\ c_2 &= x_2(1), ..., x_2(m), x_1(m+1), ..., x_1(n) \end{aligned} \tag{2.27}$$

Next, we apply the simulated binary crossover (SBX) [82] to newly created children. SBX performs best for problems with non-binary decision variables as is our case. The creation of mth features of two child solutions c_1 and c_2 as a result of crossover of the parents p_1 and p_2 is as follows:

$$\begin{aligned} c_1(m) &= \frac{(1-\beta_m)x_1(m) + (1+\beta_m)x_2(m)}{2} \\ c_2(m) &= \frac{(1+\beta_m))x_1(m) + (1-\beta_m)x_2(m)}{2} \end{aligned} \tag{2.28}$$

where β is a random number generated from following probability density function.

$$PDF(\beta) = \begin{cases} (1+\eta)\beta^{\eta})/2 & \text{if } 0 \leq \beta \leq 1 \\ (1+\eta)\beta^{-(\eta+2)})/2 & \text{if } \beta > 1 \end{cases} \tag{2.29}$$

In (2.29) η is a non-negative number generally in the range of 0 and 5 [78].

The last operation, mutation, helps the evolutionary algorithms explore search space rigorously and avoid being stuck in a local optimum. The mutation generates a new solution from Uniform or Gaussian distribution whose mean is either at the center of the search domain or at the non-mutated value of the individual itself [84]. In this work, we chose to generate mutated solutions from a normal distribution with mean at the individual itself. For a solution x_i, Gaussian mutation can be written as follows:

$$x_i(k) = \begin{cases} x_i(k) & \text{if } r_m > p_m \\ max[min(x_{max}(k), N(x_i(k), & \text{if } r_m < p_m \\ \sigma^2(k)), x_{min}(k)] & \end{cases} \tag{2.30}$$

where p_m is the mutation probability and $r_m \in U[0,1]$ is a random number generated from the uniform distribution and $x_i(k)$ is the kth feature of ith member of the population.

Finally, the two important parameters related to the genetic operations are the crossover p_c and mutation p_m probabilities. Their values determine the fraction of the elite population that would participate in a crossover or undergo a mutation. A low value of p_c means a longer convergence time, whereas a very high value would force an algorithm to converge prematurely. On the other hand, a higher p_m may turn the optimization into a random search, and with a lower value of p_m, the algorithm may not explore the search domain rigorously and may produce a lower quality solution.

To assess the effectiveness of hybrid recombination and the impact of crossover and mutation probabilities, we used the simulation setup given in Section 2.5.1 and compared the resultant net system profit. In the first experiment, Fig. 2.7, the single crossover plot shows results from SBX only case, whereas multiple crossovers plot demonstrates the system profit when it is used in combination with single point crossover. The evaluation ascertains a significant improvement in profit by combining two types of crossovers. In the second evaluation, Fig. 2.8, we assessed the impact of the selection of crossover and mutation probabilities on system profit. The results show that when the p_c is 0.75 with p_m 0.25, the algorithm achieves the maximum profit and maintains it for a broader range of price gradients.

Solution Selection

On completion of each phase, Fig 2.2, multiple solutions emerge as Pareto front. We select the solution with the highest profit. The selected solution, either resource allocation or

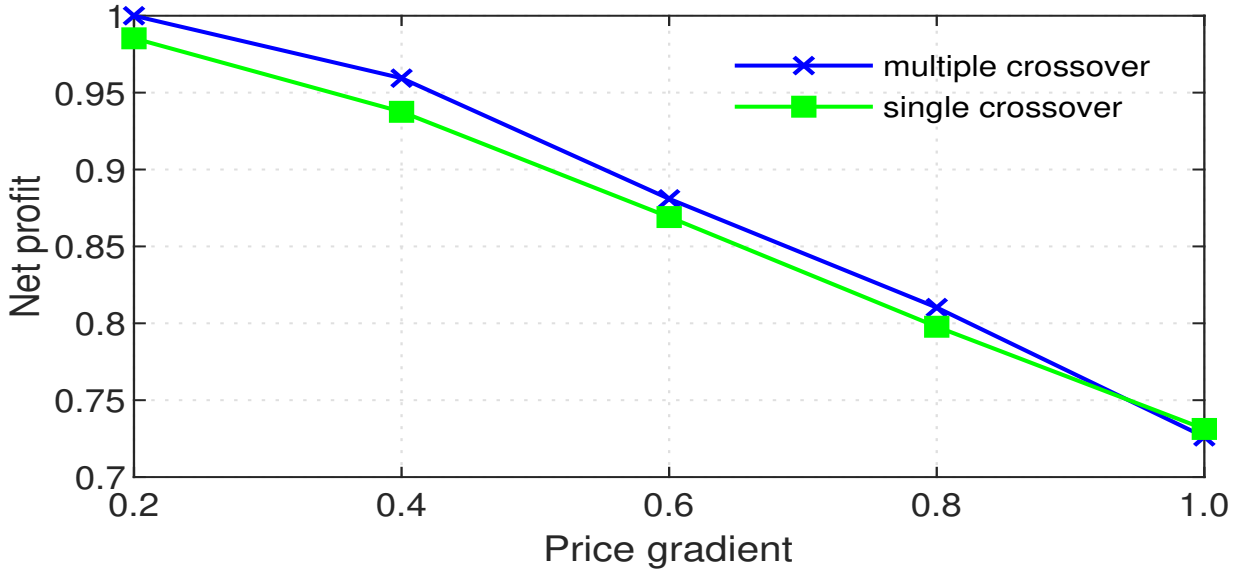

Figure 2.7: Impact of combining recombination operation.

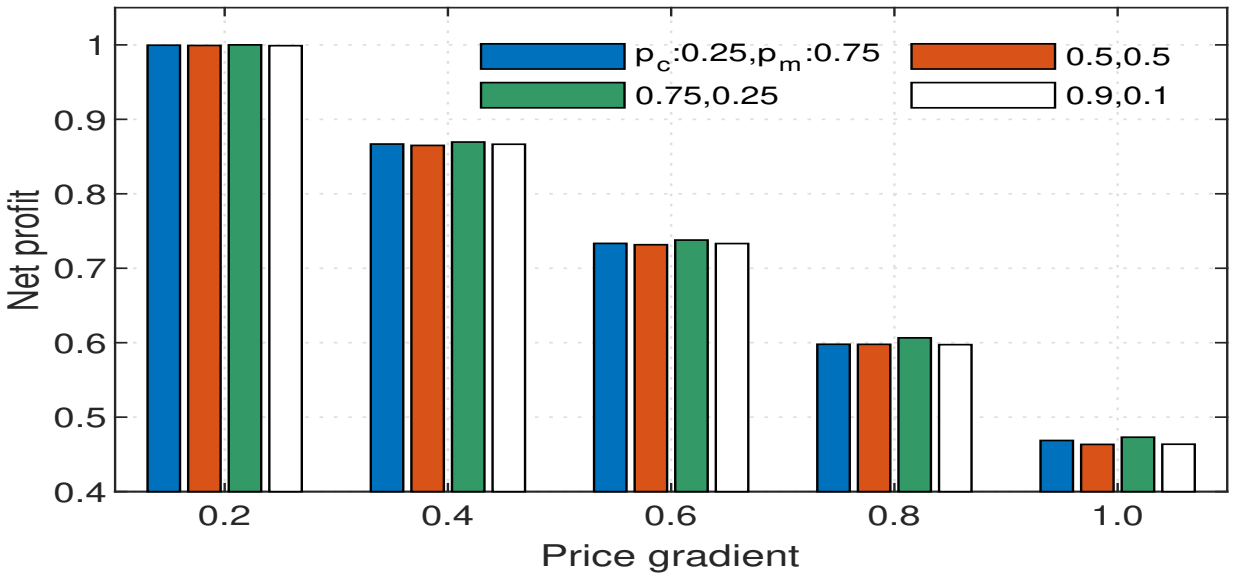

Figure 2.8: Impact of crossover and mutation probabilities. The highest net profit is when crossover probability (p_c) and mutation probability (p_m) are set at 0.75, 0.25 respectively.

request dispatch probabilities, serves as an algorithm parameter for the subsequent phase of optimization. The process continues as per Fig. 2.2 updating the selected solutions alongside if the increase in profit, from the previous run, is more than ϵ. Finally, multiple Pareto optimal solutions, Pareto front, are available to the cloud system operator for a request assignment schedule and resource allocation configuration. A snapshot of Pareto fronts showing scatter plots of normalized revenue (first objective) and the expense (second objective) under different load and price conditions are in Fig. 2.9. In the request assignment phase, the fronts are sparse, indicating hard constraints, whereas, in the re-

source allocation phase, they are relatively dense, showing the availability of more feasible solutions.

2.5 Performance Evaluation

In this section, we evaluate the algorithm performance and the impact of the selection of system parameters on data center profit.

2.5.1 Simulation Setup

To evaluate the proposed scheme, we consider three clouds computing systems designated as small, medium and large with 4, 5, and 7 data centers respectively. Table 2.1 summarizes

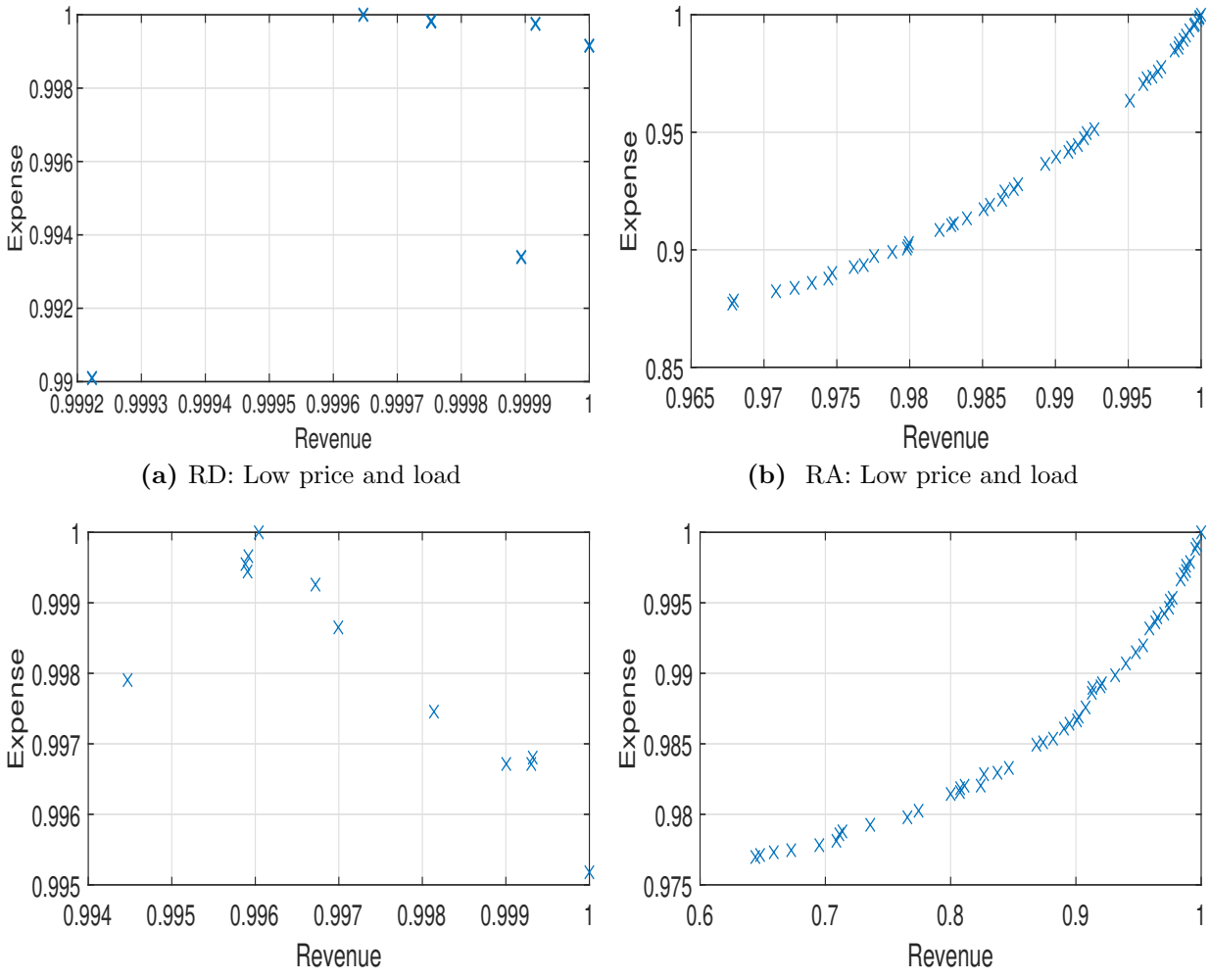

(a) RD: Low price and load

(b) RA: Low price and load

(c) RD: high price and load

(d) RA: high price and load

Figure 2.9: Pareto fronts generated in two phases: Request dispatch (RD) and Resource allocation (RA) under different load and price scenarios.

the values used for the system and the evolutionary algorithm parameters during the simulation. In the table, the quantities, e.g., $p_r := U[0, 5]$ show a uniformly distributed parameter in the range of 0 to 5. For the simulation, we kept the base electricity price C_b as same i.e. 0.3, for all data centers to evaluate algorithm performance under real-time demand dependent pricing specifically.

We evaluate the algorithm at three different levels of computing load, i.e., low, medium, and high. The system utilization ρ for these levels is set at 0.4, 0.6, and 0.8 inline with the practical workload of the large data centers [85]. The rate of request arrival λ in the cloud system is calculated from ρ as $\lambda = \rho \sum u_{ij}$. We compare the performance of the proposed algorithm with a resource allocation technique that follows a fixed request assignment schedule irrespective of electricity prices and only optimizes resources. We refer to this technique as the Baseline approach during analysis. The simulator itself is implemented in Matlab.

Table 2.1: System Parameters

Parameter	**Value**
Cloud data centers	4 (Small), 5 (Medium), 7 (large)
Number of servers	500 (Small), 2000 (Medium), 5000 (large)
P_{nr}	175 (small), 700 (medium), 980 (large)
P_r	$U[0, 5]$
P_o	$U[5, 10]$ if data center connected and
	$U[20, 40]$ otherwise
$\bar{P}^s, \bar{P}^d$	$U[0.5, 1]$, $U[0.5, 1.5]$
μ	$U[1, 3]$
ζ	215 (small), 800 (medium) and 1100(large)
h	0.003
Evolutionary Algorithm Parameters	
Population size	50
Max generations	120
p_c	0.75
p_m	0.25
ϵ	0.05%

2.5.2 Performance Measures

Impact of system utilization

System utilization ρ is the ratio of the number of requests arriving in the system to the processing power of the cloud computing system —an aggregate of server processing capacities. Fig. 2.10 shows the profit compared to the system utilization for three cloud sizes. The results indicate that an increase in the value of ρ results in the system profit increase. However, as ρ reaches 0.7, the profit shows a downward trend.

Impact of dynamic pricing on cloud revenue and expense

In this experiment, we examine the effect of the real-time price changes on the revenue and expenditure of a cloud computing system. Since the system revenue depends on the number of requests serviced (2.12) and is independent of the cost of the energy, the results remains nearly the same across the price gradients; therefore the plots are not included here. In contrast, as we can deduce from Fig.2.11, the expense increases with the increase in the price of electricity. The plot shows the expense function for a small, medium, and large cloud in low, medium, and high computing load scenarios. The proposed algorithm minimizes the expense much better than the Baseline approach over a broad range of price gradients regardless of the data center size and load conditions.

Impact of dynamic pricing on cloud Profit

In this case, we analyze the effectiveness of the proposed algorithm under dynamic pricing scenario in a bulk power network. Fig.2.14 shows the cloud system profit versus price changes in three cloud systems and under low, medium, and high load conditions. The

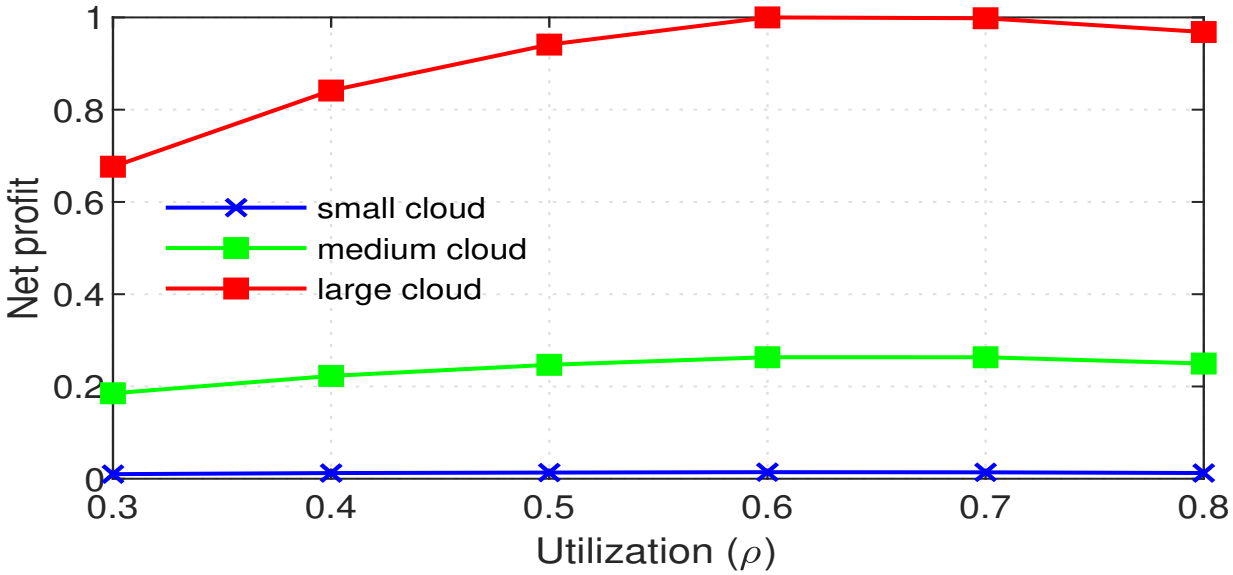

Figure 2.10: Impact of system utilization.

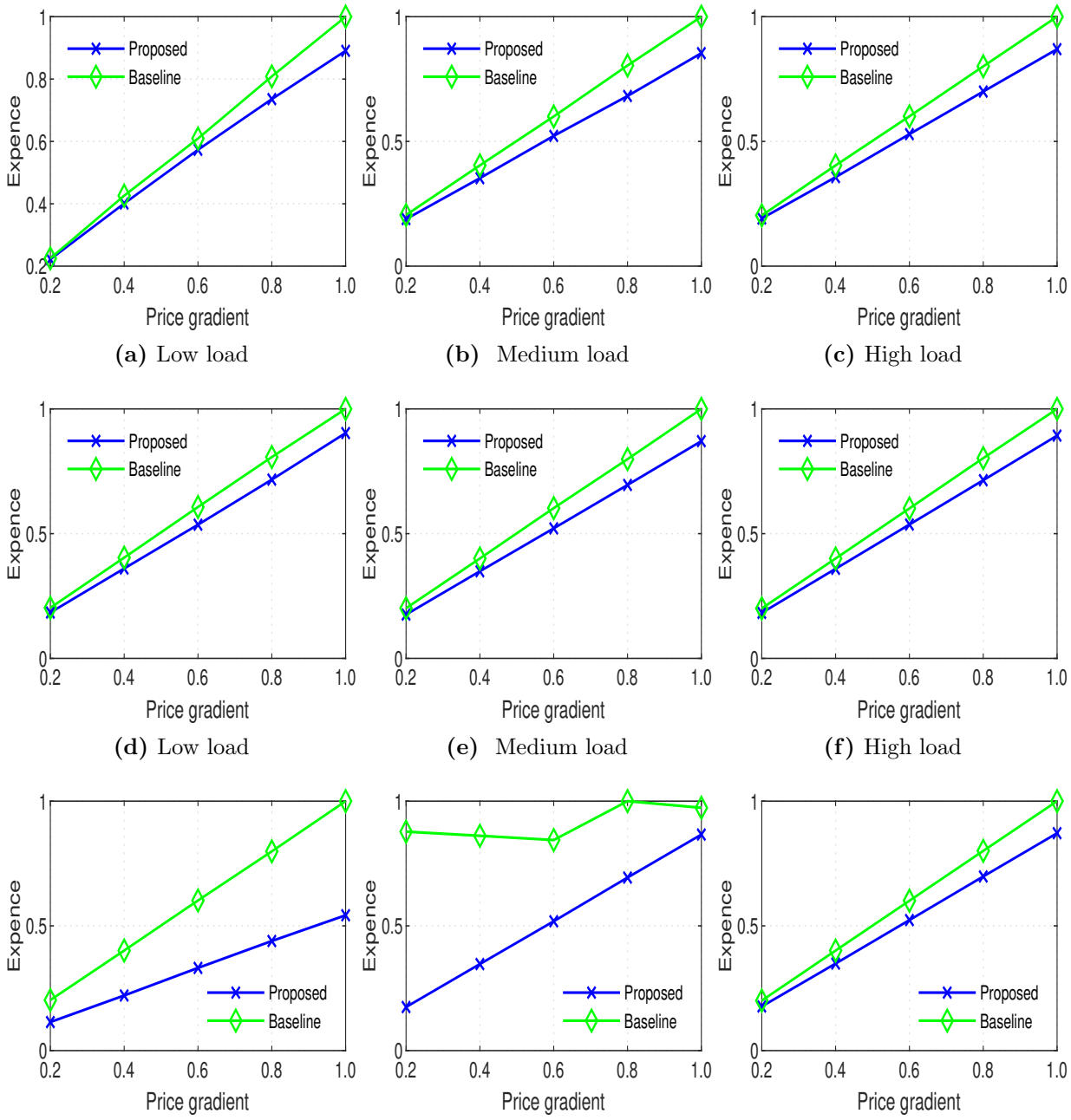

(a) Low load **(b)** Medium load **(c)** High load

(d) Low load **(e)** Medium load **(f)** High load

(g) Low load **(h)** Medium load **(i)** High load

Figure 2.11: Impact of dynamic pricing on data center expense under low, medium, and high load conditions in small cloud (Fig. a,b,c), medium cloud(Fig. d,e,f), and large cloud (Fig. g,h,i)

results show a decrease in profit as the price of electricity increases. The proposed scheme achieves higher profit compared to the Baseline algorithm regardless of the cloud size and load conditions. The higher profit stems from the price-aware routing decisions due to which the proposed approach reroutes the computing tasks with the increase in power

prices. In contrast, the Baseline approach follows a fixed request dispatch schedule regardless of the energy prices, and just to optimizes resources suffers from lower profit.

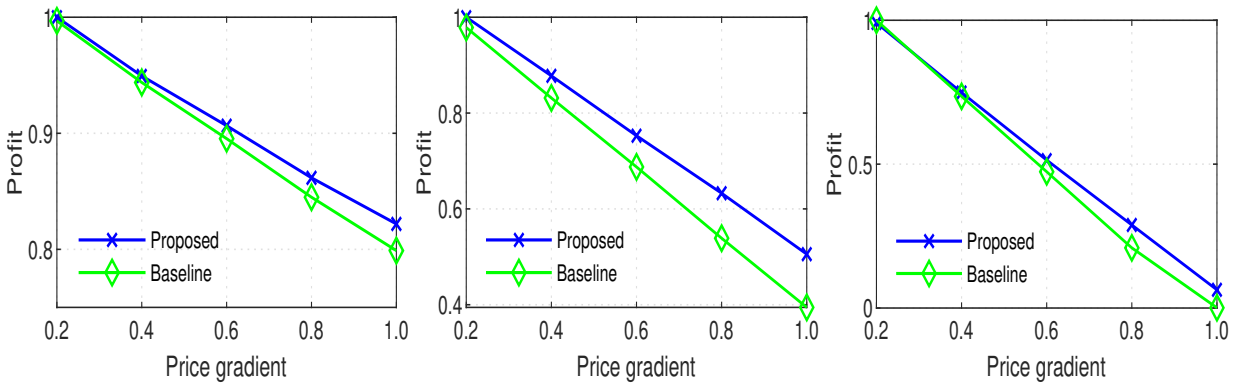

(a) Low load **(b)** Medium load **(c)** High load

Figure 2.12: Comparison of normalized profit of proposed and baseline approaches in the small cloud.

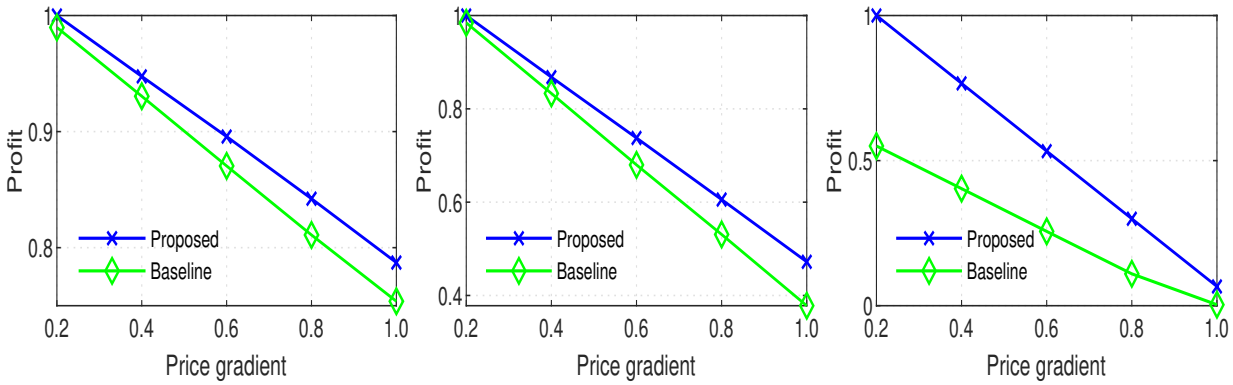

(a) Low load **(b)** Medium load **(c)** High load

Figure 2.13: Comparison of normalized profit of proposed and baseline approaches in the medium cloud.

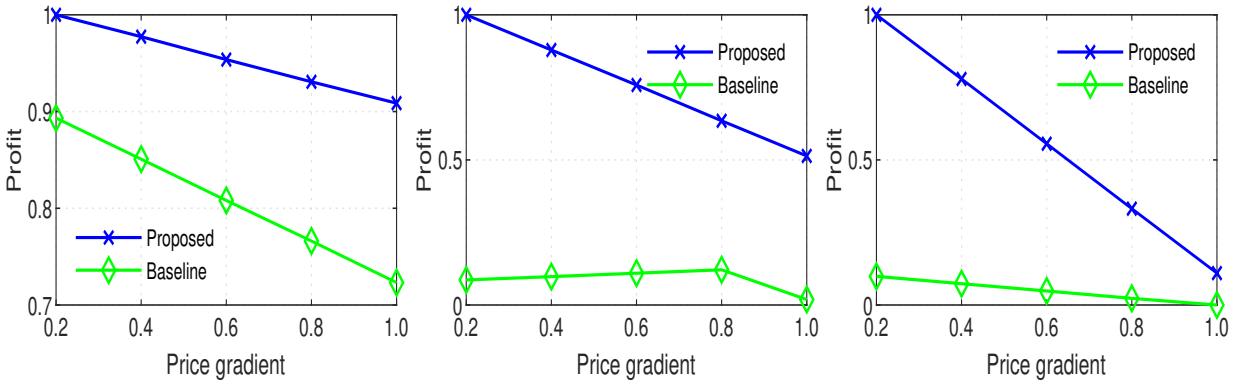

(a) Low load **(b)** Medium load **(c)** High load

Figure 2.14: Comparison of normalized profit of proposed and baseline approaches in the large cloud.

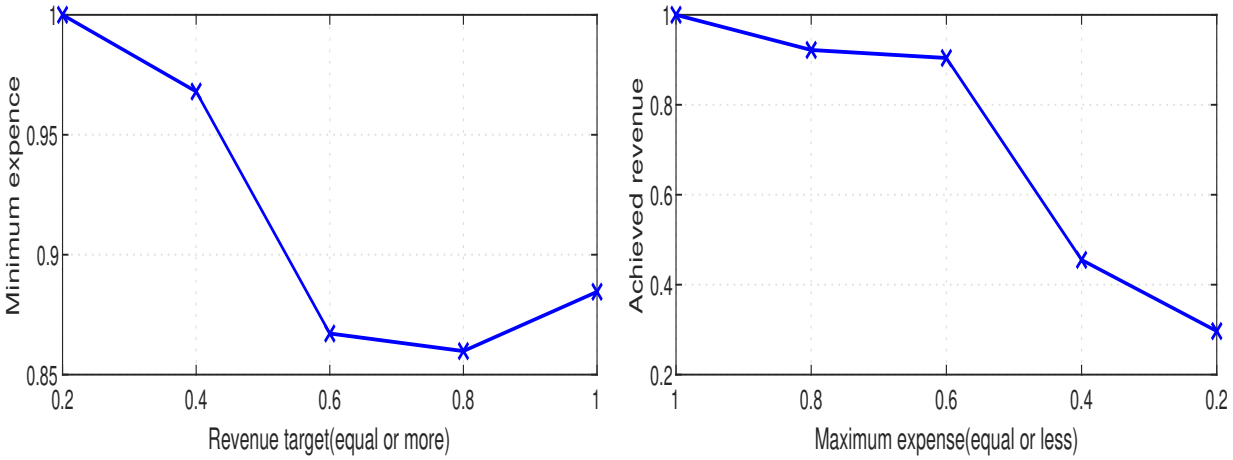

(a) Meet a revenue target **(b)** Meet an expense constraint

Figure 2.15: Meeting revenue target or an expense constraint.

Impact of a revenue target or a fund constraint

In this experiment, we analyze an operational scenario where the cloud service provider operates under a revenue target or an expense limit. The operator tries to meet the target objective by varying the other one. The results are generated in the small cloud with a price gradient m and system utilization ρ set as 0.6. Fig. 2.15(a) shows the normalized expense when normalized revenue is equal or greater than the amount shown along the x-axis. We see that when the revenue target is greater than 1, no feasible solution is possible. Fig. 2.15(b) shows the value of the revenue when the expense limit is less than the values shown along the x-axis. In this case, as the maximum allowed expense decreases, the algorithm tries to maintain the revenues till expense is 0.6; afterward, the expense constraint becomes so inflexible that the revenue starts to decrease. When the expense decreases to a value of 0.2, the algorithm is unable to find any feasible solution thereafter that meets the set objective.

2.6 Conclusion

The chapter showed that the geo-distributed data centers maximize their profit by optimizing resource allocation and request routing considering diversity at power prices available in the smart. The proposed evolutionary algorithm based upon a higher-level heuristic achieves dual objective optimization by finding Pareto optimal decisions for a cloud controller. Simulation results prove that our scheme is effective and outperforms the Baseline approach with higher profit over a broad range of energy prices, cloud sizes, and utilization levels. The proposed scheme provides trade-off solutions, and hence various choices to the system manager. In the future, we intend to enhance the system model by incorporating

the deactivation of the underutilized servers while providing QoS grantees.

Chapter 3

QoS and Power Network Stability Aware Simultaneous Optimization of Data Center Revenue and expenses

Data center profits are directly impacted by electric power consumption, which in turn has critical environmental implications. Geo distributed data centers maximize profits by optimizing resource allocation and leveraging diverse power tariffs available in a deregulated market. However, a power network state apathetic profit maximization can destabilize the grid and hamper a data center's sustainability goals. In this chapter, we formulate the data center profit maximization as a constrained optimization problem. We then propose a multi-level algorithm where the lower level scheme is based on evolutionary optimization. The algorithm simultaneously optimizes revenue and expenses while preserving QoS and power network stability. The proposed approach considers real-time demand-based energy price variations to orchestrate request routing and resource allocation. The approach is suitable for heterogeneous and homogeneous data center architectures. The proposed scheme is also thermal-aware and considers both computing and cooling consumption. Simulation results show that the proposed technique is effective; it achieves a higher profit over a broad range of price variations and data center utilization levels. Data center; Resource allocation; Quality of Service; Evolutionary optimization; Smart grid; Voltage stability

3.1 Introduction

Global data centers consume $5 - 9\%$ of the world's electricity [86]. The enormous power consumption is a financial burden for providers and has severe implications for the environment. Data center (DC) design caters to the quality of service requirements (QoS) according to users' service level agreement (SLA) even during the peak load periods. This

results in overprovisioning and is a major contributor to excessive consumption. Data center consumption growth is likely to continue due to the ever-increasing demand for digital services. At present, the fossil fuel used to power world data centers produces carbon dioxide equal to the whole of the airline industry [53]. The excessive consumption and reliance on the power grid on brown energy sources would hamper the achievement of sustainable and carbon-neutral data centers. Therefore, a well-coordinated approach involving regulators, the data centers, and smart grid operators is vital to reverse the course. For this, the data centers need to be energy efficient and contribute to integrating renewable energy sources and the power grid's smooth functioning [87].

A smart grid with renewable energy resources like solar and wind faces the challenge of intermittent generation. Therefore, the network maintains brown energy-based costly generation reserves to stabilize supply. Data centers with massive consumption and capabilities to adaptively change demand pose huge challenges to grid stability and offer tremendous opportunities. Greedy profit maximization by data center can destabilize the power grid. On the other hand, it can also act as a dispatchable load that the power network can utilize to cater to generation and user demand uncertainties. Thus, the data centers can help the power grid assimilate renewable energy sources without maintaining costly reserves.

The power grid employs dynamic pricing of electricity where prices vary depending on real time demand, generation, and network conditions. The energy prices change from one region to another, across grid nodes, and time intervals. Geo distributed data centers utilize lower power tariffs by routing computing traffic to areas with minimum electricity costs [6–8]. However, these dynamic changes in the data center load can destabilize the power grid and stimulate major voltage collapses. In such circumstances, the power grid raises energy prices to incentivize users to do demand-side management. As a result, the data center may have to reroute traffic, thus stimulating a chain reaction or counteracting the objective of availing lower power prices. This mutual interaction of demand, cost, and price paradoxically continues to create a vicious cycle [9]. By embedding power stability in the optimization process, the data center can utilize lower power tariffs, minimize geographic load balancing overheads, and fulfill social responsibilities towards a greener future.

Data center profit maximization research branch into two main directions: First, the approaches that focus on improving data center efficiency by optimizing request routing, resource allocation, and environmental control [23, 56–58]. Second, the group that has additionally strived to reduce power bill by harnessing diversity at power prices offered in a deregulated energy market [13, 28, 30–33].

The relevant research works have sought to address the problem only from the data centers' perspective making the benefits flow unidirectional [9]. Most solutions seek to maximize revenues, reduce the cost of operation, and maintain a higher availability of data center [35]. Only a handful of these studies have explored the interaction of a data center

with a power grid [9–14]. In general, these works have not evaluated the impact of dynamic changes in data center load on power system stability. At best, some of these researches have tried to curtail power grid load imbalances and consequent instability through indirect performance measures. For example, [11, 12] uses electric load imbalance index —the ratio of demand to system capacity . Therefore, to the best of our knowledge, no contemporary work has directly incorporated power networks' operational constraints into the data center optimization process.

This article proposes a data center profit maximization approach utilizing a higher-level algorithm that uses an evolutionary optimization technique. We formulate the profit maximization problem with multiple geo-distributed data centers. The proposed algorithm uses the Strength Pareto Evolutionary Algorithm (SPEA-II) [63] as a base framework and adapts it to devise an algorithm. The algorithm simultaneously maximizes SLA revenues and minimizes expenses while providing guaranteed QoS and satisfying power network operational constraints.

This chapter's key contributions are as follows: First, we formulate profit maximization as a multi-objective constrained optimization problem and propose an SPEA-II-based higher-level algorithm to solve it. Second, the proposed scheme harnesses spatiotemporal diversity and real time demand or renewable generation based price changes for assigning tasks to servers. Third, the algorithm finds Pareto optimal solutions for data center request routing and resource allocation for use in varied operational scenarios. The algorithm minimizes energy consumption on computing and considers machine temperature for task placement to avoid hot spots and reduce environment control expenses. Our approach achieves a higher profit over a broad range of prices and utilization levels of the cloud. Finally, to the best of our knowledge, this is the first scheme that incorporates power grid stability into the data center optimization process. Simulation results in the IEEE-33 bus system ascertain the effectiveness of the proposed approach.

The rest of the chapter is organized as follows: Section II presents the related work, summarizing and highlighting the differences with our work. Section III elaborates the problem formulation. Section IV explains the design of the proposed optimization scheme and its operation. Section V presents the performance evaluation and analysis of results. Section VI concludes the chapter by providing some highlights of the future work directions.

3.2 Related work

Data center profit maximization research has taken two main courses. The first category includes the approaches that try to make data center operation efficient by optimizing request routing, resource allocation, and environmental control [23, 56–58]. For instance, Ardagna *et al.* proposed a framework for increasing SLA revenues and reducing energy consumption by virtual machine allocation and using server hardware features. The schemes

in this category face many challenges that limit their practical use. For instance, some works have not considered environmental control that accounts for 40—50% of data center net power consumption. Others only cater to homogeneous data center architecture, and some have left out the QoS aspects. Most importantly, price apathetic nature inhibits their ability to use spatiotemporal price diversity in the smart grid. In comparison, the proposed approach optimizes both cooling and computing-related power and is equally applicable to homogeneous and heterogeneous DC architectures. The scheme also carries out price aware routing of request while providing QoS grantees as per SLA.

The next group has additionally focused on reducing the power bill by harnessing diverse power prices offered in the smart grid [13, 28, 30–33]. For example, [31] addressed the trade-off between minimizing a data center's energy cost versus maximizing the revenue. Kiani and Ansari [32] proposed a workload distribution strategy aimed at maximizing the profit of geo-distributed green data centers. However, these schemes have sought to broadly address the profit maximization from the data center's perspective, and here, the benefits flow is unidirectional [9]. The research focus is contracted to maximize data center revenue, reduce the cost of operation, and maintain high data center availability [35]. This unidirectional optimization can potentially destabilize power grid operations and hamper the integration of renewable generation sources into the power grid. On the contrary, the proposed approach considers power network operational constraints in the optimization process to help the grid to provide a stable supply to users.

A small number of related studies, however, have also explored interactions of the data center and the power grid [9–14] but, in general, they have not evaluated the impact of dynamic changes in data center load on power system stability. The researchers have tried to curtail power grid load imbalances and consequent instability through indirect performance measures. For example, [11, 12] use electric load imbalance index —the ratio of load to system capacity. Such high-level measures have limitations compared to incorporating power network operational constraints into the data center optimization process. Motivated by this, the proposed algorithm considers the power network's operational parameters in the optimization process instead of taking indirect measures to safeguard power network stability.

Achievement of the futuristic objective of sustainable power systems and carbon-neutral data centers require close coordination among power network, data centers, and the regulators. Future data center and power grid (microgrid) may be owned by the same entity so that an integrated optimization approach would become more plausible. Otherwise, the regulators can facilitate cooperative operational arrangements among the grid and data centers. The integrated data center and smart grid paradigm has recently gained the attention of many researchers. The new paradigm hinges on three salient features: First, integrating data center into the power system as dispatchable load, e.g., Koronen *et al.* [35, 87] investigated the data center integration into the European energy system via

DC demand response. The DC could provide more than 10 GW of demand response in the European Energy System by 2030, facilitate the transition to renewable sources, and render other societal benefits. Second, a socially conscious optimization of the data center operations, e.g., Liu *et al.* [88], explored the social impacts of the geographic load balancing specifically to increase renewable penetration and reduce the use of brown energy. Third, incorporating operational constraints of power network into the DC optimization process, e.g., Aksanli *et al.* [14] analyzed effects of changes in the data center consumption on power grid stability by incorporating bus voltage deviations. In comparison, our approach is more rigorous as it uses both voltage deviations and voltage stability index.

3.3 Problem Formulation

We consider a cloud computing system consisting of $\mathcal{N}$ geographically distributed data centers. The data centers are connected to a smart power grid that comprises $\mathcal{W}$ nodes (buses) and $\mathcal{E}$ branches. The grid has distributed renewable alongside bulk generation. The service requests land at front end portals of the cloud and then are assigned to specific servers in the different data centers. The probability of assigning a request to a server depends upon the energy price in that region. Data centers form the major load on a power bus. However, other loads are also present that are assumed to be constant for the given operation slot. Data centers comprise heterogeneous servers of varying request processing capacity. The setup is shown in Fig. 3.1. In a deregulated energy market, electricity prices vary across the geographic regions primarily because of production cost factors, network congestion, and losses in an area. The prices are cleared in the day-ahead market, but due to real time generation conditions, demand uncertainties, and network dynamics, the prices may escalate in real time. The variations may be the order of magnitude higher.

Data centers operating in the realm of cloud computing can benefit from the spatiotemporal price diversity by dynamically shifting their load to areas where cheaper electricity is available. Such flexibility enables the data center to act like a dispatchable load that the power grid can utilize to address network stability issues arising due to heightened user demand. The grid, to incentivize users, dynamically changes electricity prices based on real time power consumption at a node. The system raises the prices to balance the supply and demand gap; otherwise, it lowers them at the base price level. The policy aims at achieving demand response and stable supply.

A representative pricing scheme that embeds the price diversity in the day-ahead market and a component that depends on the real time load and the available power supply is available in [71]. Accordingly, the unit price of electricity on ith power bus (node) is given

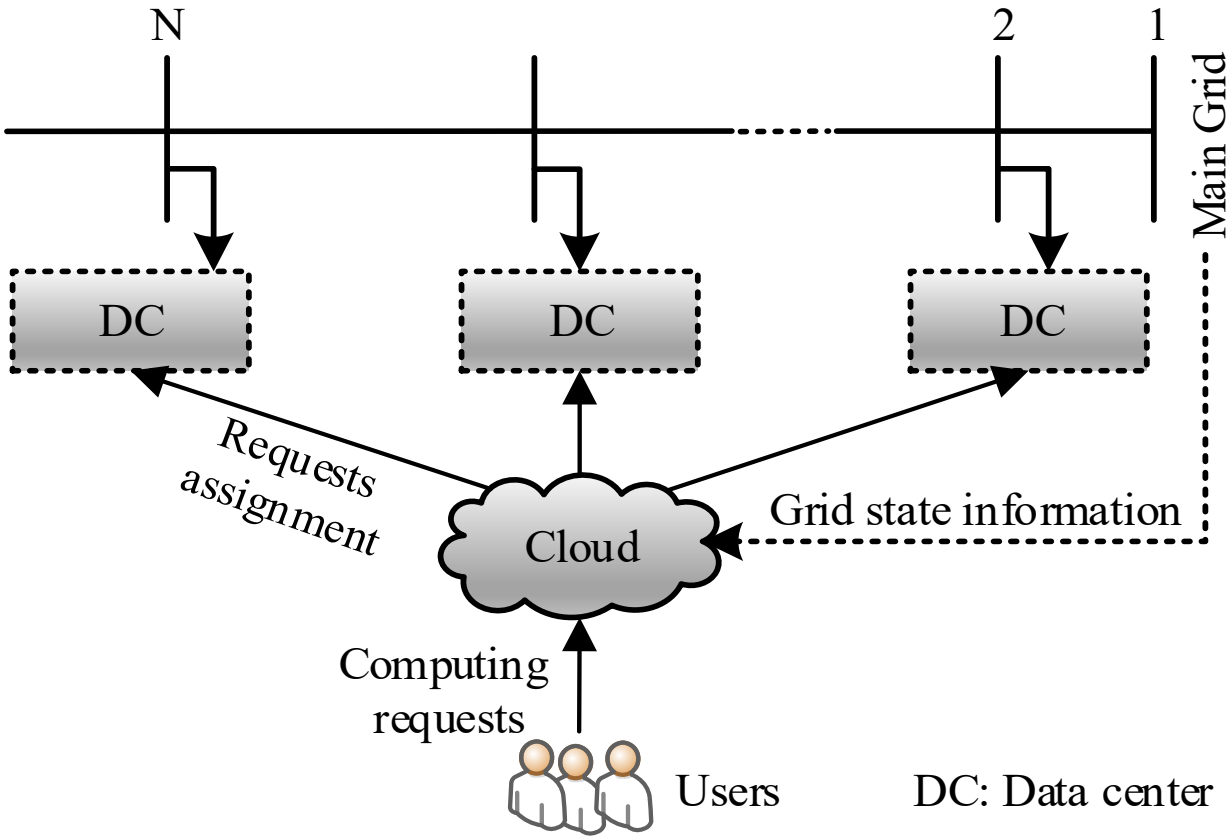

Figure 3.1: Geo distributed data centers and power grid infrastructure.

as

$$C_i^l = \begin{cases} C_b - mS_{in} & \forall \;\; S_{in} < 0 \\ C_b & \text{Otherwise} \end{cases} \tag{3.1}$$

where $S_{in} = S_g - L$, is the power injection, $\mathcal{S}_g$ is the scheduled power from distributed renewable and non-renewable source, and $\mathcal{L}$ the load on the node.

When $\mathcal{S}_{in} \geq 0$, i.e., generation exceeds demand, the grid charges the energy at the base price $\mathcal{C}_b$. Otherwise, the grid increase energy prices proportional to the difference in supply-demand to assert demand response. The base component $\mathcal{C}_b$ encompasses the geographic factors and the day-ahead price clearing. The factor m regulates the rate of change of the price. The grid controller tries to determine an optimal value for m, considering the requirement of load balancing and grid stability.

We assume that grid state information, including energy consumption data on a particular bus and other system parameters, are available to the cloud controller. In anticipation of price change due to load conditions, the cloud controller shifts the computing load to areas with cheaper electricity. The state information becomes available as a result of load flow analysis [89] by the grid or the cloud controller.

3.3.1 Data Center Power Consumption

Data center consumption comprises the power utilized in computing equipment and environmental control. The later accounts for up $40 - 50\%$ of the net consumption with the computer room air-conditioner (CRAC) being the main contributor. The consumption on cooling depends on two factors. First, the maximum temperature T_{max} allowed inside data center—higher temperature limit results in to lower consumption in CRAC, but it can impact equipment safety and efficiency. T_{max} has an optimal range of $18 - 27$ degrees Celsius [72]. Second is the units' coefficient of performance (CoP). CoP depends on the temperature of the air supplied by a CRAC also called the server inlet temperature T_{in}. For water chilled unit [58], the CoP is given as $CoP(T_{in}) = 0.0068T_{in}^2 + 0.0008T_{in} + 0.458$.

A common strategy to reduce power consumption consolidates load on to fewer servers. However, the consolidation increases machine temperatures, creates load imbalance among servers, and hot-spots inside a data center. As a result, the system controller has to lower the temperature of the cool air supplied to the data center, thus increasing consumption on cooling. One remedy for this is the thermal-aware task placement on servers. Under this scheme, the scheduler monitors machine temperature before assigning a computing task to a server.

The server temperature depends on its utilization and also on the cross-interference from other machines. For this work, we use the model [57] that considers the interference from servers located in the same rack below the machine under consideration and ignores the effect from the others. The scheme includes a cross-interference coefficients matrix $\mathcal{D}$ that is used to convert the server consumption to the temperature domain. Using $\mathcal{D}$, server temperature can be modelled as $T_i = T_{in} + max(\mathcal{D}P_j^c)$, where P_j^c is a vector consumption of servers housed in the same cabinet. The cooling related power consumption of a data center in terms of CoP is given as

$$P_{dc}^{cool} = P_{dc}/CoP_{dc} \tag{3.2}$$

where P_{dc} is the data center consumption on computing.

For a data center, computing power consumption P_{dc} is the net energy consumed by individual servers. A server consumption comprises two components; the dynamic component depends on its utilization level, and the static component is determined by hardware configuration. The static consumption always exists as long the server is powered on. A majority of studies for reducing the static consumption propose consolidating computing to the minimum servers and shutting down underutilized machines. However, the efforts in this direction increase the complexity of the algorithms and challenges to provide quality of service.

In a cloud computing system, the service requests arrive at front end portal servers. The requests are then assigned to servers in different data centers. The scheduling decision

is based on the price of electricity in that region. The controller schedules requests to data centers with minimum cost.

Let x be the probability of assigning a request to a server in a data center that has request processing capacity μ. By adopting a queuing theoretic approach [13,29], computing consumption of the data center is given as:

$$P_{dc}^{comp} = \sum_{j \in K} (P_j^d + P_j^s) \tag{3.3}$$

where $P_j^d := \frac{x\lambda}{\mu} \bar{P}^d$ is dynamic and $P_j^s := h + r(\bar{P}^s - h)$ is the static power consumption of jth server in ith data center. $\bar{P}^d$ and $\bar{P}^s$ are the maximum dynamic and the static consumption of a server, h is the consumption due to the server base hardware. The parameter r represents the computing resources allocated to service requests. Combining (3.2) and (3.3), power consumption of ith data center is as following:

$$P_{dc,i} = \left(1 + \frac{1}{CoP_i(T_{in})}\right) P_{dc,i}^{comp} \tag{3.4}$$

Now, for a cloud with $\mathcal{N}$ data centers, the net power consumption is $\sum_{i \in \mathcal{N}} P_{dc,i}$.

3.3.2 Power Network Stability

Maintaining bus voltages at nominal levels is critical for power network stability. Sudden variations in load can destabilize the power network and stimulate a voltage collapse, especially if compensation for real and reactive power is not available. System operators employ voltage stability index to monitor and compensate real and reactive power if required. Geo distributed data centers offload computing to ones located in regions with lower power tariffs. Thus, data center load varies in real time, making the power system vulnerable to voltage collapses. In such circumstances, the power grid operator raises power prices to incentivize users to do demand-side management. As a result, the data center may have to shift the computing load again. This sets up a vicious cycle, and the operations may get highly destabilized. Otherwise, data center risks counteracting the objective of availing lower power tariffs. So grid stability aware optimization of data center operation is important.

By embedding power stability in the data centers' optimization process, the data center can help the smart grid balance load and provide a stable supply. In addition, the data center can also benefit from lower power tariffs and reduced overheads due to geographic load balancing of its traffic. More importantly, power stability aware data center optimization can ultimately lead to greater integration of renewable energy sources into the power grid.

We consider a voltage stability index (SI) to evaluate the stability margin at a power bus to which a data center is connected. The voltage stability index has attracted vast

research in the past. Many indices for analysing instability along the nodes and lines are available in literature [90–94]. For this work, we adopt an approach proposed in [94]. The proposed power stability index is suitable for an active distribution network as it accounts for distributed generation and the voltage angle variations. The index is given as follows:

$$SI = \frac{4\Omega_{ij}(P_L - P_G)}{[|V_i|Cos(\theta - \delta^p]^2} \leq 1 \tag{3.5}$$

where Ω_{ij} is the effective line resistance from node i to j and V_i is the sending end node voltage. Next, P_L, P_G are load and power compensation on a node, δ^p is angle variation between two nodes and θ is the impedance angle.

During optimization, the cloud system controller evaluates a solution for voltage stability value (SI) for buses where data centers are located. If the index value is closer to unity, it shifts some load to other data centers and re-evaluates SI.

3.3.3 Objective Function

A cloud earns revenue by servicing requests according to user SLA. Typically, a cloud computing systems' income is expressed as a utility function. We utilize linear non-increasing utility function $U = \zeta - \delta R^t$ [22, 34] to represent revenue; where R^t is the system response time, ζ, and δ are utility function parameters.

Given a cloud, as the request are assigned to individual servers from the front end portal, the system forms a $M/M/1$ queuing model with response time is given as

$$R^t = \begin{cases} (r_{ij}\mu_{ij} - x_{ij}\lambda)^{-1} & \text{if } x_{ij} > 0 \\ 0 & \text{Otherwise} \end{cases} \tag{3.6}$$

where μ_{ij} shows processing capacity, x_{ij} the probability of assignment of request to a server, λ is mean arrival rate of request in cloud system, and r_{ij} is the fraction of server resources assigned for processing the assigned tasks. In order to provide QoS as per the SLA, a data center allocates sufficient resources such that $R^t \leq D^{sla}$ where D^{sla} are the ervice delivery deadlines specified in SLA.

The system profit, a difference of revenue and expense, depends on the number of requests serviced according to SLA and the cost of power consumed while servicing these requests. The revenue and expense functions for cloud computing system are as per (3.7) and (3.8) respectively.

$$Rev = \lambda(\zeta - \delta \sum_{i \in N} \sum_{j \in K} \frac{x_{ij}}{r_{ij}\mu_{ij} - x_{ij}\lambda}) \tag{3.7}$$

$$Exp = \sum_{i \in N} C_i^l P_{dc,i} \tag{3.8}$$

The cloud controller tries to simultaneously maximize revenue and minimize expenses in an effort to maximize profit. The optimization problem is given as following:

$$
\begin{aligned}
&max\ Rev \\
&min\ Exp \\
&\text{Subject to:} \\
&\qquad 0 \leq x_{ij} \leq 1 \ \ \forall i,j \\
&\qquad 0 \leq r_{ij} \leq 1 \ \ \forall i,j \\
&\qquad R^t \leq D^{sla} \ \ \forall i,j \\
&\qquad x_{ij}\lambda < r_{ij}\mu_{ij} \ \ \forall i,j \\
&\qquad T_{in} + max\{D_{dc,i}P_{dc,i}\} < T_{max} \\
&\qquad SI < 1 \\
&\qquad V_{min} \leq V_i \leq V_{max}
\end{aligned}
\tag{3.9}
$$

The optimization objectives are conflicting and the functions are nonlinear. However, if one decision variable is fixed, the objective is modeled as a convex function. Therefore, we take an iterative approach and optimize the request dispatch and resource allocation in successive phases. The constraints on the optimization problem come from both the data center and the power grid domains. The first two specify bounds on the decision variables, whereas the third is QoS constraint to ensure the system meets response time requirements specified in SLA. Next is the resource constraint that allows for allocating adequate resources to provide services as per SLA. The fifth one is the thermal constraint; it safeguards against a rise in the server temperature beyond permissible limits due to consolidation. The last two are the operational constraints from the power grid. SI is the voltage stability index, and the last constraint deals with voltage levels on power buses. These constraints ensure that the data center optimization does not cause instability in the power network, and voltage levels stay in permissible bounds.

3.4 Proposed Solution

Given conflicting objectives, the optimization transforms into Pareto optimality. Thus, solutions are selected based on Pareto dominance. We propose a multi-level technique that uses a multi-objective evolutionary optimization algorithm called SPEA-II [63] at lower level for simultaneous optimization of both objectives. However, even the lower-level algorithm is not a direct variant of SPEA-II; rather, it involves multiple additional components like a custom diversity-oriented initialization and constraints handling and genetic operations. Figure 3.2 shows the salient steps of the proposed algorithm. Next, we describe various algorithmic components.

Algorithm: Optimization Approach

Require: System parameters, power network data, initial guess for $\mathbf{r_{ij}}$ or $\mathbf{x_{ij}}$
Ensure: Pareto optimal request routing schedule ($\mathbf{x_{ij}}$) and resource allocation configuration ($\mathbf{r_{ij}}$)

1: **while** ΔProfit $> \epsilon$ **do**
2: **Step 1: Optimize request routing given $\mathbf{r_{ij}}$**
3: Execute CORE BLOCK ▷ Steps {9 - 20}
4: $\mathbf{x_{ij}} \leftarrow$ Pareto front member with maximum profit
5: **Step 2: Optimize resource allocation given $\mathbf{x_{ij}}$**
6: Execute CORE BLOCK ▷ Steps {9 - 20}
7: $\mathbf{r_{ij}} \leftarrow$ Pareto front member with maximum profit
8: **end while**

9: **procedure Core Block**
10: Generate initial population —$\mathbf{x_{ij}}$[1] or $\mathbf{r_{ij}}$[2]
11: **for all** $i \in$ *generations* **do**
12: Run load flow[3]
13: Determine voltage stability index SI
14: Invoke constraint handling procedure
15: Perform environmental selection
16: Run hybrid recombination operation
17: Apply mutation
18: **end for**
19: Return Pareto front
20: **end procedure**

[1] Decision variable in request routing optimization. [2] Decision variable during resource allocation optimization. [3] May be performed by power grid and state information shared with the data center.

Figure 3.2: Evolutionary algorithm based higher level optimization approach

3.4.1 Constraints Handling

We employ a hybrid constraint handling approach that uses two approaches for two phases of the algorithm. We use self-adaptive penalty approach [79] for the request dispatch and constrained dominance [78] for the resource allocation optimization.

The self-adaptive penalty function approach [79] adaptively varies penalty depending upon the number of feasible solutions during each generation of evolution. First, when no feasible member exists, the scheme uses the violation magnitude to penalize infeasible individuals. Next, if feasible solutions are less, it applies a higher penalty on the infeasi-

ble solutions with a greater violation. Subsequently, as the feasible solutions increase in number, it penalizes solutions with poor objective value more severely.

The constrained dominance approach [78] uses a binary tournament to select solutions based on the constrained dominance. A solution s_i is said to constraint dominate another solution s_j, if any of the following conditions is true: first, solution s_i is feasible and s_j is not, second, solution s_i and s_j are both infeasible, but solution s_i has smaller constraint violation, and third, both solutions are feasible, but solution s_i dominates solution s_j.

3.4.2 Initial Population

The initial population impacts the convergence of an algorithm, and its size determines the size of the Pareto front. Diversity in initialization helps an algorithm to explore search space rigorously and evolve to the best solutions. For this work, we generate the initial population from a uniform distribution. The population includes 10% infeasible solutions. The remaining feasible solutions constitute two equal-sized groups. The first group, biased toward the first objective, comprise solutions with better revenue. In contrast, the second group includes solutions that produce the highest expenses. The initialization scheme is designed to promote diversity in the evolved solutions.

3.4.3 Environmental Selection

During each iteration, the algorithm evaluates the objective values and determines the fitness for each member of the current population. The fitness has two components, i.e., the domination strength or the frailty and the solution density. The frailty is a measure of the number of elements dominated by the solutions which dominate the solution under consideration, whereas density is a distance measure of a solution from its kth nearest neighbor. The fitness of the ith solution is as

$$fitness_i = \frac{1}{(frailty_i + density_i)} \tag{3.10}$$

The algorithm maintains two types of population, the current P and the elite population $\hat{P}$. At the start, the elite pool is empty. After current population members are assigned fitness, $|\hat{P}|$ nondominated solutions with the highest fitness are copied to the elite set. If the number of nondominated solutions are less than $|\hat{P}|$, the unfilled pool is filled with best-dominated solutions. As the population evolves, $\hat{P}$ is updated with best-nondominated solutions from the set $P \cup \hat{P}$. If the size of updated $\hat{P}$ exceeds $|\hat{P}|$, then the weak individuals are removed from the elite set using the truncation operator. The operator, while removing the weak member, considers the region's density where the solution resides. The solutions from most dense regions are removed first to enhance diversity in the Pareto front.

After filling the elite set, mating pairs are selected to undergo genetic operations, using the binary tournament. For this, two elite pool members are randomly drawn each time, their fitness values are compared, and the superior contestant is selected. The scheme chooses the fittest members of each generation. An individual participates in the tournament with probability $1/|\hat{P}|$.

3.4.4 Genetic Operations

Elite group members undergo two genetic operations. The first operation is a hybrid crossover that comprises single-point crossover [81] and simulated binary crossover [82] and next is the mutation.

In a single-point crossover, each pair swap their decision variables to the end of a chromosome, starting at a random index, thus producing two child solutions. Next, we apply the simulated binary crossover (SBX) [82] to newly created offspring. SBX demonstrates the best performance for problems with nonbinary decision variables, as is our case.

Mutation operation helps the evolutionary algorithms explore search space rigorously and avoid being stuck in a local optimum. In this work, we generate mutated individuals from a normal distribution whose mean is at the individual being mutated.

3.4.5 Solution Selection

During each iteration, multiple Pareto optimal solutions emerge as a Pareto front, as shown in Fig. 3.3. In the request assignment phase, Pareto fronts are sparse, indicating hard constraints, whereas, in the resource allocation phase, they are relatively dense, indicating more solutions comply with the constraints. A feasible solution with the highest profit is selected and used as an algorithm parameter for the subsequent phase. The selected solutions are updated if the increase in profit, from the algorithm's previous run, is more than a threshold. Finally, obtained feasible solutions in the form of the Pareto front are used as a request assignment schedule and resource allocation configuration for the cloud.

3.5 Performance Evaluation

We test the proposed algorithm's performance in a cloud computing system comprising five data centers with 500 servers. The data centers are connected to buses 2—6 of a smart grid represented by the IEEE-33 bus system [95]. Table 3.1 shows system simulation parameters along with the distributed generation in a given operation window. The load from other sources for buses with data centers is as per [95]. Next, we set the base electricity price C_b as same, i.e., 0.3, for all data centers to evaluate algorithm performance under real time

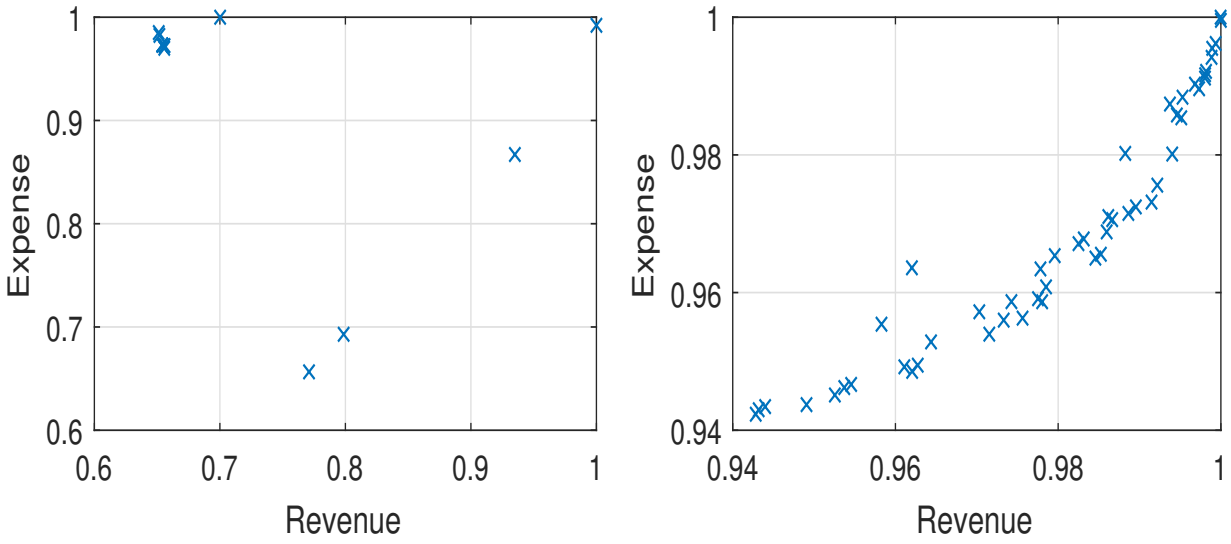

(a) Request dispatch **(b)** Resource allocation

Figure 3.3: Pareto fronts for two phases of algorithm

load dependent pricing specifically. We evaluate the algorithm at three levels of computing load, i.e., low, medium, and high. The system utilization (ρ) for these levels is set at $0.3, 0.6,$ and 0.9. The rate of request arrival λ in the cloud system is calculated from ρ as $\lambda = \rho \sum u_{ij}$.

3.5.1 Performance Comparison

In this section, we evaluate algorithm performance compared to the baseline approach which is an identical algorithm except that it is insensitive to energy prices. The baseline algorithm follows a fixed assignment schedule irrespective of the energy prices and only

Table 3.1: Simulation Parameters

Evolution parameters		**System parameters**	
Population size	50	$\bar{P}^s$	$U[0.5, 1]$
Generations	80	$\bar{P}^d$	$U[0.5, 1.5]$
Crossover Probability	0.75	μ	$U[1, 3]$
Mutation Probability	0.25	ζ	215
Distributed generation			
Bus	**P(pu)**	**Q(pu)**	
3	0.7381	0.6190	
18	0	0.0476	
33	0.1190	0.0476	

tries to optimize resources.

The first experiment investigates the impact of real time price changes on the cloud computing system's revenue and expenditure. As we can see from (3.7), system revenue is independent of the cost of the energy and is solely a function of requests serviced according to the SLA. Therefore, changing energy prices do not affect revenues. On the other hand, Fig. 3.4 shows a direct relationship between the energy price and cloud system expenses. As the energy price increase, the data center expenses increase as well. The results, Fig. 3.4, show that the proposed algorithm meets the objective of expense minimization much better than the baseline approach.

In the second case we analyzes the effectiveness of the proposed algorithm to maximize data center profit under dynamic pricing scenario in a bulk power network. We compare system profit for the proposed and the baseline algorithms with changes in power prices. The results are shown in Fig. 3.5. The analysis indicate a decrease in profit as the price of electricity increases due to increasing expenses. The proposed algorithm maximizes the profit better than the baseline as it shifts computing loads with the price changes to areas with lower power tariffs. On the other hand, the baseline approach that does not consider electricity in routing requests demonstrates a lower profit.

3.5.2 Voltage Stability

This experiment analyzes the impact of data center resource and request optimization on power network stability by investigating voltage stability index. The index is plotted in Fig. 3.6 for three solutions selected from two extremes and the middle of a Pareto front. The stability index in all cases is well below the unity value indicating that the algorithm meets network stability constraints during optimization.

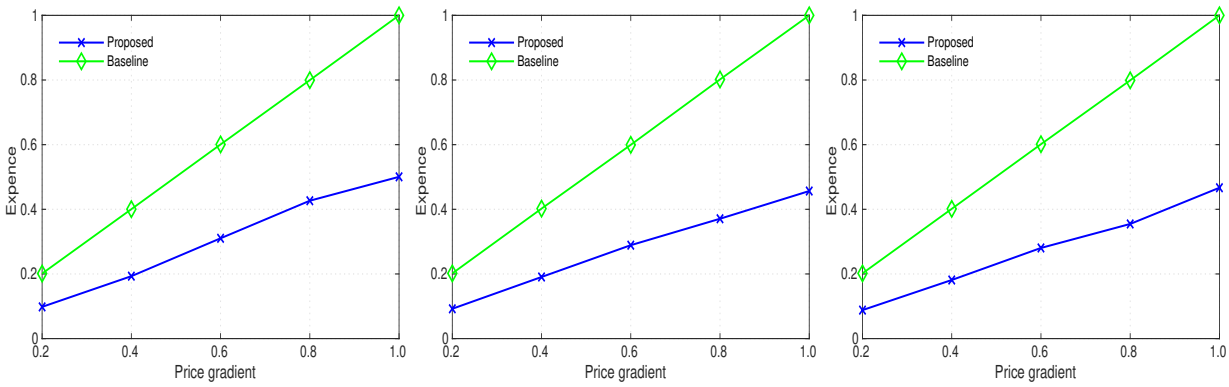

(a) Low load **(b)** Medium load **(c)** High load

Figure 3.4: Comparison of normalized expense of the proposed and baseline approaches under low, medium, and high load conditions

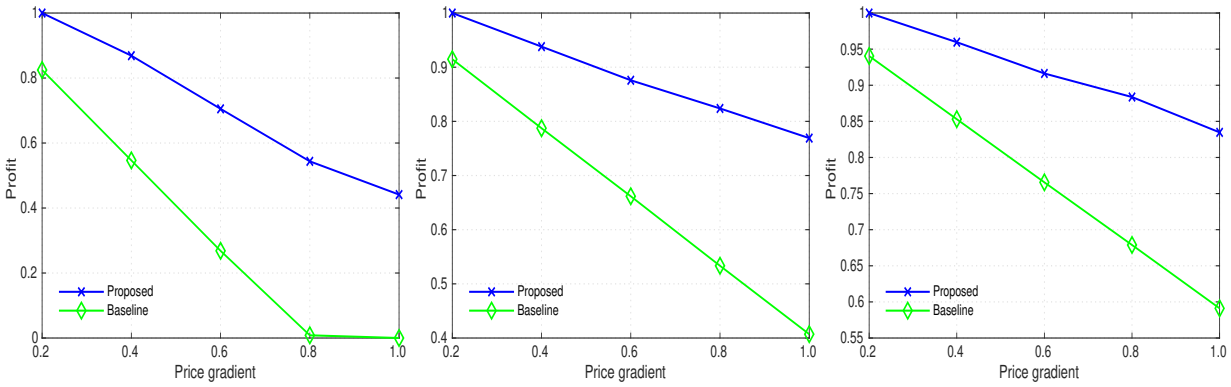

(a) Low load **(b)** Medium load **(c)** High load

Figure 3.5: Comparison of normalized profit of the proposed and baseline approaches under low, medium, and high load conditions

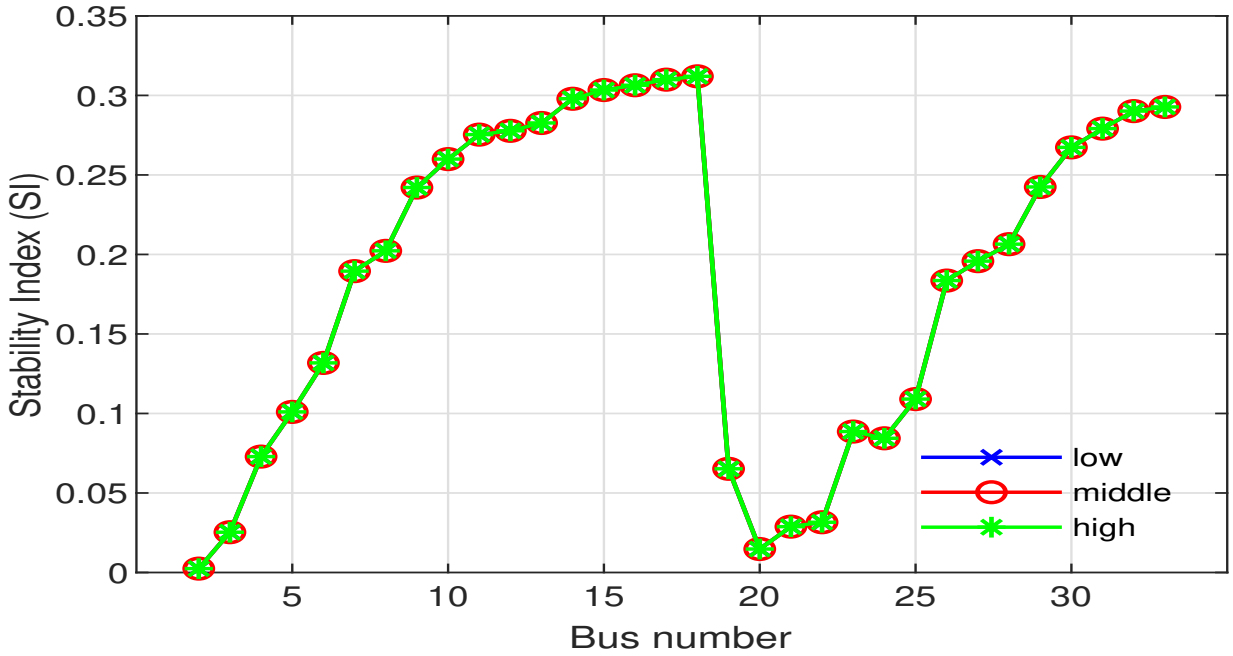

Figure 3.6: Voltage stability index for three Pareto optimal solutions from two extremes and middle of a Pareto front.

3.5.3 Voltage Profile

This experiment analyses the impact of data center optimization on the power networks' bus voltage profile. We select three representative solutions from two extremes and the middle of a Pareto front. The extremes represent solutions with lower revenue and higher expenses and vice versa. In all cases, as shown in Fig. 3.7, the bus voltages are closer to unity, which indicates that the data center optimization follows power network constraints and does not hamper network stability.

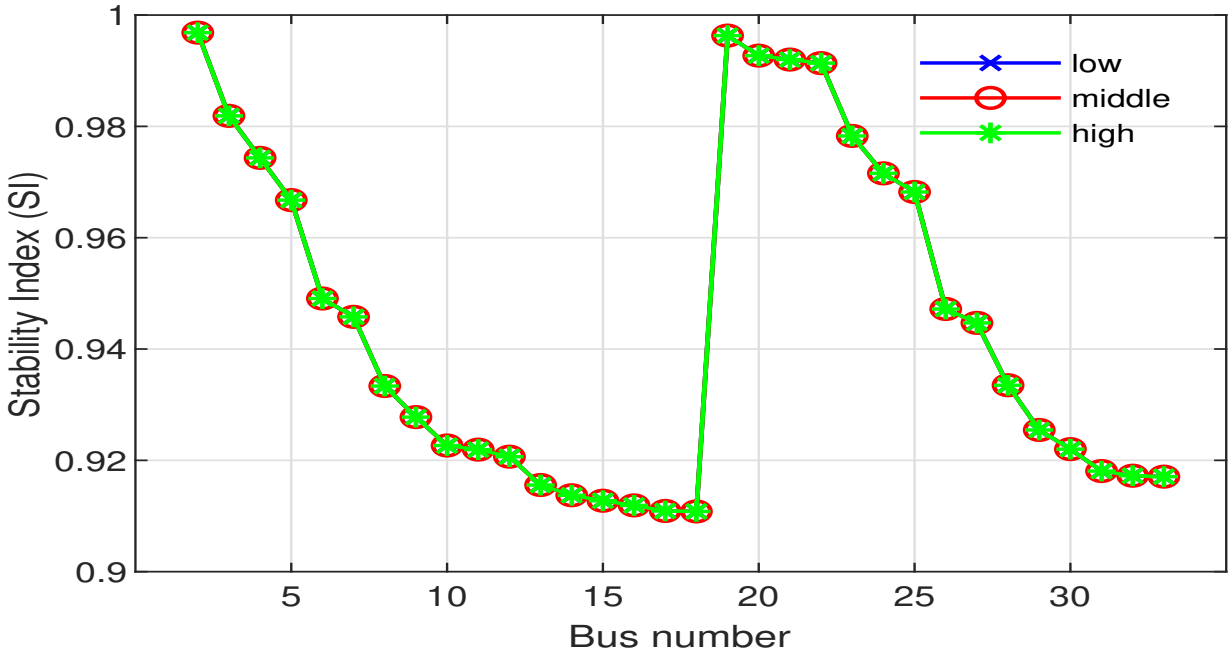

Figure 3.7: Voltage profile for three Pareto optimal solutions from the initial, middle and end parts of the front.

3.6 Conclusion

Power network state aware optimization of resource allocation and request routing in geo-distributed data centers maximizes data center profit. It also enables the power grid to reduce operation costs, integrate renewable sources, and stabilize power supply. An integrated approach that considers energy prices, grid stability, server temperature, and QoS is investigated. The proposed evolutionary optimization based multi-level algorithm simultaneously maximizes data center revenue and minimizes expenses, thus achieving higher profit. Simulation results prove that the proposed technique is effective; it maintains a higher profit over a broad range of price variations and cloud utilization levels. We intend to enhance the system model by incorporating the deactivation of the underutilized servers in the future.

Chapter 4

Optimizing Energy Donation for Service Restoration in a Power Distribution System

Natural hazards and technical malfunctions often cause widespread outages of power networks that can affect the communities and critical infrastructures. Microgrids with distributed power generation and backup storage can help mitigate some of these devastating effects. However, not many communities and infrastructures are equipped with energy storage or alternative power generation mechanisms. In an hour of need, microgrids may help needy neighbors or critical communities, such as hospitals, by donating or trading surplus capacity. Energy donation in a smart grid is a viable and highly effective restoration option to mitigate the effects of a disaster. In this chapter, we propose a pioneering framework for enabling energy donation in a smart grid during a crisis when the main supply is cut off. The proposed algorithm allocates energy using rationing and back-filling approaches to utilize the limited supply optimally. It does so by catering to the load critically and users' historical contribution during restoration. The proposed algorithm is based on an evolutionary optimization technique that maximizes social welfare and minimizes losses while satisfying the resource and the network constraints. The extensive simulation results ascertain the effectiveness of the proposed approach across a myriad of system parameters.

4.1 Introduction

Climate change and the resultant extreme weather events have a significant impact on power systems. The power grid, designed to operate under stable weather conditions, is exceedingly vulnerable to severe weather. Hurricanes with powerful winds and rains can be devastating, while extremes of heat or cold result in overloading the systems; hence, they cause equipment failures. Likewise, snowstorms and wildfires are the other major causes

of power system interruptions. A more recent example of weather-related interruptions is Public Safety Power Shut-off (PSPS) [96], where power is turned off for public safety when heightened fire risk exists. This intentional power interruption in California affected 600,000 users in 2019 and caused estimated losses of $2.5 billion to the economy [97]. The phenomenon may impact communities beyond the high fire-prone neighborhoods if they rely upon a power line that runs through an area experiencing gusty winds and dry conditions. In addition, weather events pose long-term risks to power systems' operation as the hardening of infrastructure is likely to take years and is often cost-prohibitive [98].

In the aftermath of a disaster, the power distribution system splits into islands that generally have an intact network but no connection to the central generation. However, a limited supply from distributed energy resources (DERs) in the form of microgrids may be available that the grid can use for speedier localized restoration [45]. Given a disaster, the local power supply often falls short of demand, so the operators prioritize restoring the critical loads. Naturally, the hospitals and public safety installations come first, whereas ordinary neighborhoods get the lowest precedence. Still, extended power outages may have life-threatening consequences in some situations. In this context, to render relief, the grid must adopt an energy allocation policy that maximizes coverage with the limited supply, prioritizes restoration of the critical load, and is fair to incentivize participants successfully. It must also consider resource and distribution system constraints to cater to a highly unstable post-disaster distribution network.

A disaster may encourage or invigorate prosocial behavior in a community, thereby increasing a collective desire to assist those in need [99]. The grid can tap this emphatic sentiment to crowdsource energy for restoration. MGs with surplus capacity may share their excess energy either by donating or trading. The energy can be utilized to restore service to the critical load and provide relief to those without alternate power arrangements. Thus, energy donation in the smart grid is a viable and highly effective option for mitigating disaster effects. We propose a novel approach that enables and optimizes energy donation. Essentially, our approach optimally uses limited energy to restore critical load and achieve social welfare while building upon the economic and market aspects fairly and equitably. The work, including the problem formulation and solution, is novel and unprecedented.

In a smart grid, energy sharing or trading takes place directly among peers —users, houses, MGs. For example, [15, 16, 36–38] proposed direct energy sharing among multi-microgrids, [39] studied peer-to-peer energy trading among users within a microgrid, and [40–42] explored sharing of energy among neighbouring homes. In other cases, the sharing or trading are facilitated by a central entity, e.g., a DSO [15, 16, 43]. Here, the controller manages energy allocation and transactions from DERs to loads thereby avoiding problem caused by uncoordinated energy exchanges [44]. However, many contemporary works have overlooked critical aspects of restoration in both scenarios, particularly when supply is limited. For example, [15,16] ignored distribution systems' operational constraints so their

solution may destabilize distribution system. Furthermore, neither works used a pricing mechanism, so all transactions carry the same value irrespective of supply-demand conditions. It adversely affects the fairness and thus lowers the incentive for the participants. In contrast, Kim *et al.* [36] handled power balance and network constraints but did not address prioritized allocation. Another issue across these schemes is their sole focus on the participants' benefit rather than the collective interest of the community affected by a disaster. For example, in [40–42] houses participate in trading as long as the payoff is significant; otherwise, they defect.

Similarly, traditional restoration approaches become ineffective when supply from the central generation is not available [45]. So, a body of research exists that have studied DER-based restoration after a high impact event [45–50]. For example, Xu *et al.* [46] utilized microgrids' resources to restore critical loads when utility power is interrupted. They form a minimum length restoration tree rooted at the closest MG that can provide sufficient energy to restore a load group. Similarly, [47] adopted a two-level restoration approach in that they establish restoration paths followed by restoration through solving a linear program. An identical approach in [48] used a spanning tree to divide the distribution system into microgrids and restore the critical loads utilizing locally available combined heat and power units. Authors' prior work [43] presented a restoration technique using energy crowdsourced through donation or trade. We formalize and extend the underlying donation framework in this manuscript.

In contrast to these notable efforts, the proposed scheme is highly flexible and comprehensive. It offers multiple energy allocation criteria, uses a valuation system to appraise energy transactions according to the supply-demand gap, and determines user contribution based on allocation and energy value. In addition, the scheme tries to maximize coverage beyond critical loads to provide relief to the maximum users. Most importantly, it captures resource and network constraints into the allocation process to address stability issues prevalent in post-disaster networks.

The chapter proposes an energy donation framework for service restoration in a post-disaster distribution system. We formulate energy donation as a multi-objective constrained optimization problem and devise an evolutionary technique-based algorithm to solve it. The proposed approach utilizes the Strength Pareto Evolutionary Algorithm (SPEA-II) [63] as the base framework and adapts it to devise an algorithm. The technique finds Pareto optimal solutions for energy allocation to microgrids against their demand considering service priorities, contribution, and system objectives.

The proposed algorithm maximizes social welfare and minimizes losses while satisfying the resource and power network constraints. Specifically, the chapter's key contributions are as follows: First, we design an effective algorithm that uses an evolutionary technique to optimize energy donation in an islanded post-disaster distribution network with multi microgrids. Second, the algorithm embeds an allocation technique that uses rationing and

back-filling strategies to cater to the supply-demand gap, maximize coverage, and prioritized allocation considering load criticality and historical contribution of a microgrid. Third, we propose a commodity valuation-driven contribution mechanism for appraising energy transactions based on energy availability through donation and trade processes. Fourth, the proposed algorithm includes a problem-specific operator to partially repair infeasible solutions in recombination and mutation stages of the evolution. The framework is fair over an extended operation horizon. Finally, the chapter includes extensive simulation results that ascertain the effectiveness of the proposed approach.

The rest of the chapter is organized as follows: Section II presents the problem formulation and Section III elaborates on the design of the proposed optimization scheme and its operation. Performance evaluation and analysis of results are presented in section IV. Finally, section V concludes the chapter and highlights future work directions.

4.2 Problem Formulation

The microgrids with surplus supply donate or trade electricity to help needy neighbors. The energy donors make charitable donations or may receive some benefits in return. The rewards may take different forms, e.g., an increased reputation for getting subsidized or priority services from the local community or the grid. In another scenario, a microgrid may trade its surplus with the grid for later use once the main grid restores. The framework is fair over an extended operation horizon. Next, we specify assumptions and give the formulation of the donation problem.

4.2.1 Network Model

We consider a radial distribution system represented as graph $\mathcal{G}(\mathcal{W}, \mathcal{E})$ where $\mathcal{W}$ is the set of nodes and $\mathcal{E}$ is the set of branches. The distribution system operates in island mode with most of the infrastructure intact but no connection to the central generation. The network comprises $\mathcal{N}$ microgrids interconnected by the branches $\mathcal{E}$. MGs have local backup storage and generation from solar, wind, and limited supply from a small brown energy source. We assume a system controller or donation coordinator, which, together with local microgrid controllers, enables a two-way exchange of electricity. Moreover, the system controller matches the peers using relevant techniques considering voltage issues at local level [100, 101]. MGs have data on their historical demand and locally available energy. The layout of the donation network is given in Fig. 4.1. The systems' operation horizon $\mathcal{T}$ comprises n slots normalized to unit time so that we can use power and energy interchangeably.

Let g_i and d_i be the local generation and demand of ith MG during a given operation slot. A microgrid donates or trades energy if $g_i > d_i$ or borrows it if $g_i < d_i$. Let $\mathcal{N}^s$ be the

group of MGs with surplus and $\mathcal{N}^c$ be the group with deficient supply, then, for a given slot, the relationship $\emptyset = \mathcal{N}^s \cap \mathcal{N}^c$ holds. The set $\mathcal{N}^s$ comprise the donors $\mathcal{N}^{sd}$ and $\mathcal{N}^{st}$ traders. In each operation window, based on their local supply and individual demand, MGs pledge the amount of energy they can provide to the donation controller or publish their demand if they require energy to meet their needs.

We consider two kinds of energy contributions to the system: first, a philanthropic donation E_d and second, energy supply available through trade E_t. The net amount of energy available for exchange during jth window is as follow:

$$E_j^{net} = Ed_j + Et_j \tag{4.1}$$

where $Ed_j := \sum_{i \in \mathcal{N}^{sd}} Ed_{ij}$ and $Et_j := \sum_{i \in \mathcal{N}^{st}} Et_{ij}$ are the energy donation or energy traded by ith microgrid during jth operation window, respectively.

4.2.2 Commodity Valuation and User Contribution

The framework adopts a commodity valuation based system to determine the intrinsic value of an energy transaction [15, 102]. The energy value depends on the supply conditions, i.e., net pledged energy from all microgrids in an operation window. Let v_d and v_t be the commodity values for an energy donation and trade transactions, respectively. The value v_d may be zero or some value mutually decided by the donor and the utility, but it is always less than v_t. Given the two commodity values and the amount of energy available,

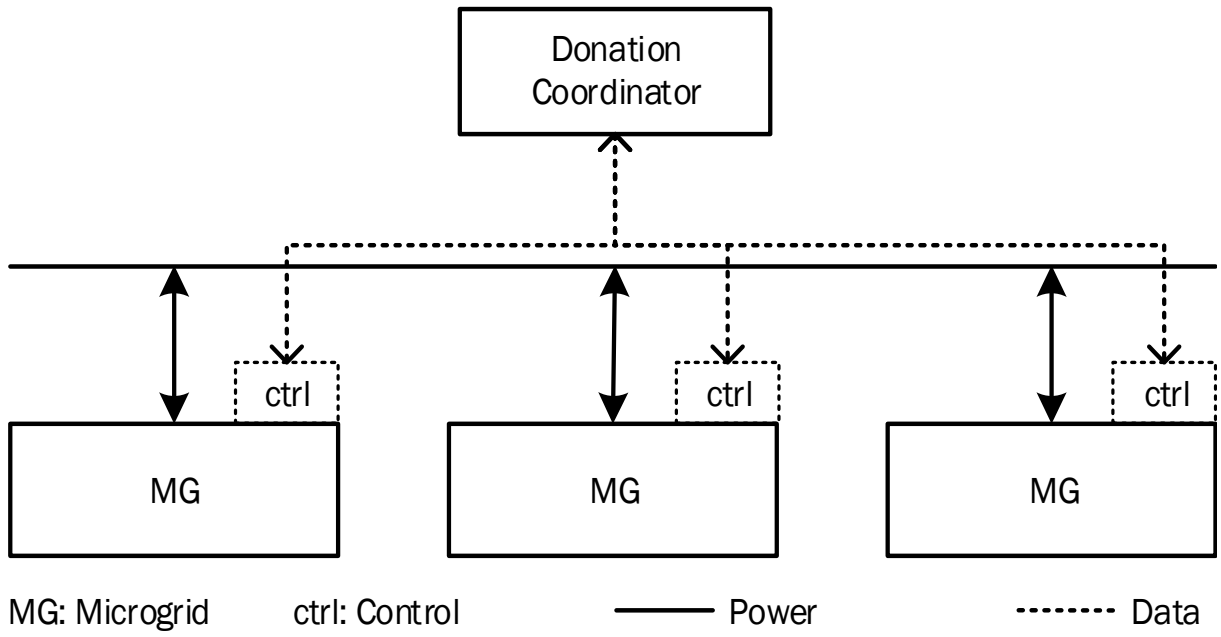

Figure 4.1: Energy donation network model.

we define a new rationalized value $\mathcal{V}_j^{rat}$ for each window as follow:

$$\mathcal{V}_j^{rat} = \frac{v_d Ed_j + v_t Et_j}{E_j^{net}} \text{ s.t. } v_d \leq \mathcal{V}_j^{rat} \leq v_t \tag{4.2}$$

Next, the historic contribution depends on two factors, i.e., the amount of energy exchanged and commodity value in a given time slot. The historical contribution c_i of an MG is given as:

$$c_i = \sum_{j \in \mathcal{T}} sgn(\alpha) \mathcal{V}_j^{rat} E_{ij} \ \ \forall \alpha \in \{1, 0, -1\} \ \& \ i \in \mathcal{N} \tag{4.3}$$

where E_{ij} is the energy transaction, $\mathcal{T}$ is the operation horizon across which the donation controller maintains contribution data. The parameter $\alpha := \{1,\ 0,\ -1\}$ indicates the type of transaction namely trade, donation, or borrowing, respectively.

The donors' contribution value may be zero across the operation horizon, whereas it accumulates for the trading microgrids. The grid compensates them once they require energy. When a microgrid receives energy, its reputation reduces correspondingly in relation to the amount of energy and the commodity value. A reduced reputation lowers future allocation priority, discouraging MGs from cheating by artificially raising demand in a given operation slot.

4.2.3 Energy Allocation

This work provides a flexible mechanism to allocate energy to a demanding microgrid based on the criticality of load they serve, historical contribution, or a composite index based on their combination.

From the criticality point of view, the load may have varying impacts on the functioning of public services, so they are assigned different service priorities. For example, a hospital located in the area may need the energy to take care of the patients, a pumping station to supply water to households, and a gas station to provide fuel to the rescuers. Moreover, the duration of being without an electric supply is another important factor in determining the need for a microgrid. For example, suppose an area is without supply for an extended period. Then, the people may drain out batteries of their communication devices and even medical aids, which may have life-threatening consequences in an emergency. Therefore, the load criticality requires due consideration in energy allocation. On the other hand, the faithful members of the system need compensation in the hour of need; therefore, the donation framework accounts for the historical contribution along with the load criticality. For implementing load priority or contribution-aware allocation, the system controller uses the rationing approach.

Given a crisis, generation falls short of the demand thus the energy allocation in this situation is a bankruptcy case. The coordinator rations the resource among the demanding

microgrids (agents) each with an individual demand (claim) and priority (weight) of the allocation [103]. Generalized rationing problem is given as

$$\begin{aligned} &(\mathcal{N}, E_j^{net}, \vec{\mathcal{D}}) \text{ s.t.} \\ &0 \leq E_j^{net} \leq \sum d_i \quad \text{and} \quad 0 \leq d_i \; \forall \; i \in \mathcal{N} \end{aligned} \tag{4.4}$$

where $\mathcal{N}$ is the number of agents, E_j^{net} is the energy resource to be distributed, and $\vec{\mathcal{D}}$ is the vector of claims. The solution to the problem is vector of shares $\vec{Y}$ of each agent such that

$$\sum y_i = E_j^{net} \quad \text{and} \quad y_i \leq d_i \; \forall \; i \in \mathcal{N} \tag{4.5}$$

where y_i is the individual share, an agent gets against its demand d_i.

For allocation, the system solves the rationing problem in two steps. In the first phase, it uses the uniform gains rationing method [103]. Particularly, it employs the weighted version of the method to prioritize servicing critical loads and recompense faithful subscribers. The weighted rationing assigns more significant weight to a user with a higher priority of claim in contrast to the uniform gains where equals get an equal share. The formulation for the first step is described next.

Given power network consisting of $\mathcal{N}$ microgrids with individual demand $\vec{\mathcal{D}} := \{d_1, d_2, d_3, \ldots, d_{\mathcal{N}}\}$[1], historical contribution $\vec{C} := \{c_1, c_2, c_3, \ldots, c_{\mathcal{N}}\}$, and service priority $\vec{P} := \{p_1, p_2, p_3, \ldots, p_{\mathcal{N}}\}$. We define rationing index $\mathcal{R}_i$ as follows

$$\mathcal{R}_i = \begin{cases} \dfrac{p_i}{\sum_{i \in \mathcal{N}} p_i} & \text{if } \psi = 1 \\ \dfrac{c_i}{\sum_{i \in \mathcal{N}} c_i} & \text{if } \psi = 2 \\ \dfrac{h_i}{\sum_{i \in \mathcal{N}} h_i} & otherwise \end{cases} \tag{4.6}$$

where ψ is the rationing basis with its values $\{1,\ 2,\ otherwise\}$ representing load criticality, user contribution, and their combination, respectively. The parameter h_i defined as $h_i := \gamma p_i + (1-\gamma)c_i$ forms the hybrid allocation basis. Here γ is used as the weighting factor for contribution and priority. Next, using $\mathcal{R}_i$ and available energy E_j^{net}, we solve a variation of the weighted gains problem in first step as follows

$$e_i^w = f^w(\mathcal{N}, E_j^{net}, \vec{\mathcal{D}}) = min\{\mathcal{R}_i E_j^{net}, d_i\} \tag{4.7}$$

where f^w is the weighted gains rationing function and $\mathcal{R}_i$ the represents the weight assigned to a claim of a microgrid.

[1]For simplicity, we assume $d_i = 0 \;\; \forall i \in \mathcal{N}$ if $g_i > d_i$

In second step, to complete the rationing process, the system allocates the leftover energy $E_j^{res} := E_j^{net} - \sum_{i \in \mathcal{N}} e_i^w$ using optimization algorithm considering the objective performance, the residual demand $d_i^r := d_i - e_i^w$, and constraints compliance. The second phase rationing is given

$$e_i^o = f^o(N, E_j^{res}, \vec{\mathcal{D}}^r) \tag{4.8}$$

where f^o is the optimization function. Finally, energy allocation E_i to ith MG, is as follows

$$E_i = min\{e_i^w + e_i^o, d_i\} \text{ s.t.} \sum_{i \in \mathcal{N}} E_i + \mathcal{L}_i = E_j^{net} \tag{4.9}$$

where $\mathcal{L}_i$ is the loss incurred to provide energy E_i to a given MG. The allocated energy comprises two components, i.e., e_i^w allocated in weighted rationing step and e_i^o allocated through optimized rationing by the optimization algorithm specified in section 4.3.

4.2.4 Social Welfare

Given limited supply-demand scenario, we take the aggregation based resource allocation approach where small gains for maximum individuals determine overall good of the system [104]. The system allocates energy to meet users' demand. The unmet demand adds to

Algorithm: Energy Allocation

Require: Load criticality $\vec{P}$, historical contribution $\vec{C}$, user demand $\vec{\mathcal{D}}$, available supply E_j^{net} and system parameters
Ensure: Energy allocation $\vec{\mathcal{E}} := \{e_i\}\ \forall i \in \mathcal{N}$

1:
2: **if** $E_t^{net} - \sum_{i \in \mathcal{N}} d_i \leq 0$ **then**
3: Determine rationing index $\mathcal{R}_i$ (4.6)
4: Solve weighted rationing problem (4.7)
5: Determine residual energy E_j^{res} and demand d_i^r
6: **if** E_j^{res} & $d_i^r > 0$ **then**
7: Solve optimal rationing problem (4.8)
8: **end if**
9: Back-fill allocation (4.9)
10: **end if**

Figure 4.2: Energy allocation based on load criticality, users' historical contribution, or both using rationing and back-filling.

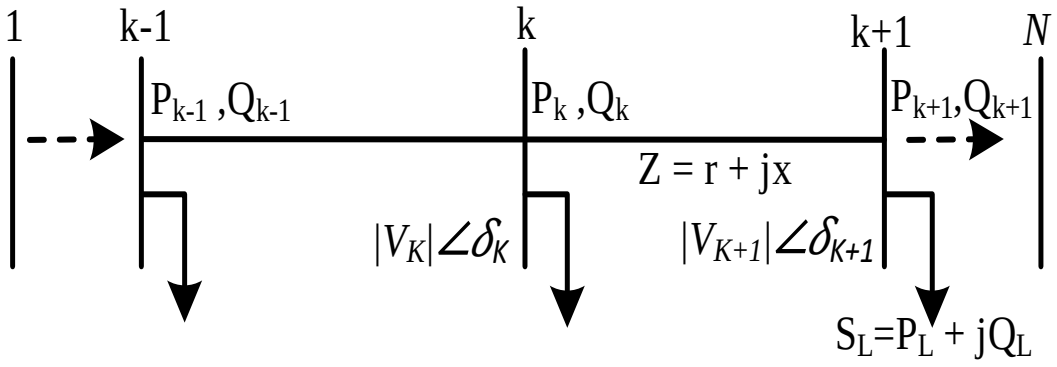

(a) Single line diagram

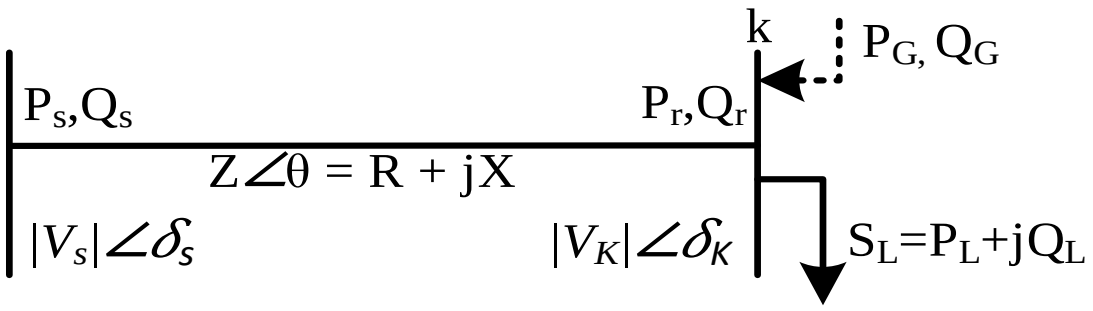

(b) Two bus network

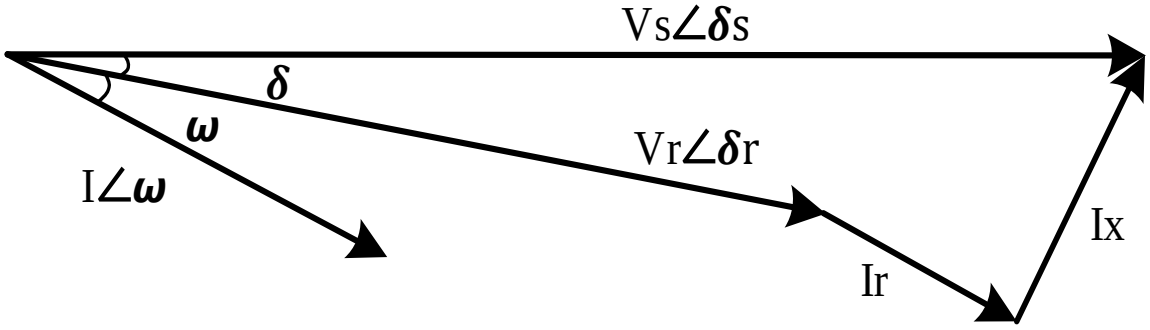

(c) Phasor diagram

Figure 4.3: shows a single line diagram and two bus equivalent of a radial distribution system. Next is the phasor diagram of two bus network.

the dissatisfaction. A utility function can represent users' satisfaction and aggregation of the individual utility determines the social welfare achieved with limited energy. The donation coordinator tries to maximize social welfare thus its objective can be modeled as

an optimization problem, as follows:

$$\begin{aligned} & max \sum_{i \in \mathcal{N}^c} U(E_i) \\ & \text{subject to:} \\ & e^w \leq E_i \leq d_i \\ & \sum_{i \in \mathcal{N}^c} E_i + \mathcal{L}_i \leq E_j^{net} \end{aligned} \tag{4.10}$$

Where $U_i(E_i)$ is the utility achieved by ith user through allocated energy E_i. The objective has two constraints: the first restricts the coordinator to allocate energy more than the user demand, whereas the second ensures that the net allocation is at the most equal to the available energy.

User satisfaction follows the law of diminishing utility. Therefore, at a certain point, the satisfaction achieved with allocating additional units of electricity results in a smaller increase in user satisfaction. In such a case, the $U(E_i)$ takes the form of a logarithmic utility function [105] and is given as follows:

$$U(E_i) = \log(1 + \frac{E_i}{d_i}) \tag{4.11}$$

The utility function has the following inherent features: 1) The function is concave on allocated energy. 2) Follows the law of marginal utility, so the rate of satisfaction decreases with the subsequent allocation of energy. 3) $U(E_i)$ is a non-negative real-valued function, as the satisfaction is never negative. 4) The satisfaction increases with an increase in allocated energy which is a function of users' priority or contribution and the system objectives.

Next, transporting the energy to the users incurs losses that depend on allocation and network conditions. The system runs load flow to establish network parameters and determine losses for different MGs. Minimization of losses becomes critical in the backdrop of limited supply.

4.2.5 Power Flow

The power flows in the network are determined using a set of recursive power flow equations [106]. We use a single line diagram of a radial distribution system as in Fig. 4.3a to illustrate the equations. We represent line impedance as $Z = r + jx$ and the load as $P_L + jQ_L$. The real power, reactive power, and the voltage at the end of the branch

connecting node k and $k+1$ are as follows:

$$\begin{aligned} P_{k+1} &= P_k - \frac{P_k^2 + Q_k^2}{V_k^2} Z - P_{Lk+1} \\ Q_{k+1} &= Q_k - \frac{P_k^2 + Q_k^2}{V_k^2} Z - Q_{Lk+1} \\ V_{k+1}^2 &= V_k^2 - 2(r_k P_k^2 + x_k Q_k^2) + (r_k^2 + x_k^2) \frac{P_k^2 + Q_k^2}{V_k^2} \end{aligned} \tag{4.12}$$

where P_k, Q_k are the real and reactive power at the receiving end of the branch $k,\ k+1$, V_k is voltage magnitude at node k whereas P_{Lk+1}, Q_{Lk+1} are the active and reactive load connected to bus $K+1$ and $\frac{P_k^2+Q_k^2}{V_k^2} Z$ is the loss on the branch.

4.2.6 Distribution Losses

The distribution network has high resistance to reactance (R/X) branch ratios which cause higher losses. Moreover, lack of voltage regulation and poor feeder configurations may further worsen the situation. More importantly, minimizing losses is essential due to supply scarcity in a post-disaster distribution system. Therefore, the donation controller, while allocating the energy, tries to minimize network losses, given as follow

$$\mathcal{L}_k = \frac{P_k^2 + jQ_k^2}{|V_k|^2} R_k \ \ \forall k \in \mathcal{W} \tag{4.13}$$

4.2.7 Voltage Stability

Excessive losses increase post-disaster distribution networks' vulnerability to voltage collapses. A major collapse can happen if the load overshoots permissible limits and the network does not compensate for the real and reactive power. The utilities use the voltage stability index to monitor and compensate for real and reactive power.

Several recent works have analyzed voltage instability in distribution systems and proposed approaches for determining network stability indices [91, 93, 94, 107, 108]. For this work, we use the index proposed in [94]; the method is suitable for an active distribution network as it caters to the distributed generation and the voltage angle variations. To illustrate formulation of the voltage stability index, we use a two bus equivalent, Fig. 4.3b, and phasor diagram, Fig. 4.3c, of the radial distribution system shown in Fig. 4.3a. For a simple two bus network, the losses are:

$$P + jQ = I^2(r + jx) \tag{4.14}$$

and the current is given as:

$$I = \frac{V_s \angle \delta_s - V_r \angle \delta_r}{r + jx} \tag{4.15}$$

where

$$\begin{aligned} V_s\angle\delta_s &= V_s(Cos\delta_s + jSin\delta_s) \\ V_r\angle\delta_r &= V_r(Cos\delta_r + jSin\delta_r) \end{aligned} \tag{4.16}$$

from (4.14) and (4.15), we have

$$(V_s\angle\delta_s - V_r\angle\delta_r)^2 = (P + jQ)(r + jx) \tag{4.17}$$

The complex power at the receiving end of the bus,

$$S_L = V_r I_r^* \tag{4.18}$$

$$\overline{V_r} = V_s - \overline{I_r Z} \tag{4.19}$$

where

$$\overline{I_r} = \frac{P_L - jQ_L}{V_r^*} \tag{4.20}$$

with power compensation from DG, we re-write (4.20)

$$\overline{I_r} = \frac{(P_L - P_G) - j(Q_L - Q_G)}{V_r^*} \tag{4.21}$$

From above we can drive following relationship for the real and reactive power:

$$P_L - P_G = \frac{|V_r||V_s|}{V_r^*}Cos(\theta - \delta_s + \delta_r) - \frac{|V_s|^2}{Z}Cos\theta \tag{4.22}$$

$$Q_L - Q_G = \frac{|V_r||V_s|}{V_r^*}Sin(\theta - \delta_s + \delta_r) - \frac{|V_s|^2}{Z}Sin\theta \tag{4.23}$$

From (4.22), we get

$$|V_r|^2 - \frac{|V_r||V_s|}{V_r^*}Cos(\theta - \delta) + \frac{Z(P_L - P_G)}{Cos(\theta)} = 0 \tag{4.24}$$

where $\delta = \delta_s - \delta_r$ and θ is the impedance angle. The equation (4.24) is quadratic and for stable node voltages, it should have real roots, i.e. discriminant $B^2 - 4AC > 0$. The voltage stability index for a generalized system with $\mathcal{N}$ buses is given as as follows:

$$SI = \frac{4r_{ij}(P_L - P_G)}{[|V_i|Cos(\theta - \delta)]^2} \leq 1 \; \forall i, j \in \mathcal{W} \tag{4.25}$$

where r_{ij} is the effective line resistance between nodes i & j and V_i is the sending end node voltage. During optimization, after allocating energy, the algorithm determines the SI value for every bus. If the index approaches to unity, it sheds some load or in other words reduces allocation and re-evaluates the stability.

4.2.8 Optimization Objectives

During the second phase rationing (4.8), the fundamental goal of the donation coordinator is to optimally allocate residual energy to fully or partially restore user loads and thus mitigate the effects of a disaster. The realization happens in the form of two objectives, i.e., achieving maximum social welfare measured in terms of users' satisfaction or minimize unserviced load and minimize the losses. Besides, the framework incorporates resource and network constraints for stable distribution system operation. Combining the two objectives (4.10) and (4.13), the optimization problem is given as:

$$
\begin{aligned}
& max \sum_{i \in \mathcal{N}^c} U(E_i) \\
& min \sum_{i \in \mathcal{W}} \mathcal{L}_i \\
& \text{subject to:} \\
& e^w \leq E_i \leq d_i \ \ \forall i \in \mathcal{N}^c \\
& \sum_{i \in \mathcal{N}^c} E_i + \mathcal{L}_i \leq E_j^{net} \\
& V_{min} \leq V_i \leq V_{max} \ \ \forall i \in \mathcal{W} \\
& SI_i \leq 1 \ \ \forall i \in W
\end{aligned}
\tag{4.26}
$$

As the system tries to increase welfare by increasing allocated energy to users against demand, the distribution losses also increase. Therefore, both objectives are conflicting; in this scenario, the notion of optimality transforms into Pareto-Optimality.

4.3 Proposed Solution

The proposed solution is an evolutionary algorithm based upon a higher-level heuristic, as shown in Fig. 4.4. The algorithm starts with solving the weighted rationing problem; next, it generates the initial population and runs power flow analysis to assess the impact of the generated solutions on network operations. Then, the evolution continues until the maximum generation limit reaches.

The optimization problem (4.26) is a multi-objective-constrained optimization case with conflicting objectives—maximization of welfare and minimization of loss. A constrained

multi-objective problem is mathematically represented as follows:

$$\begin{aligned}
&\min\ f_i(x) = f_i(x_1, x_2, ..., x_n) \quad \forall i \in 1, 2, ..., p \\
&\text{subject to:} \\
&g_j(x) = g_j(x_1, x_2, ..., x_n) \leq 0 \quad \forall j \in 1, 2, ..., q \\
&h_j(x) = h_j(x_1, x_2, ..., x_n) = 0 \quad \forall j \in q+1, 2, ..., m \\
&x_k^{min} \leq x_k \leq x_k^{max} \qquad k \in 1, ..., n
\end{aligned} \tag{4.27}$$

The formulation (4.27) involves p objective functions, $f_i(x)$, defined over an n dimensional search space R^n with upper and lower bounds given by x_k^{min} and x_k^{max}. The objectives, may be conflicting, are simultaneously optimized subject to q inequality and $m-q$ equality constraints. In (4.27), $g_j(x)$ and $h_j(x)$ are jth inequality and equality constraints, respectively. The constraints restrict the solutions to the feasible regions.

For an optimization problem with multiple conflicting objectives, the optimization transforms into Pareto optimality that is defined based on the dominance relationship between feasible solutions. For example, given two solutions, x_i and x_j in a feasible design space S, the dominance relationship is as follow:

$$\begin{aligned}
&x_i \preceq x_j \text{ iff} \\
&f_i(x_i) \leq f_i(x_j) \quad \text{for } i \in 1, 2, ..., p \\
&f_i(x_i) < f_i(x_j) \quad \text{for at least one } i \in 1, 2, ..., p
\end{aligned} \tag{4.28}$$

So, solution x_i is said to dominate solution x_j if x_i is no worst than x_j in all objectives and solution x_i is better than x_j in at least one objective. Such non-dominated solutions in a feasible space are called Pareto optimal. In other words, for x_i to be Pareto optimal point, no other point exists in the feasible design space S that improves at least one objective function while keeping others unchanged. The non-dominated solutions evolve in the form of Pareto fronts (PF), as in Fig. 4.12.

The basis of the proposed algorithm is built on the principles of a multi-objective evolutionary optimization algorithm called SPEA-II [63]. SPEA-II has been reported to be effective in a diverse set of problems. It operates on a set of initial candidate solutions iteratively, applying natural selection based on fitness, removing weak members, and introducing randomness through mutation, resulting in gradual evolution. The fitness assignment function guides the selection operation, and the genetic operations are used to produce new offspring. The base framework of SPEA-II, including initial population selection, the fitness assignment, and the genetic operations, must be adapted according to the nature of the problem. More importantly, the framework does not have a constraint handling mechanism, but constraint handling is fundamental for most practical problems. Therefore, the proposed algorithm is not a direct SPEA-based technique. Instead, ours is a higher-level algorithm that systematically employs SPEA-II to determine optimization.

Besides, the SPEA-II component, with its parameters and evolution process, is designed with several problem-specific steps, including constraints handling approach, techniques for determining the initial population of the solutions, and genetic operators specific to this problem. The main steps of the proposed technique are given in Fig. 4.4. We describe these algorithmic components in the following sections.

4.3.1 Constraints Handling

The donation problem has both equality and inequality constraints. The bounds on the decision variables take the form $0 \leq E_i \leq d_i$ and are different for each element, which contrasts with the box constraint, where all features of a chromosome have the same upper and lower bounds. Therefore, due to the equality constraint and the varying bounds, the probability of feasible solutions is very low, making constraint handling a challenging task. In this work, we adopt the constraint dominance [78] approach to handle constraints. The method is widely used because of its performance and simplicity.

The constraint dominance algorithm uses a constrained binary tournament to select a solution based on its dominance status, i.e., a solution s_i is said to constraint dominate solution s_j if any of the following conditions are true: first, s_i is feasible and s_j is not, second, both solutions are infeasible, but s_i has smaller constraints violation. Third, both are feasible, but s_i dominates s_j.

4.3.2 Initial Population

The composition of the initial population impacts the diversity of solutions, the size of the Pareto front, and algorithm convergence, especially in constrained optimization problems. For this work, the initial population includes 20% infeasible solutions [80], while the remaining comprises two equal-sized sets of feasible individuals. The solutions in the first group are biased towards the first objective, thus produce higher welfare. In contrast, the second set with a bias towards the second objective renders higher losses. The initialization scheme aims at building diversity and thus evolving to more diverse solutions. A snapshot of chromosome composition representing energy allocation is shown in Table. 4.1.

Table 4.1: Chromosome - energy allocation vectors

MG	1	2	3	...	$\mathcal{N}-2$	$\mathcal{N}-1$	$\mathcal{N}$
P	0.030	0.034	0.046	...	0.002	0.006	0.022
Q	0.013	0.028	0.016	...	0.001	0.007	0.025

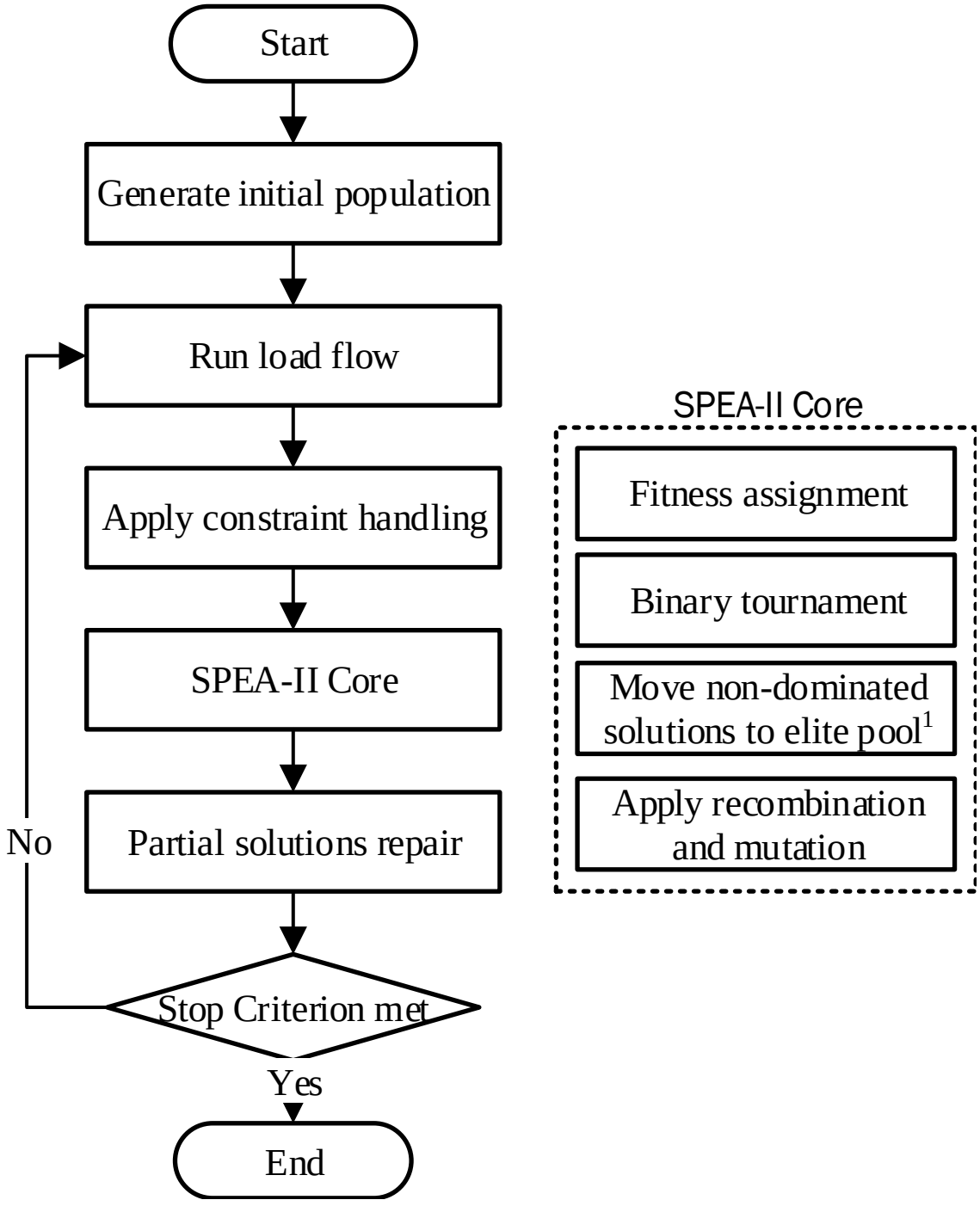

Figure 4.4: Evolutionary technique based optimization algorithm.

[1] If non-dominated solutions are less than the size of the elite pool, the best dominated solutions fill remaining members.

4.3.3 Genetic Operations

Depending on the crossover and mutation probabilities, a fraction of the whole population undergoes recombination —simulated binary crossover (SBX) [82] and a mutation operation. The creation of mth features of two child solutions c_1 and c_2 as a result of crossover of the parents p_1 and p_2 is as follows:

$$\begin{aligned} c_1(m) &= \frac{(1-\beta_m)x_1(m) + (1+\beta_m)x_2(m)}{2} \\ c_2(m) &= \frac{(1+\beta_m))x_1(m) + (1-\beta_m)x_2(m)}{2} \end{aligned} \tag{4.29}$$

where β is a random number generated from following probability density function.

$$PDF(\beta) = \begin{cases} (1+\eta)\beta^{\eta})/2 & \text{if } 0 \leq \beta \leq 1 \\ (1+\eta)\beta^{-(\eta+2)})/2 & \text{if } \beta > 1 \end{cases} \tag{4.30}$$

Here η is a non-negative number generally in the range of 0 and 5 [78].

The next operation, mutation, helps the evolutionary algorithms explore search space rigorously and avoid being stuck in a local optimum. The mutation generates a new solution from Uniform or Gaussian distribution whose mean is either at the center of the search domain or at the non-mutated value of the individual itself [84]. In this work, we generate mutated solutions from a normal distribution with mean at the individual itself. For a solution x_i, Gaussian mutation is given as follows:

$$x_i(k) = \begin{cases} x_i(k) & \text{if } r_m > p_m \\ max[min(x_{max}(k), N(x_i(k), & \text{if } r_m < p_m \\ \sigma^2(k)), x_{min}(k)] & \end{cases} \tag{4.31}$$

where p_m is the mutation probability and $r_m \in U[0,1]$ is a random number generated from the uniform distribution and $x_i(k)$ is the kth feature of ith member of the population.

The selection of crossover p_c and mutation p_m probabilities determine the fraction of the elite population participating in a crossover or undergoing a mutation. An analysis of the impact of the selection of crossover and mutation probabilities on unmet demand is shown in Fig. 4.11. The results show that when the p_c is 0.75 with p_m 0.25, the algorithm achieves the minimum unmet demand and produces the maximum feasible solutions.

4.3.4 Repair Operator

As discussed in Section 4.3.1, the probability of finding feasible solutions is extremely low. In such cases, the evolutionary algorithms employ operators [84, 109] to repair a fraction of infeasible solutions and make them feasible. Repair operators' design and the

probability of replacing solutions with repaired ones depends on the nature of the problem, e.g., 5% and 15% repair and replacements are proposed in literature [84]. In this work, the proposed operator partially repairs a fraction of infeasible solutions by applying the bound constraint, followed by a back-filling process to satisfy the equality constraint. The design of the operator is as follows:

Let $\vec{\mathcal{E}} := \{e_1, e_2, e_3, \ldots, e_N\}$ be a solution produced either as result of recombination or mutation and $\vec{\mathcal{D}} := \{d_1, d_2, d_3, \ldots, d_{\mathcal{N}}\}$ be the demand, repair steps are is as follows

$$e_i^r = min\{e_i, d_i\} \;\; \forall i \in \mathcal{N} \tag{4.32}$$

Next, we execute back-filing step with the residual energy $E_j^{res} := E_j^{net} - \sum_{i \in \mathcal{N}} e^r$ and the residual demand $d_i^u := d_i - e_i^r$. The residual energy is rationed among MGs based on the residual demand using uniform gains method as follow

$$e_i^{ug} = f^{ug}(\mathcal{N}, E_j^{res}, \vec{\mathcal{D}}^u) = min\{\bar{d_i^u} E_j^{res}, d_i^{rat}\} \tag{4.33}$$

where $\bar{d_i^u} = d_i^u / \sum_{i \in \mathcal{N}} d_i^u$ is the proportional division factor. The solution elements are updated as

$$s_i = min\{e_i^r + e_i^{ug}, d_i^{rat}\} \text{ s.t.} \sum_{i \in \mathcal{N}} s_i = E_j^{net} \tag{4.34}$$

In this work, we repair solutions with a 0.7 probability in the recombination stage and 0.15 during the mutation. The repair process only takes care of the bounds and the equality constraint. The SI constraint being nonlinear is left for the constraint handling approach to address.

4.4 Performance Measures

We test the proposed algorithm in 33-bus [95] and 69-bus [106] radial distribution systems. Each bus in the test systems is assumed to represent a microgrid. The system data and cumulative demand of the MGs are as given in [95,106]. As shown in Table 4.2, some MGs have surplus supply, whereas the others require additional energy to meet their needs. We use the method given in [89] to carry out load flow. The evolutionary algorithm parameters, including initial population, number of generation, mutation, and crossover probabilities, are set to 50, 75, 0.25, and 0.75, respectively.

4.4.1 Demand, Priority, and Phase 1 Allocation

The result shows the impact of individual demand and priority on phase 1 allocation. Figure 4.5 shows third-degree polynomial curves fitted on demand, priority, and phase 1 allocation data sets. The data elements are not shown to avoid clutter. The allocation in phase 1 follows the demand and priority curves showing their influence.

Table 4.2: Microgrids with surplus supply

33-Bus			69-Bus		
Bus	P	Q	Bus	P	Q
3	0.7381	0.6190	3	0.1608	0.4019
18	0	0.0476	11	0.2130	0.2460
33	0.1190	0.0476	14	0.338	0.1112
			17	0.9968	0.3738
			20	0.3288	0.2809
			26	0.0209	0.0161

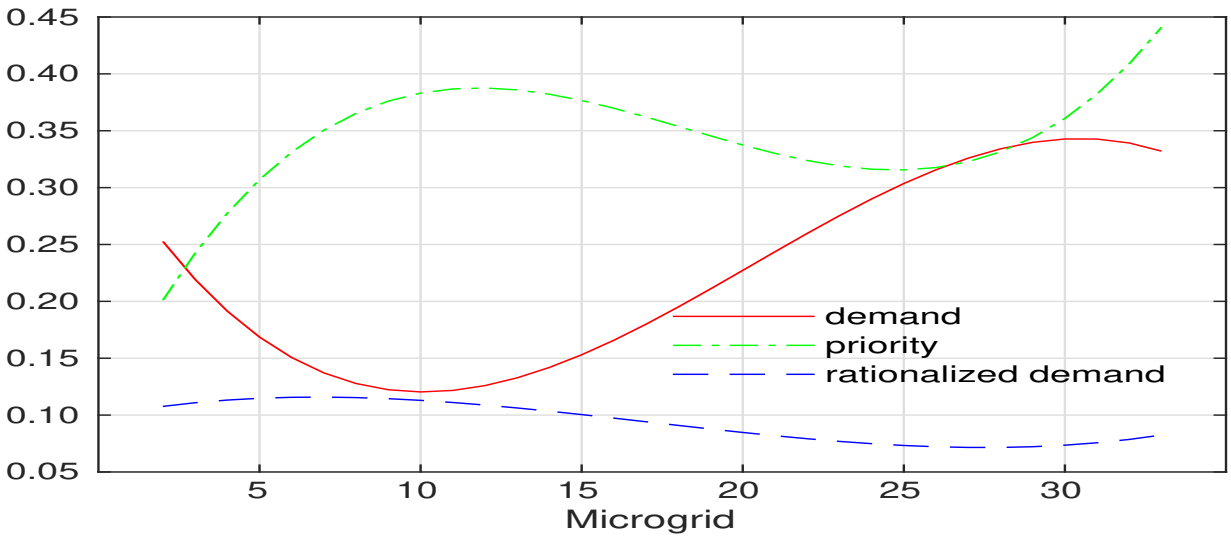

Figure 4.5: Polynomial curve fitted on demand, priority, and phase 1 allocation data.

4.4.2 Phase 1 vs. Final Allocation

Figure 4.6 shows third-degree polynomial curves fitted on the phase 1 and final allocation data. For avoiding clutter and see trends, elements of the data sets are not shown and a factor of 3 amplifies phase 1 allocation. The plots (a)(b)(c) show results for three solutions selected from the middle and two extremes of the Pareto front. The results show that the final energy allocation curve generally follows phase 1, but the distance varies for different members. This varying distance indicates that the algorithm allocates energy, considering the two optimization objectives besides the rationing index used in phase 1. Also, the allocation curves vary for three solutions according to the performance of Pareto optimal objectives.

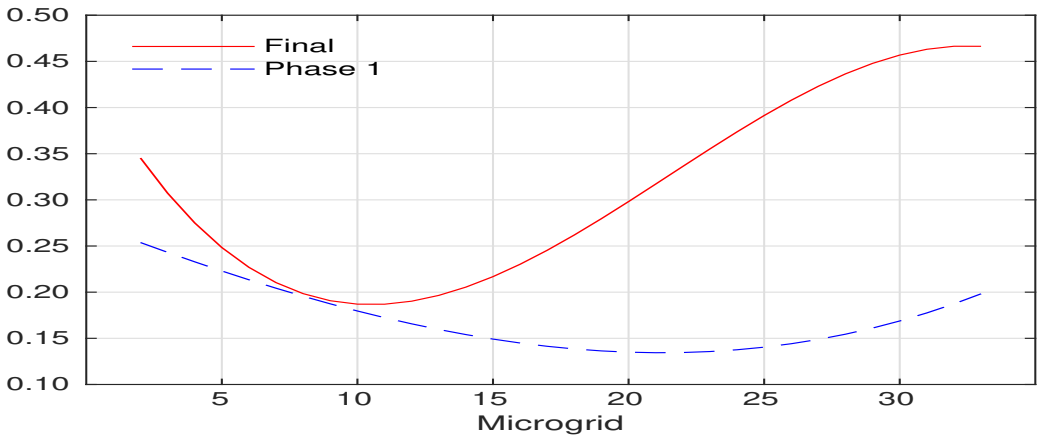

(a) Low

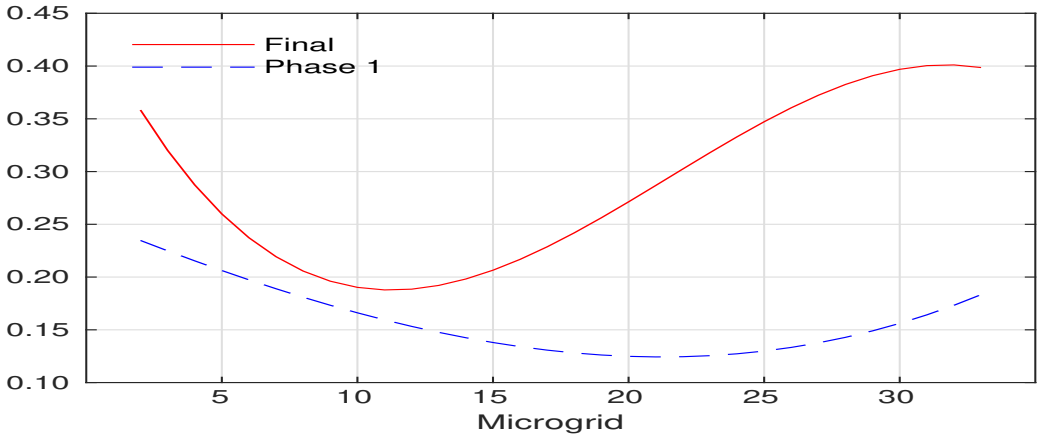

(b) Middle

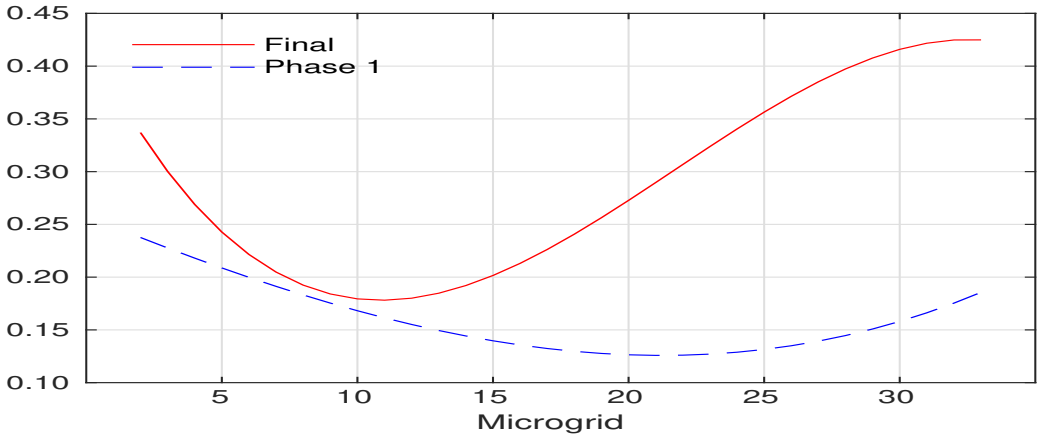

(c) High

Figure 4.6: Polynomial curve fitted on phase 1 and final allocations for solutions selected from middle and two extremes of Pareto front.

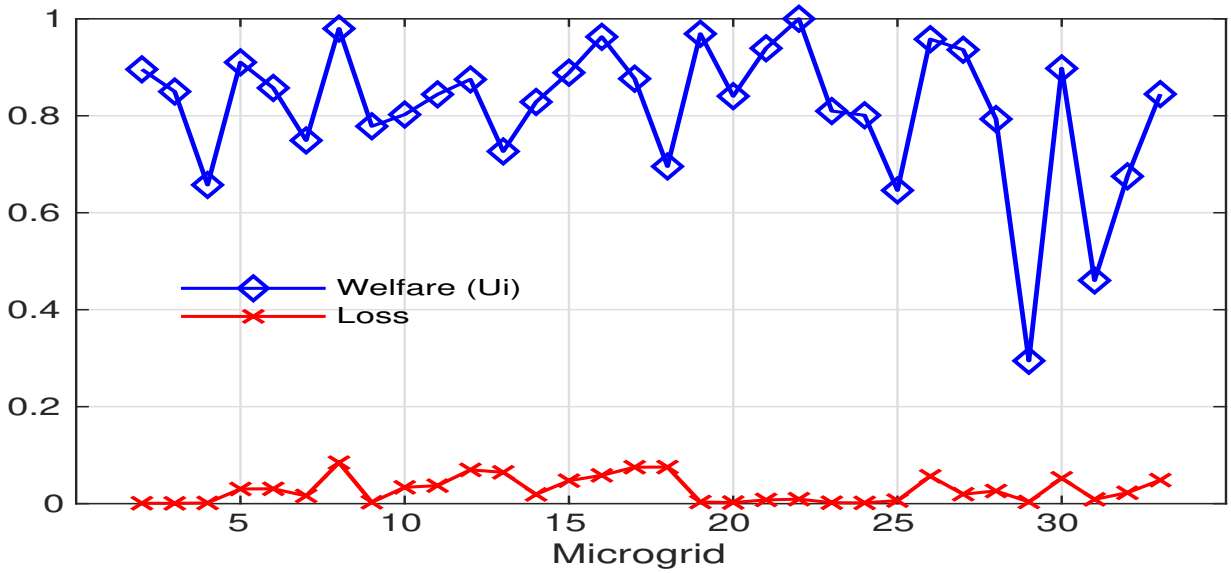

Figure 4.7: Welfare and loss plot

4.4.3 Welfare and Loss

The results in Fig. 4.7 show values of the two optimization objectives, i.e., welfare and power loss. Welfare is a function of energy a user gets against its demand. The system, while making an allocation, tries to minimize losses. The user losses vary depending on the individual allocation and resultant network conditions. For plotting, the loss values are amplified by a factor of 200; otherwise, relatively higher welfare values obscure loss values.

4.4.4 Load Priority vs. Allocation

In this experiment, we examine the impact of load priority on energy allocation to a microgrid. We compare the unmet demand when the microgrids have equal priorities and otherwise. Figure 4.8 shows six sets of microgrids from 33 and four from 69 Bus systems that have equal demand within the set. Figure 4.8(a)(c) show the results when MGs in each group have equal priority of allocation. Though the priority and demand are the same, the unmet demand varies because the system also considers Pareto Optimal objectives during allocation. In other cases, Fig. 4.8(b)(d) shows a case where the group members have different priorities. The results, in this case, also support findings from equal priority case.

4.4.5 Demand vs. Allocation

In this experiment, we examine the impact of individual demand on energy allocation to a microgrid by comparing the unmet demand when the microgrids where have equal priorities and otherwise. Figure 4.9 shows microgrids from 33 and 69 Bus systems where

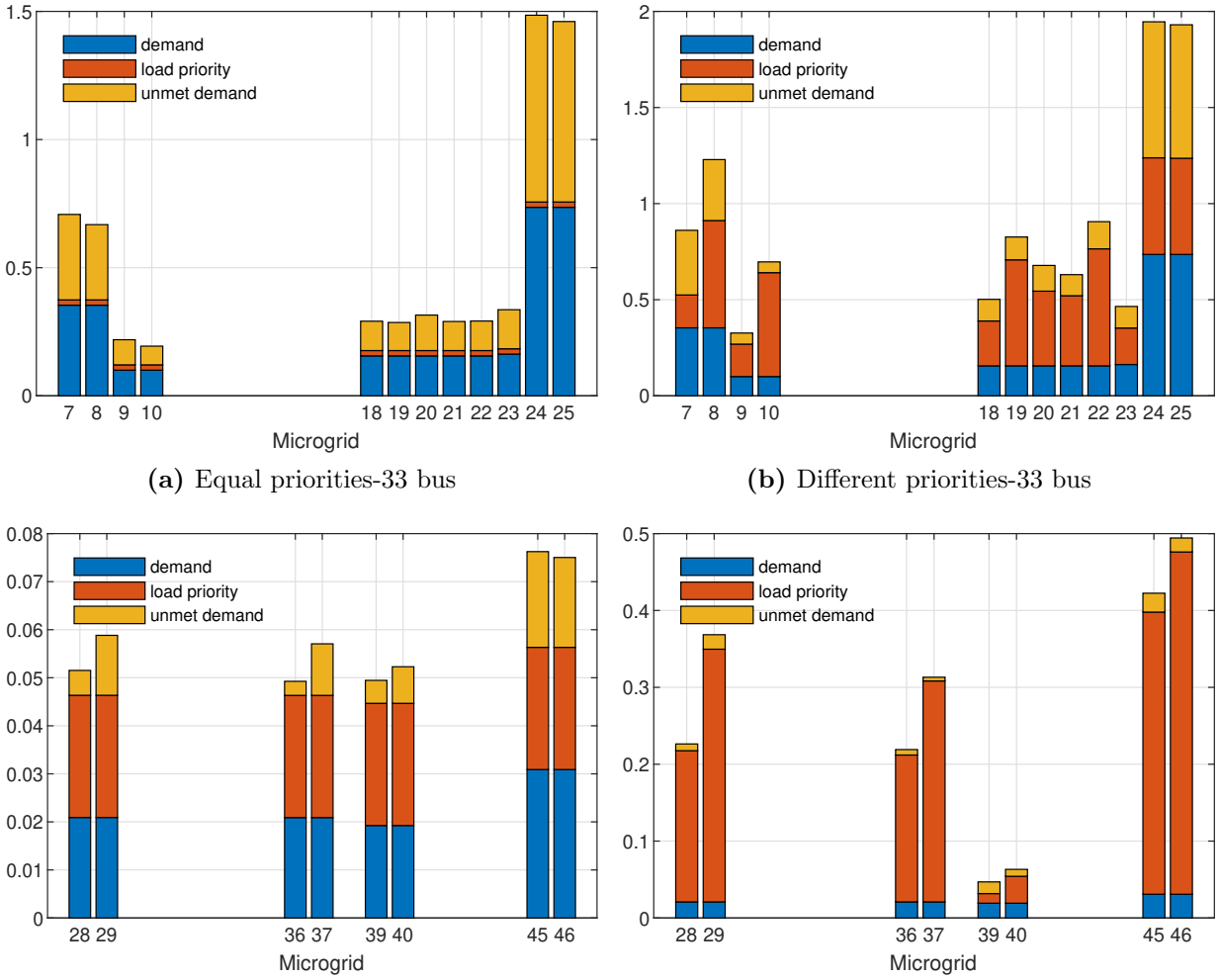

(a) Equal priorities-33 bus

(b) Different priorities-33 bus

(c) Equal priorities-69 bus

(d) Different priorities-69 bus

Figure 4.8: Impact of load priority on allocation: Four sets of MGs with identical demand are shown, (a)(c) show the the unmet demand when load priorities are equal whereas in (b)(d) priorities are different.

each one has different demand. Figure 4.9(a)(c) show the case where allocation priorities are same for all MGs and Fig. 4.9(b)(d) are for unequal allocation priorities. The unmet demand generally follows the priority and demand, but the effect is not easily discernible due to optimization.

4.4.6 Contribution vs. Allocation

In this experiment, we examine the impact of microgrid contribution on energy allocation by the system controller. Figure 4.10 shows four sets of microgrids with equal demand. In the first case, all microgrids have an equal historical contribution, but as shown in Fig. 4.10 (a)(c) each user has different unmet demand. It is because the system also considers

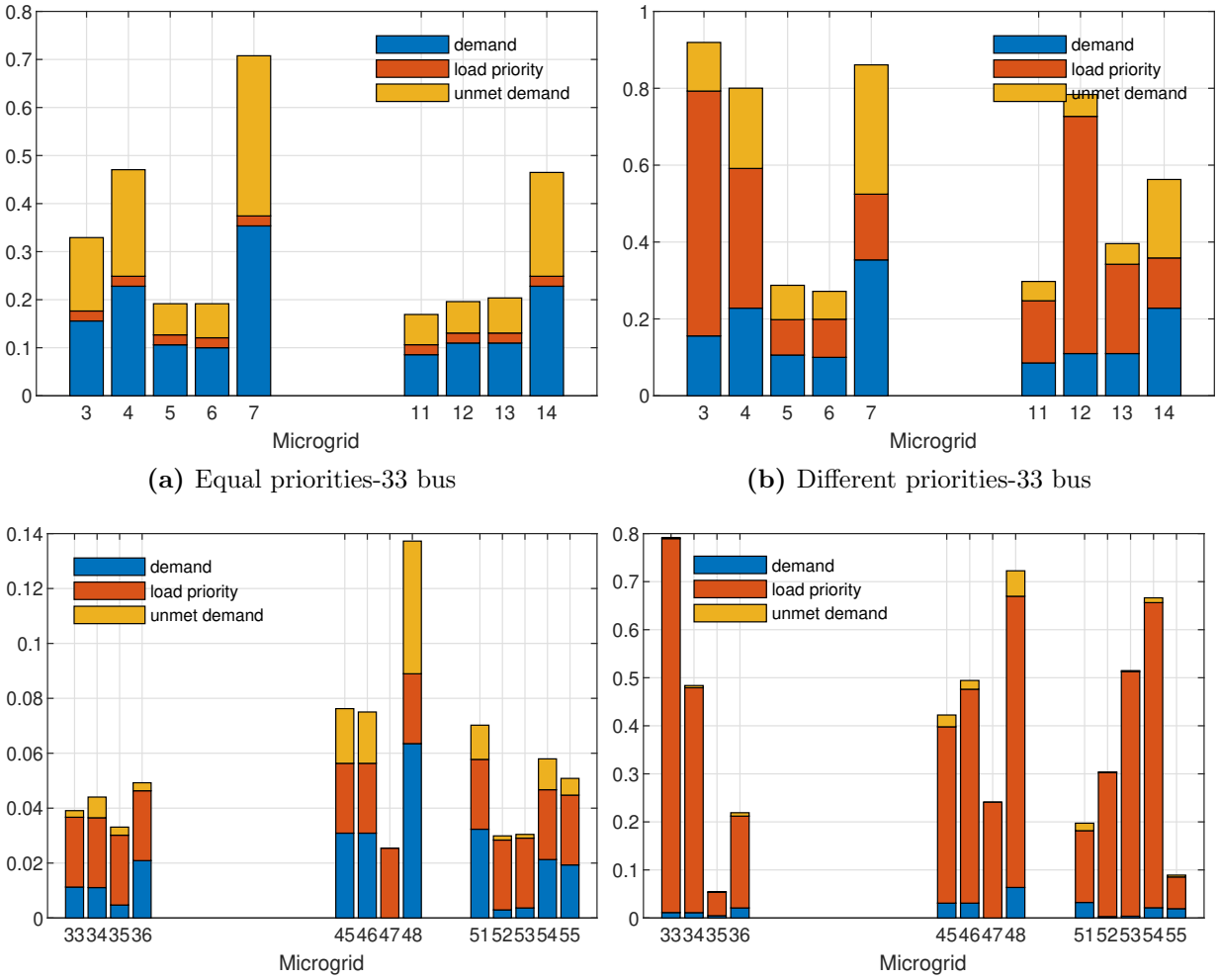

(a) Equal priorities-33 bus **(b)** Different priorities-33 bus

(c) Equal priorities-69 bus **(d)** Different priorities-69 bus

Figure 4.9: Impact of demand on allocation: microgrids with different demand are shown. (a)(c) shows the the unmet demand when load priorities are equal whereas (b)(d) represents the case where both demand and priorities are different.

Pareto Optimal objectives during allocation besides contribution and demand. In the other case, Fig. 4.10 (b)(d), each microgrid have different contribution. In this case, the unmet demand varies in direct relation to contribution and also based on the Pareto optimality of the optimization objective.

4.4.7 Impact of Crossover and Mutation Probabilities

In this experiment we examined the the impact of selection of different crossover and mutation probabilities on unmet demand and number of feasible solutions. As the crossover probability increase the unmet demand remains same largely and on the contrary the number of feasible solution increase with increasing crossover probability. Figure 4.11

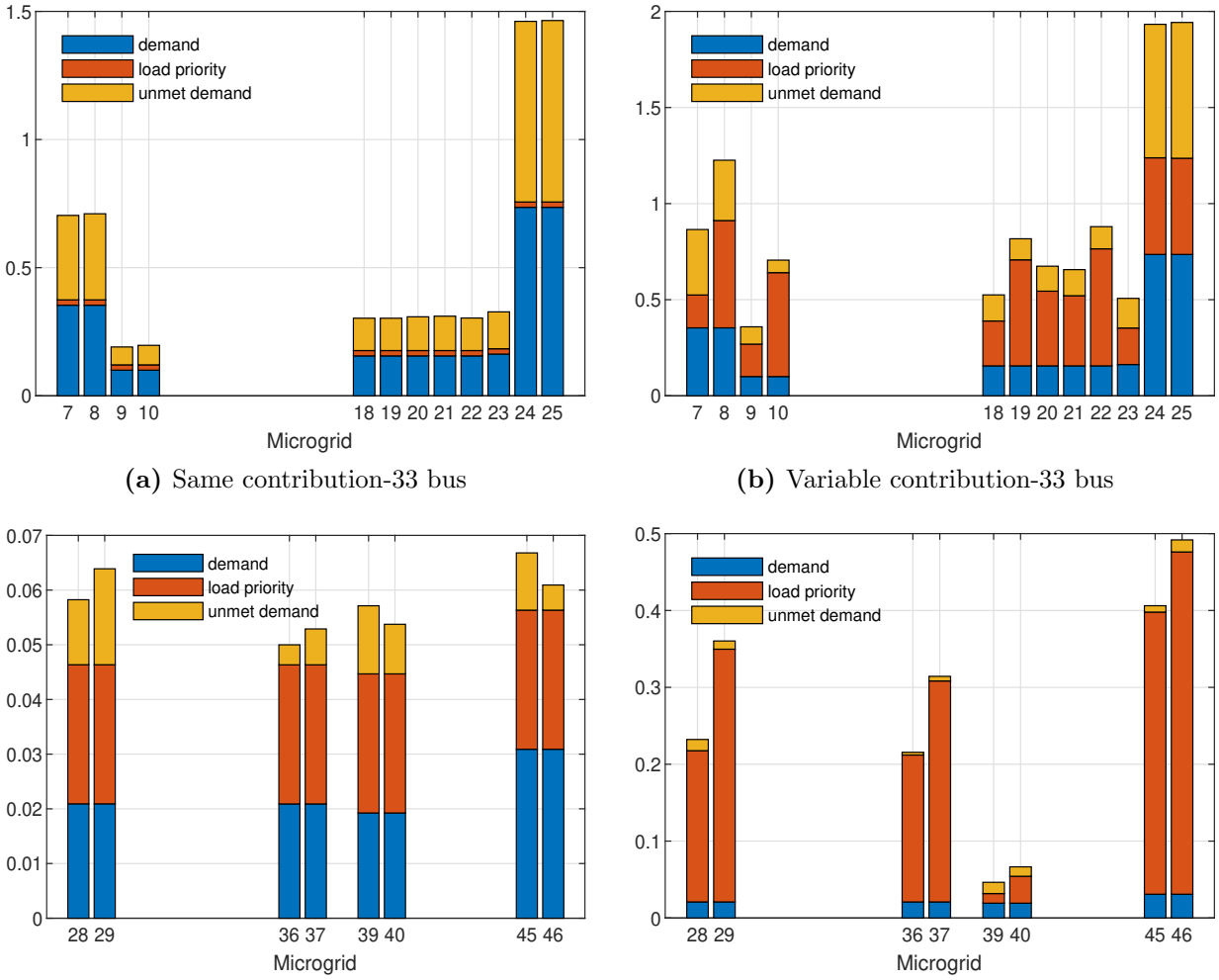

(a) Same contribution-33 bus

(b) Variable contribution-33 bus

(c) Same contribution-69 bus

(d) Variable contribution-69 bus

Figure 4.10: Impact of contribution on allocation: Four groups of microgrids with equal demand are shown. (a)(c) shows the the unmet demand when users' contributions are equal whereas in (b)(d), contributions of microgrids within each groups are different.

shows the results, the algorithm find maximum solutions when p_c is set to 0.75 and p_m to 0.25

4.4.8 Voltage Stability Index

This experiment analyses the impact of allocation on network stability in terms of voltage stability index. Figure 4.13, shows the voltage stability index in IEEE-33 and IEEE-69 bus systems for three representative solutions. The solutions include two selected from the two extremes of an evolved Pareto front that represent low welfare and high loss and vice versa. The third solution is from the middle part of the Pareto front. An index value closer to unity show a network that is vulnerable to collapse, whereas lower values indicate a more

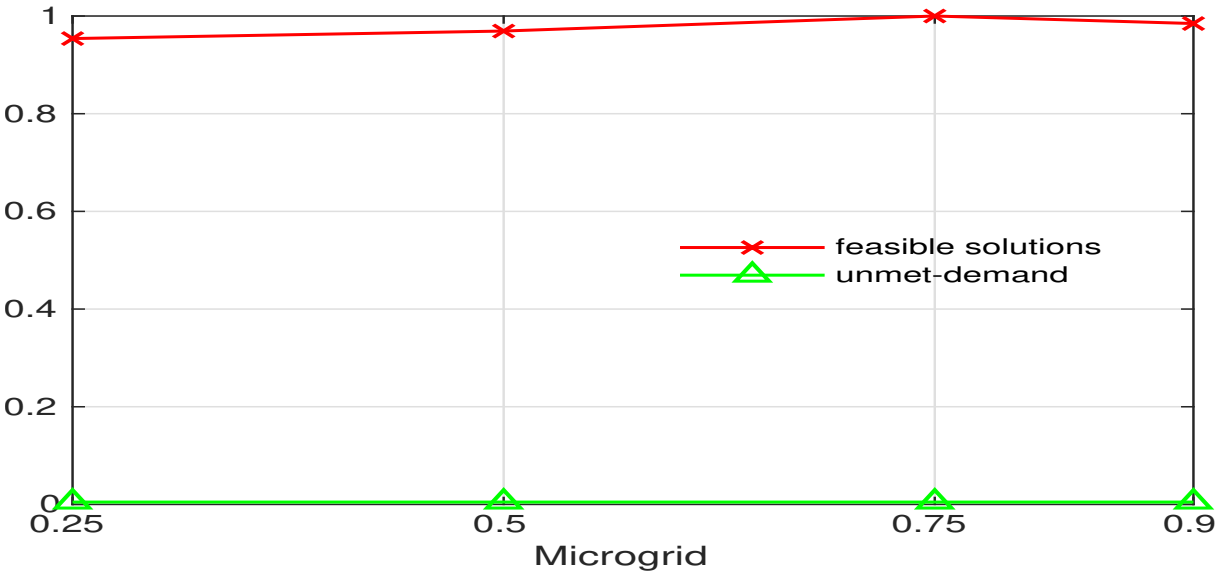

Figure 4.11: Impact of crossover and mutation probabilities on unmet-demand.

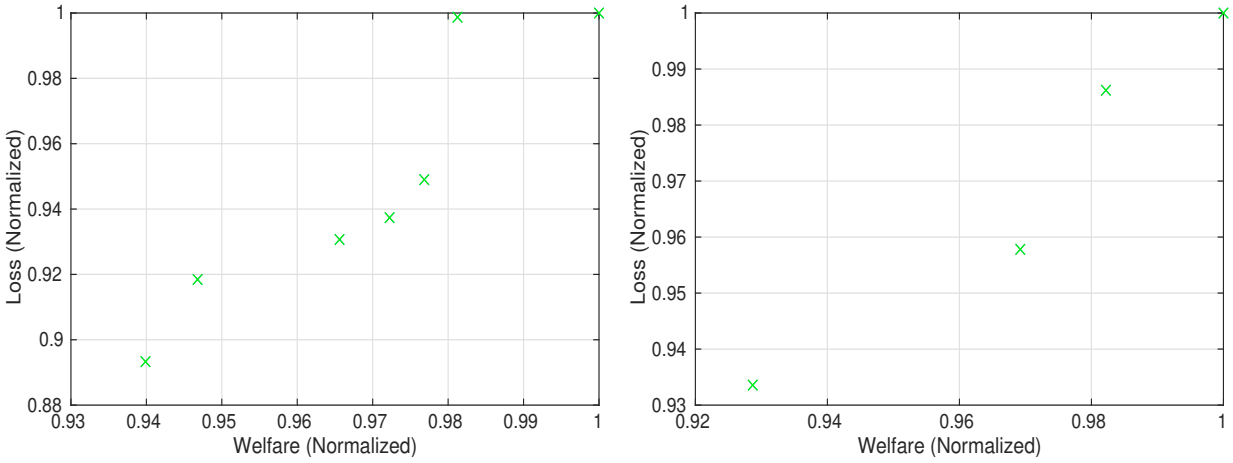

(a) IEEE-33 Bus System **(b)** IEEE-69 Bus System

Figure 4.12: Pareto optimal front plot. The graph show scatter plot of normalized values of objective functions i.e., welfare and loss.

stable network. The stability index in all solutions is well below the unity value. Therefore, the algorithm meets network constraints during optimization and achieves better stability.

4.4.9 Bus Voltage Profile

This experiment analyses the impact of allocation on network stability in terms of bus voltages. Figure 4.14 shows the normalized voltages on various buses in IEEE-33 and IEEE-69 systems for three representative solutions. The solutions include two selected from the two extremes of an evolved Pareto front that represent low welfare and high

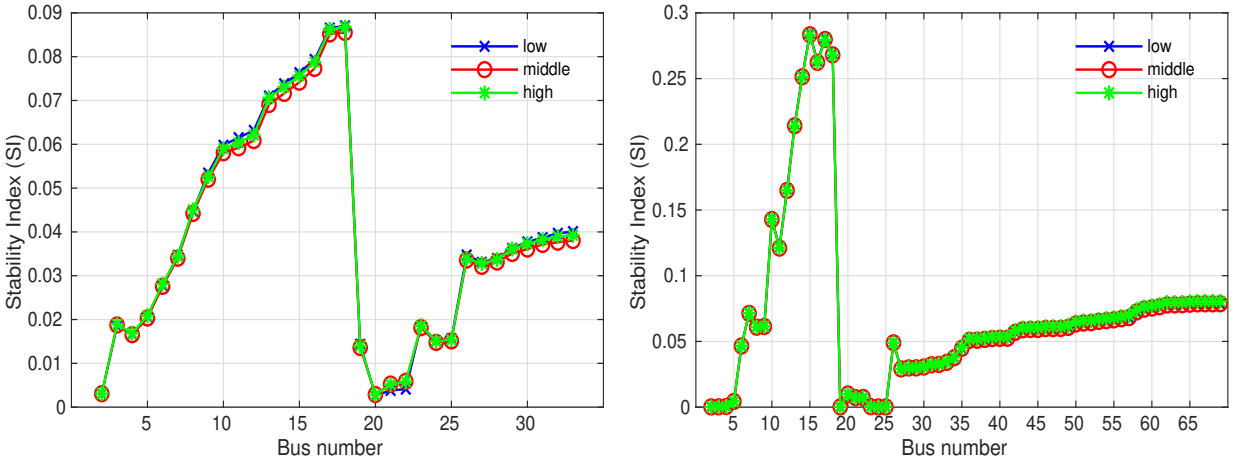

(a) IEEE-33 bus system **(b)** IEEE-69 bus system

Figure 4.13: Voltage stability index for three Pareto optimal solutions from two extremes and middle of the front.

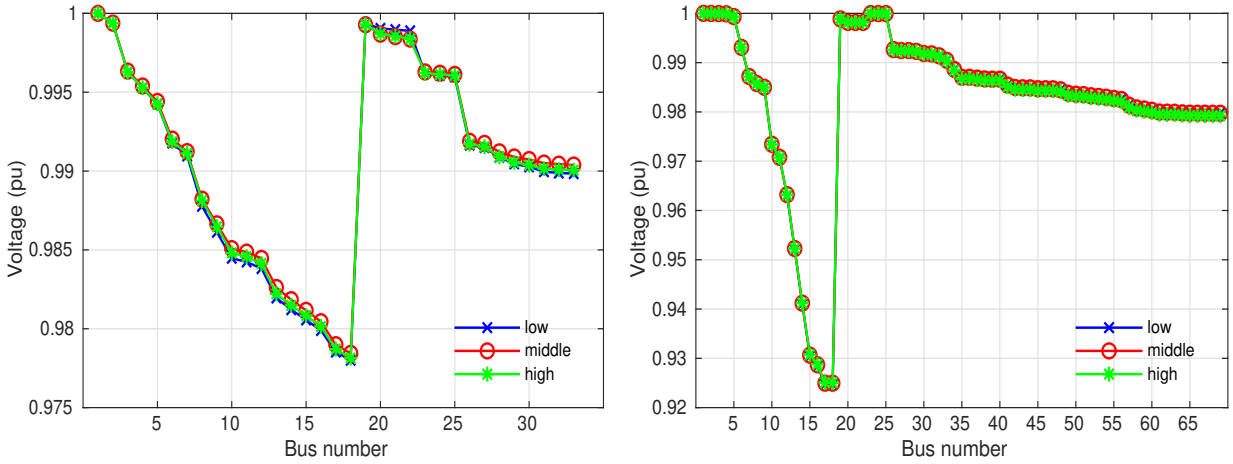

(a) IEEE-33 bus system **(b)** IEEE-69 bus system

Figure 4.14: Voltage profile for three Pareto optimal solutions from the initial, middle and end parts of the front.

loss and vice versa. The bus voltages for selected solutions are within 5% of the nominal voltage, showing that the algorithm meets network constraints during optimization and achieves better stability. However, in this experiment we assume existence of local voltage mechanism, e.g., selecting a source MG considering its location and impact on network conditions as discussed in [100, 101].

4.5 Conclusion

Energy donation is an attractive mechanism to mitigate the effects of the power crisis resulting from a weather-related interruptions. By tapping enhanced philanthropic senti-

ment invigorated during a crisis and encouraging the trade of user-owned surplus capacity, the grid can restore critical loads and provide a degree of relief to the affected users. We proposed a novel and completely new framework to enable and optimize energy donation for service restoration. The proposed algorithm embeds weighted and evolutionary optimization-based rationing techniques to prioritize critical load restoration and meet system objectives of maximizing welfare and minimizing losses. Furthermore, it embeds resource and distribution system constraints in the allocation process to ensure a stable network operation. Extensive performance analysis in IEEE 33 and 69 bus system shows the effectiveness of the proposed approach. As an extension of this work, one avenue is to incorporate techniques for managing stability issues resulting from energy exchanges in DERs-based restoration at the local level.

Chapter 5

Energy Sharing for Service Restoration using a Consortium Blockchain Approach in a Power Distribution System

Power network disruptions triggered by weather events or otherwise leave devastating effects on communities. Microgrids with distributed energy resources can help swift localized restoration following the interruption of utility power. However, because of the limited generation and storage capacity of microgrids, service restoration would require prioritizing critical load and optimality of operations for rendering relief to those in dire need. Moreover, fair energy allocation, trust-free energy exchanges, and the integrity of transactions are crucial. We propose a blockchain-based energy sharing approach for service restoration using energy crowdsourced through donation or trade. The proposed framework utilizes microgrids' supply situation and reputation as consortium admission criteria for optimizing the blockchain operations' energy cost. The proposed approach utilizes a measure called proof of welfare (PoWel) which solves the rationing problem to produce an energy allocation block accordingly by utilizing weighted rationing for prioritizing critical load restoration and an evolutionary optimization algorithm for maximizing social welfare and minimizing power losses. The winner block selected through consensus intrinsically preserves network stability while conforming to resource and stability constraints. An extensive performance and security analysis ascertains the effectiveness of the proposed approach.

5.1 Introduction

Weather events, technical malfunctions and sometimes sabotage are the maincauses of power failure. These disruptions leave devastating effects on communities. The frequency

and intensity of weather-related catastrophes are projected to increase with climatic deterioration. The events may cleave power networks into islands with unimpaired distribution infrastructure, having no or limited supply. These islands may be organized into microgrids (MGs) for speedier localized service restoration utilizing distributed energy resources (DERs. A grid can power up critical loads locally before the main generation becomes available. However, since available distributed generation is limited, a restoration strategy should prioritize loads, optimize network operations, and maximize coverage to provide relief to those severely affected.

Disasters may positively impact communities' pro-social behavior, increasing their motivation to help others in need [99]. The availability of technological means can facilitate or accelerate to do that. For example, a grid can crowdsource energy from the microgrids with excess capacity and supply it to those without alternative power arrangements. MGs may either donate their surplus energy or opt to trade it with the local grid. However, transparency and fairness are key ingredients for the success of such community-driven initiatives. Such a system requires an accurate accounting of energy contributions, a fair allocation criterion, and integrity of transactions. Blockchain, an emerging distributed ledger technology with inherent transparency, accountability, and fairness features, is an apt candidate for such applications.

Blockchain has found applications in many areas; it has especially revolutionized financial transactions by decentralizing and eliminating third parties' involvement. A blockchain system generally constitutes a distributed ledger, a consensus protocol, smart contracts, mining or validating nodes, and a registration authority. The ledger comprises a series of data blocks linked together through a cryptographic hash. It provides features such as immutability, integrity and authentication, fault tolerance, and above all, trust-free operation [110]. The registration authority uses a private-public key pair-based identification system to provide anonymity and privacy protection services to system users. On the other hand, the miners or validators run the consensus protocol for maintaining a common state of the distributed ledger across the network. These characteristics of the blockchain technology make it suitable for smart grid applications, particularly energy sharing or trading and DER-based service restoration [111].

DER-based service restoration strategy embeds a network reconfiguration component and an energy management scheme. The scheme allows for energy allocation based on load service priorities and system objectives. It also manages the energy sharing or trading from distributed sources to the loads. In a distribution system, the sharing or trading can take place directly among peers —users [39], houses [40–42], MGs [15,16,36–38]. In other cases, a central entity, e.g., a DSO may facilitate energy allocation or exchanges between DERs and loads [15,16]. The latter approach helps mitigate the problem caused by uncoordinated energy exchanges [112]. However, energy sharing or trading during major power disruptions presents additional challenges because of limited supply, unstable network, the requirement

of prioritizing critical load while providing relief to those in dire need. In this context, many contemporary energy-sharing works have overlooked critical aspects of restoration. For example, [15,16] ignored distribution systems' operational constraints so their solution may destabilize distribution system. Furthermore, neither works used a pricing mechanism, so all transactions carry the same value irrespective of supply-demand conditions. It adversely affects fairness and thus lowers the incentive for the participants. In contrast, Kim *et al.* [36] handled power balance and network constraints but did not address prioritized allocation.

Several recent works have studied critical load restoration following an interruption using energy from DERs [45, 46, 48, 113–121]. A common strategy across these works is to aggregate DERs into MGs for garnering sufficient supply for restoration. For example, [45, 46, 113, 121] provide framework for restoring critical loads using DERs when utility power is interrupted. Chen *et al.* [114] studied formation of the microgrids dynamically in a distribution system for restoration given an outage. Similarly, [48] uses spanning tree to divide a distribution system into MGs and restore the critical loads using CHP units within distribution system. Similarly, [121] sectionalize distribution network into isolated MGs and propose a two level simulated assisted strategy for service restoration.

DER-based restoration manifests exchanges from distributed sources to the loads either directly or through aggregators. In both cases, efficient accounting and integrity of transactions are essential. Despite a widely sought research area, few approaches currently exist that utilize blockchain for DER-based energy sharing for restoration [17–21]. A prominent example of blockchain application is the Brooklyn microgrid [17]. The grids' architecture embeds a blockchain-based peer-to-peer energy market. The system provides uninterrupted supply to critical facilities, but lesser critical, i.e., houses and businesses compete for the remaining supply. In [18] Wang and Taha proposed a blockchain-assisted energy crowdsourcing system using DERs and controllable loads. The proposed system uses a Hyperledger [122] with Practical Byzantine Fault Tolerance (PBFT) as a consensus mechanism for managing peer-to-peer energy transactions.

The architecture of a blockchain system depends on a particular application [111]. Moreover, it may require case-specific optimization to improve energy efficiency, computation complexity, and transaction throughput. In a post-disaster distribution network, several options for blockchain system design optimization exist: First, a power distribution system predominantly forms a closed network where the subscribers register with a utility for services. This feature adds a security layer; therefore, relatively less complex blockchain systems, e.g., permissioned blockchain, may accomplish the task. Second, an islanded network has limited users. Therefore, it ameliorates the blockchain systems' scalability requirements and opens up opportunities for private or permissioned instead of the public blockchain that has better scalability. Third, power networks impose hard technical constraints on peer-to-peer energy exchanges. Besides, uncoordinated energy sharing may compromise network stability, making it a crucial consideration for underlying trading or

allocation models in blockchain systems [112]. Finally, energy scarcity is the most critical factor in the design of blockchain operations, particularly consensus mechanism.

A blockchain consensus is key to ensuring that all nodes agree on a common state of a distributed ledger. However, due to the scarcity of supply in a disaster-ridden power distribution system, complicated consensus protocols such as proof-of-work (PoW) may not be viable because of their high power consumption and complexity. Some researchers have proposed lightweight, customized consensus mechanisms designed particularly for power systems applications [123–127]. For example, Liu *et al.* [126] proposed a consensus mechanism to minimize power grids' load variance. Similarly, [124] proposed a reputation-based consensus and validation protocol. The authors' prior work [127] presented a consensus mechanism, called proof of welfare (PoWel), considering post-disaster network characteristics. These approaches, however, are not applicable in our context because they do not consider limited supply scenario and optimize blockchain operations. We propose a consensus protocol that allows nodes to select energy allocation block that meets system objectives, i.e., restoring critical load, maximizing social welfare, and minimizing losses without compromising network stability.

A blockchain system for power networks with DERs requires addressing stability concerns by embedding underlying network physical constraints into allocation or trading models [112]. It translates to adding constraint compliance in a consensus protocol as an additional criterion for block selection. Thus, the mining nodes run powerflow analysis to evaluate the impact of a proposed block on the network stability and assess constraints compliance. The feature adds to the complexity of blockchain consensus, increasing its energy consumption. Therefore, a blockchain system needs active measures, e.g., consortium formulation, to improve the consensus protocols' energy efficiency. The consortium mechanism achieves this by limiting the number of miners running consensus protocol and powerflow analysis.

In this context, we propose a consortium blockchain approach for energy sharing during service restoration in a post-disaster distribution system using energy crowdsourced from MGs through donation or trade. We formulate energy allocation as a rationing problem to prioritize critical load, minimize losses and maximize welfare for the communities without alternate power arrangements. The proposed approach considers distribution network characteristics —closed nature and limited size, to optimize blockchain design. It incorporates resource and underlying networks' stability constraints into the consensus mechanism to preserve network stability. Finally, to address blockchain systems' energy consumption and complexity concerns, we adopt blockchain nodes' reputation and supply state-based consortium formulation to limit the number of miners running consensus and powerflow analysis. More specifically, the chapter's key contributions are:

1. A consortium blockchain-based energy sharing approach for service restoration in a post-disaster distribution system using energy crowdsourced through donation and

trade.

2. A blockchain design for limited supply scenarios that uses distribution network characteristics and a consortium formulation based on nodes' reputation and supply state to reduce complexity and energy cost of blockchain operations.

3. A unified consensus protocol that solves a rationing problem to enable prioritized restoration of critical loads, minimize losses, and maximize welfare for those in dire need. The protocol incorporates resource and voltage stability constraints into the consensus; thus, a selected energy allocation block maintains distribution system stability.

The rest of the chapter is organized as follows: Section II presents the problem formulation. Section III explains the blockchain system model components including the consensus mechanism. Section IV summarizes the operation of the blockchain-enabled service restoration framework. Section V presents the security and performance analysis of the proposed scheme. Finally, section VI concludes the chapter by providing some highlights of the future work directions.

5.2 Problem Formulation

This section describes the network model for the service restoration and formulation of energy allocation as a rationing problem along with the solution approach.

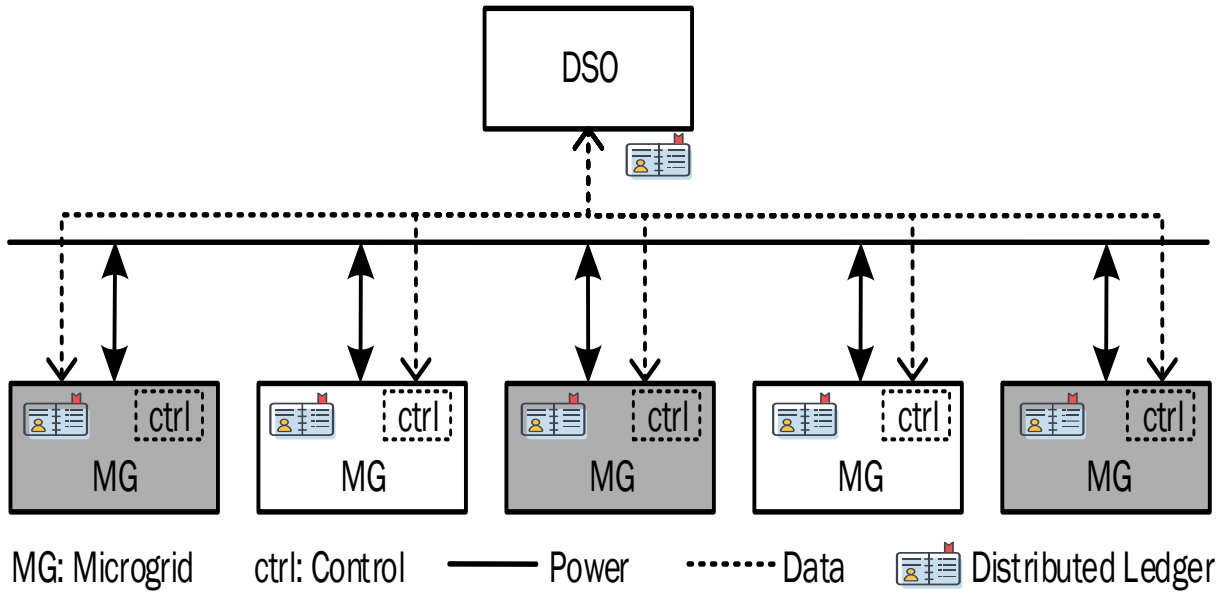

Figure 5.1: Blockchain model for service restoration. Shaded MGs are consortium nodes whereas the others only have read access to blockchain ledger.

Table 5.1: Blockchain System Key Elements Defined

Name	Description
Node	A microgrid or DSO; A node acts as a miner or validator if it has sufficient supply and reputation. The others have read access to the blockchain ledger. Nodes' roles change over time with changes in supply and reputation situation. DSO is a special node.
Transaction	Smallest building block of a blockchain system contains information about energy exchanges between demanding MG and suppliers.
Block	A set of energy transactions not yet validated and added, it has a specific structure, and after validation, get added to the blockchain. Besides energy transactions information, a block contains other system parameters as well.
Chain	An ordered sequence of energy allocation blocks added after consensus. New block links to the previous through a cryptographic hash.
Miner	A microgrid, which is a consortium member, runs a consensus algorithm and proposes an energy allocation block. Also, it verifies blocks proposed by other miners for addition to the blockchain.
Consensus	A set of rules for achieving agreement on the common state of blockchain ledger, e.g., PoW, PoS. Proposed frameworks' consensus is based on solving rationing problem to achieve energy allocation block with the best proof.
Smart contract	Set of self-enforceable and tamper-proof rules stored as a computer program in blockchain to make changes in the ledger. They activate when a set condition is met, thus eliminating the need for intermediaries reducing transacting, contracting, and compliance costs
Consortium	A selected set of nodes in consortium blockchain, e.g., MGs, undertake the mining and validation tasks. A nodes' admission to consortium often follows a set criterion; it limits the number of miners and the consensus protocol instances.

5.2.1 Network Model

The problem is set in an islanded radial distribution network organized around multi-microgrids. The network comprises $\mathcal{N}$ nodes and $\mathcal{B}$ edges (branches). The supply from the main grid is not available due to disaster. However, a limited local generation is available as microgrid resources including solar, wind, and limited brown energy. We assume the physical network infrastructure is largely intact. The network comprises microgrids with surplus supply that they can share with peers in need. The others lack sufficient local capacity to meet the needs of the loads they service. The network has a special entity, namely a distribution network operator (DSO), for coordinating the energy exchanges among the microgrids. MGs can either donate or trade their surplus energy to the local grid or utility for socioeconomic benefits. Requisite infrastructure is available for blockchain-based two way flow of electricity among the MGs.

In each operation slot, MGs' demand or information about the surplus supply for the next slot is available with the DSO. We consider two types of transactions for energy exchange: First, donation transaction in which MG transacts energy as a charitable donation. Second, trade transaction, where MG trades energy with the local grid and it has associated cost. The grid uses a supply-demand-based valuation system to appraise transactions [128]. It further uses it to determine users' contribution and, thus, in subsequent energy allocation. The donations may be free or may accompany some socioeconomic benefits for a donor. In contrast, trade transaction increases suppliers' reputation which it can redeem to get prioritized services and compensation from the utility when main grid restores.

Because of the limited supply, the load restoration needs prioritization. For example, public health and safety facilities get priority over other households. However, a prolonged power outage may threaten inhabitants' safety because of a lack of supply for home medical aids and communication devices. Recompensing faithful system members during the difficult time also need due consideration. Therefore, we adopt a community-centered restoration approach. It tries to achieve maximum welfare for the affectees, prioritize restoration of critical load, and factor historical contribution in allocation to recompense faithful users. The systems' operation horizon $\mathcal{T}$ comprises n slots normalized to unit time so that we can use power and energy interchangeably. The network setup is shown in Fig. 5.1.

5.2.2 Energy Allocation Model

In a disaster situation, the energy supply is limited compared to demand; thus, the energy (resource) allocation is a case of bankruptcy. We formulate energy allocation as a rationing problem and adopt a two-step solution approach. First, the system allocates energy using the uniform gains rationing method [103] based on the rationing index (5.2). Subsequently,

it optimally allocates the residual energy to MGs considering a multi-objective criterion, residual demand, and following power network voltage stability constraints. We term the allocation in the second phase as optimized rationing and employ an evolutionary algorithm for this purpose.

Let available energy from donation and trade be E^p and $\vec{D}$, $\vec{C}$, and $\vec{P}$ be demand, historical contribution, and service priority vectors for the microgrids in given operation window. The allocation in the first step is as follows:

$$e_i^w = f^w(\mathcal{N}, E^p, \vec{\mathcal{D}}) = min\{\mathcal{W}_i E^p, d_i\} \; \forall d_i \in \vec{D} \tag{5.1}$$

where f^w is the weighted gains rationing function and $\mathcal{W}_i$ represents the weight assigned to individual demand (claim) or the service priority. The weight is a function of service priority and the historical contribution and given as follows

$$\mathcal{W}_i = \begin{cases} \dfrac{p_i}{\sum_{i\in\mathcal{N}} p_i} & \text{if } \psi = 1, \; \forall p_i \in \vec{P} \\ \dfrac{c_i}{\sum_{i\in\mathcal{N}} c_i} & \text{if } \psi = 2, \; \forall c_i \in \vec{C} \\ \dfrac{h_i}{\sum_{i\in\mathcal{N}} h_i} & otherwise \end{cases} \tag{5.2}$$

where $h_i := \gamma p_i + (1-\gamma) c_i$ is hybrid allocation basis and the parameter γ is the weight factor. The parameter ψ controls the allocation or rationing basis and its values $\{1, 2, otherwise\}$ pertains to the cases of service priority, historical contribution, and their combination.

In the second phase, the system optimally allocates the remaining energy $E^{res} := E^p - \sum_{i\in\mathcal{N}} e_i^w$ considering a multi-objective criterion, unmet demand $d_i^u := d_i - e_i^w$, and in accordance with the distribution system operational constraints. Given the optimization algorithm f^o, the allocation in the second step is as follows

$$e_i^o = f^o(\mathcal{N}, E^{res}, \vec{\mathcal{D}}^u) \tag{5.3}$$

On completion of both steps, final the allocation E_i to an MG is as follows

$$E_i = min\{e_i^w + e_i^o, d_i\} \quad \text{s.t.} \sum_{i\in\mathcal{N}} (E_i + \mathcal{L}_i) = E^p \tag{5.4}$$

The allocation comprises two components, i.e., e_i^w allocated in the first step based on weighted rationing and e_i^o through optimized rationing by the optimization algorithm. The energy transport to a demanding MG incurs power losses $\mathcal{L}_i$ that need accounting in the allocation process. Lastly, the share of energy allocated in the first step is adjustable as per user preferences.

5.2.3 Optimization Problem

The system allocates energy in the second phase to achieve maximum coverage or minimize the unserviced load. The objective is to maximize user satisfaction —a social welfare indicator. But maximizing social welfare by allocating more energy or increasing coverage may increase distribution losses.

The post-disaster network has higher power losses due to poor feeder configuration and absence of adequate compensation. Moreover, in view of limited supply, the minimization of losses becomes very critical. So while allocating energy, the system tries to minimize losses and find a trade-off solution to achieve maximum coverage, i.e., reaching out to the maximum users. The power loss $\mathcal{L}_i$ on the link connecting two MGs is given as follow

$$\mathcal{L}_i = \frac{P_i^2 + jQ_i^2}{|V_i|^2} r_i \quad \forall i \in \mathcal{N} \tag{5.5}$$

where P_i, Q_i are the real and reactive power at the sending node, and V_i is voltage magnitude at the node.

Power losses, poor feeder configuration, and compensation unavailability makes the network vulnerable to voltage collapse. The operators use network stability indices for monitoring and compensating real and reactive power. A representative stability index is available in [94]. The index is suitable for a network with DERs that cause voltage angle variations.

$$SI = \frac{4 r_{ij}(P_L - P_G)}{[|V_i| Cos(\theta - \delta)]^2} \leq 1 \; \forall i, j \in \mathcal{N} \tag{5.6}$$

where r_{ij} is the effective line resistance between nodes i & j and V_i is the sending end node voltage. Next, P_L, P_G are load and power compensation on a node, δ is angle variation between two nodes, and θ is the impedance angle. During optimization, after allocating energy, the algorithm determines the SI value for every bus. If the index approaches unity, it sheds some load or, in other words, reduces allocation and re-evaluates the stability.

We model systems' objectives as an optimization problem, given as:

$$\begin{aligned}
&max \sum_{i \in \mathcal{N}} U(E_i) \\
&min \sum_{i \in \mathcal{N}} \mathcal{L}_i \\
&\text{subject to:} \\
&e_i^w \leq E_i \leq d_i \;\; \forall i \in \mathcal{N} \\
&\sum_{i \in \mathcal{N}} (E_i + \mathcal{L}_i) \leq E^p \\
&V_{min} \leq V_i \leq V_{max} \;\; \forall i \in \mathcal{N} \\
&SI_i \leq 1 \;\; \forall i \in \mathcal{N}
\end{aligned} \tag{5.7}$$

The first objective represents social welfare in terms of aggregate utility defined as $U(E_i, d_i) := log(1 + \frac{E_i}{d_i})$ which is the utility of allocated energy E_i to a user against demand d_i. The second objective relates to the losses incurred on providing energy to a user. Both objectives are conflicting in nature; therefore, the optimization, in this case, transforms to the Pareto optimality. Among the constraints, the first two relate to resource allocation, and the other two include the bus voltage limits and voltage stability index.

The optimization algorithm $f^o(5.3)$ rations the energy by solving the optimization problem described in this section and find out trade-off solutions. For this work, we utilize an evolutionary optimization technique from our earlier work [128] for simultaneous optimization of welfare and losses.

5.3 Blockchain System Model

A blockchain system design depends on the desired operation and a specific use case [111]. Power networks' operational characteristics provide several opportunities to simplify and optimize a blockchain model. Predominantly, a distribution system forms a closed network where the subscribers must register with a utility for getting services. The feature adds a security layer. Therefore, relatively less complex private blockchain systems may fulfill system objectives. Next, in a post-disaster scenario, the number of users is limited due to the smaller network island size. So the blockchain system scalability concerns are less stringent. Moreover, some users have a surplus supply that they can use to run mining and validation tasks, whereas others lack this capability because they do not have enough energy. These characteristics allow scenario-specific optimization of the blockchain system to achieve higher efficiency in energy usage, computation, and transaction throughput.

Most importantly, the scarcity of supply imposes critical operational constraints on the design of a blockchain system. Thus, a complicated consensus protocol such as proof-of-work (PoW) may not be viable in this scenario. Therefore, we propose a consortium blockchain approach and a new consensus protocol for the service restoration problem. The model structure is described next.

5.3.1 System Infrastructure

A representative model of the blockchain system for the service restoration is depicted in Fig. 4.1 and salient elements are described in Table 5.1. Microgrids form the nodes in the blockchain system. However, their roles vary depending on the available supply. MG with surplus capacity can take on a miner or validator role, whereas those who lack supply only have read access to the ledger. As the operation progresses, the nodes switch roles with the changes in energy supply. Therefore, a node may serve as a miner, but later, it switches to a limited node, losing miner status due to a lack of sufficient supply. The

distribution system operator (DSO) plays a special role in blockchain-based restoration. Its most prominent functions include: first, act as registration or certification authority for network nodes. Second, it matches the suppliers and demanding MGs using a peer matching criterion to transact energy employing smart contracts. Third, managing the commodity valuation-based energy pricing, keeping a record of users' energy contribution and reputation. Finally, we implement a consortium blockchain where DSO admits nodes to the consortium based on nodes' supply state and reputation.

5.3.2 Node Reputation

A nodes' reputation is a function of its energy contribution and the number of blocks it successfully mines. As a node contributes energy, its reputation increases based on the amount of energy and the current commodity value. However, if a node opts to donate energy, the increase depends on its agreement with the grid. Additionally, successful mining also helps increase a nodes' reputation. The system rewards a miner with a unit of energy on successful mining. Based on these factors, nodes' reputation is given as

$$\mathcal{R}_i = \sum_{j \in \tau} (c_{ij} + \Gamma_{ij} \mathcal{V}_j \bar{E}^m) \;\; \forall\, \Gamma \in \{0, 1\} \tag{5.8}$$

where c_{ij} is the historical contribution of a node in jth time slot. The term $(\Gamma_{ij} \mathcal{V}_j \bar{E}^m)$ is the reward a miner gets for mining a block. Here, $\bar{E}^m$ is an estimation of the energy consumption for mining operation by an average node, $\mathcal{V}_j$ represents the commodity valuation-based energy value for a given slot. The binary variable Γ_{ij} is set true when a node successfully mines a block, and otherwise, it is false. When a node borrows energy, the contribution c_{ij} is negative, so its reputation decreases accordingly. If a node lacks energy, it does not participate in mining or validation, so the related consumption is zero, and its reputation does not change.

5.3.3 Consortium Formulation

In consortium blockchain, consortium size directly impacts decentralization. It also shapes the resilience, energy efficiency, and security of a consensus protocol. A larger consortium implies a greater decentralized control and resilience against collusion by dishonest nodes. However, it increases the number of nodes executing consensus resulting in increased consumption. Moreover, for power applications involving DER, consensus protocol may embed powerflow studies to assess the impact of a proposed block on the network operations, which critically shapes energy cost and viability of the consensus.

In a post-disaster network, active measures to optimize consortium design considering available supply conditions and network size are necessary. Therefore, the proposed approach controls the size of the consortium by defining a mining eligibility threshold $\mathcal{R}^{con}$.

The DSO defines a mining eligibility threshold for the next slot after MGs' demand and supply data are available. It then admits nodes to the consortium if they have sufficient surplus energy and a reputation above the threshold for the operation window.

5.3.4 Consensus Mechanism

A blockchain consensus protocol aims to ensure that all nodes agree on the distributed ledger's common state. It maintains correct ordering and integrity of the transactions [129]. Consensus protocols comprise five major components, including block proposal, information propagation, block validation, incentive mechanism, and block finalization [130]. Next, we briefly specify the structure of these components relative to the proposed model.

Block Proposal

Block proposal is a major segment in a consensus protocol. Most of the new consensus research is happening in this domain [130]. The component itself deals with creating a block and attaching generation proofs.

The proposed consensus protocol is called proof of welfare (PoWel). It solves the rationing problem described in section 5.2.2 to get an energy allocation block with the highest value of the proof, i.e., PoWel. The selection of an allocation block based on PoWel caters to prioritizing critical loads and system objectives of achieving maximum coverage and minimizing losses. Besides, it complies with the resource and voltage stability constraints for preserving stable network operation.

Figure 5.2 shows the structure of the consensus algorithm. The algorithm runs on the mining nodes that are current members of the consortium. To propose a new block, first, a node solves a weighted rationing problem (5.1) i.e., step 2 in Algorithm 5.2. At this stage, energy allocation occurs based on the service priorities determined by the load criticality, users' historical contribution, or their combination. It enables prioritization of critical load and recompense faithful system contributors. Next, in step 5, the excess energy is allocated through the optimal rationing by invoking a multi-objective evolutionary technique based on SPEA-II, i.e, steps 10 - 21. Here, the allocation occurs considering the objective performance. As the evolution progresses, the algorithm performs loadflow studies for each candidate—energy allocation block in the current population to ascertain its impact on power network state and constraints compliance. The process discards infeasible solutions. Finally, as the evolution process completes, multiple Pareto optimal solutions evolve as Pareto front members. Then, for each solution in the Pareto front, PoWel value is determined using aggregation approach [131], as follows

$$PoWel = \eta_1 \frac{f_1(E_i)}{max f_1(E_i)} - \eta_2 \frac{f_2(E_i)}{max f_2(E_i)} \; \forall i \in \mathcal{N}, \tag{5.9}$$

where $f_j|\ \{j := 1,\ 2\}$ are the two objective functions and $\eta_j|\ 0 < \eta_j \leq 1,\ \sum \eta_j = 1$; set relative bias of the PoWel towards the welfare or the system losses. Finally, based on the PoWel value, a node selects the best solution from the Pareto front and proposes a new energy allocation block to the consortium members for voting and subsequent addition to the blockchain upon selection.

Block Structure

The block comprises the header and the body components. The block header's main contents include block index, timestamp, the hash of the previous block, Merkle root, and the PoWel. Mining nodes determine the PoWel value that is then used in consensus building. Blocks' body comprise parameters like $\vec{P},\ \vec{D},\ \vec{C},\ E^p,$ and PoWel. Whereas the other algorithm and system parameters used in the evolutionary process being fixed do not require storing in the blockchain.

Block Validation

The next component deals with the validation and correctness of the proposed block. A proposing MG broadcasts the energy allocation vector $\vec{E}$ and the proof, i.e., the PoWel value, to the consortium nodes. Then, the consortium nodes evaluate the objective function and constraints to verify the proof (5.9). Further, these nodes vote for the proposed block. A block becomes part of the chain if voted in favor by two-thirds validation nodes.

Incentive Mechanism

The system rewards a miner for the successful mining of a block. The reward $\mathcal{V}_j \bar{E}^m$ depends on the average energy cost of mining $\bar{E}^m$ and the energy value in the current operation window $\mathcal{V}_j$. The reward increases nodes' historical contribution, enabling it to get additional allocation once the main grid restores.

Energy Efficiency

A consensus protocols' energy efficiency is critical, especially in limited supply scenarios like in the aftermath of a disaster. Bitcoin network that uses Proof of Work (PoW) as consensus mechanism consumes 128.84 TWh [132] electricity annually, which accounts for 0.59% of the worlds' total consumption. Such a mechanism is not viable for energy sharing or trade in a limited supply scenario due to higher energy cost and complexity.

Operational Constraints

Power network imposes hard operational constraints on peer-to-peer energy exchanges. Thus, the energy transactions need coordination to avoid underlying network constraints

violation, instability, and voltage collapse. The proposed approach incorporates the operational constraints during allocation, ensuring that the winning block complies with the network constraints. The direct incorporation of the constraints into the allocation process adds resilience to power network operation [112].

Algorithm I: Proof of Welfare (PoWel) Consensus

Require: E^p, $\vec{P} := \{p_i\}, \vec{C} := \{c_i\}$, $\vec{D} := \{d_i\}$, power network data, and system parameters

Ensure: Select block with highest PoWel

1: **if** $E^p - \sum_{i \in \mathcal{N}} d_i \leq 0$ **then**
2: Solve weighted rationing problem (5.1)
3: Find residual energy E^{res} and unmet demand d_i^u
4: **if** E^{res} & $d_i^u > 0$ **then**
5: Solve optimal rationing problem (5.3):
Execute CORE BLOCK ▷ Steps {10 - 21}
6: **end if**
7: Determine PoWel (5.9)
8: **end if**
9: Select PF member with the highest PoWel

10: **procedure Core Block**
11: Generate initial population: $\mathbf{E^1}$
12: **for all** $i \in generations$ **do**
13: Run powerflow analysis
14: Determine voltage stability index SI
15: Handle constraints
16: Perform environmental selection
17: Run hybrid recombination operation
18: Apply mutation
19: **end for**
20: Return Pareto front (PF)
21: **end procedure**

[1] n x $\mathcal{N}$ matrix, where is n is user defined population size and $\mathcal{N}$ is number of MGs.

Figure 5.2: Evolutionary algorithm based consensus mechanism

Algorithm II: Blockchain Enabled Service Restoration

Require: $\overrightarrow{E^{p@}}$, $\vec{P} := \{p_i\}$, $\vec{C} := \{c_i\}$, $\vec{D} := \{d_i\}$, $\vec{\mathcal{R}} := \{r_i\}$, power system data, and other parameters

Ensure: Select a new energy allocation block $\vec{E}$

1: Establish mining eligibility threshold ($\mathcal{R}^{con}$)
2: **if** E_i^{s*} & $\mathcal{R}_i > \mathcal{R}^{con}$ **then**
3: Admit MG to consortium
4: **end if**
5: **if** Consortium Member **then**
6: Mine a new block—Execute Algorithm I
7: Broadcast new block ($\vec{E}$) & PoWel within consortium
8: Selects new block with highest PoWel value
9: Broadcast the winner block in the network
10: **end if**
11: Match supplier and demanding MGs
12: Execute smart contracts —peers transact energy
13: Update MGs' reputation considering energy contribution or allocation
14: Commit current block to the chain

@ Net energy pledged by MGs as donation and trade

* $E_i^s \in \{0, 1\}$ Nodes' energy state; 1 means node has sufficient energy for mining and consensus operations

Figure 5.3: Blockchain enabled service restoration approach

5.4 Service Restoration Framework

The section describes the operation of the blockchain-enabled service restoration framework; its architectural snapshot is as shown in Fig. 5.3. The algorithm executes on DSO and the consortium nodes. The framework has four operational phases: initialization, consortium formulation —steps 1 to 4, consensus —steps 5 to 10 , and execution —steps 11 to 14.

During the initialization, the nodes load the latest blockchain state, the available energy E^p, individual demand $\vec{D}$, load service priorities $\vec{P}$, contribution $\vec{C}$, and the other system parameters. Also, the MGs publish their demand and the surplus energy data for the future operational slot. Next, the process of consortium formation begins; first, based on the networks' state, especially the supply conditions, DSO establishes a mining eligibility threshold $\mathcal{R}^{con}$. It then admits nodes to the consortium provided they have sufficient supply for mining and validation tasks indicated by E_i^s and a reputation higher than the set threshold. Then, in the consensus phase, the consortium nodes start the mining process by executing Algorithm I and propose an energy allocation block $\vec{E}$. The proposing

node broadcasts the block within the consortium after attaching the proof value, i.e., PoWel. The nodes validate and vote for candidate blocks to select one with the highest PoWel value. Thus a block that achieves two-thirds votes wins the mining round. PoWel based selection of the winning block enables: First, restoration of critical loads based on service priorities determined through load priority, users' historical contribution, or their combination. Second, it maximizes social welfare for the disaster struck the community by maximizing coverage. Third, it optimally utilizes limited supply by considering and effectively minimizing losses. Finally, the winning block preserves the stability of the network by following resource and underlying network constraints.

Finally, in the execution phase, DSO broadcasts the block to all nodes in the network and matches peers to share energy using a peer matching algorithm available in energy sharing literature [133]. The matched peers transact energy using smart contracts. Subsequently, the DSO updates individual nodes' contribution or reputation record considering their contribution to the system or the energy allocation, and the block is committed to the blockchain.

5.5 Evaluation and Assessment

This section includes the analysis of the proposed approach from the security viewpoint following some commonly used metrics [134] and performance through simulation considering the system objectives.

5.5.1 Security Analysis

Unforgeablity

The system stores users' contribution, load priorities, node reputation, allocation, etc., securely in a blockchain. This unforgeable storage precludes manipulating these parameters by malicious users to get higher allocation or become consortium members to compromise the system. Secondly, a contribution mechanism that depends on the allocation makes the approach resilient to collusion by nodes.

Fairness

The system allocates energy solely based on load service priorities and nodes' contribution. Moreover, the contribution data is stored in an unforgeable blockchain ledger which adds to user trust. Secondly, the system uses nodes' energy state and reputation to admit nodes to the consortium. Thus it does not discriminate and provides a fair chance to all network nodes to earn rewards.

Trustless Operation

The approach uses the contribution and priority values stored in a blockchain. Therefore, it avoids most of the trust issues that can arise through collusion of nodes to increase contribution or allocation artificially. Also, fair and merit-based selection of nodes for consortium promotes user trust in the system.

Energy Consumption

The proposed approach simplifies the consensus by tapping on the power network's closed nature and limiting the consortium size to reduce nodes running the consensus algorithm. Both measures help make it very energy efficient. During the operation, a mining node calculates the PoWel value and sends the allocation vector along with other systems parameters to all validating nodes. The validation involves the evaluation of the objective function only. The process is very energy-efficient, making the approach suitable for limited supply scenarios.

Decentralization

The use of blockchain enables trustless, decentralized exchanges of energy among nodes. After DSO matches the exchanging peers, they transact energy by invoking smart contracts stored in individual nodes.

Scalablity

In a post-disaster network, the number of users is limited due to network islands' size. Therefore, a permissioned blockchain scheme like PoWel can provide adequate scalability. Similarly, if the consensus protocol operates at the MG level, the scheme can still adequately address the scalability need of the blockchain system because of the limited number of users within a microgrid.

5.5.2 Performance Results

For the performance analysis, we use IEEE 33-bus and 69-bus radial distribution system [95] where each bus represents a microgrid. The power network parameters and the demand of the individual MGs are as in [95]. We have three MGs in 33-bus and six in the 69-bus system with surplus supply as shown in Table 5.2. These MGs take part in the mining process for a new block. We use the loadflow analysis algorithm given in per [89] for this study. The evolutionary algorithm parameters, including initial population, number of generations, mutation, and crossover probabilities, are shown in Table 5.2.

Table 5.2: Simulation Parameters

Microgrids with surplus supply					
	33-Bus			69-Bus	
Bus	P(pu)	Q(pu)	Bus	P(pu)	Q(pu)
3	0.7381	0.6190	3	0.1608	0.4019
18	0	0.0476	11	0.2130	0.2460
33	0.1190	0.0476	14	0.338	0.1112
			17	0.9968	0.3738
			20	0.3288	0.2809
			26	0.0209	0.0161
Algorithm Parameters					
Population size	50		η_1, η_2	0.5	
Max generations	120		ψ	1,2,3	
Crossover prob	0.75		$\mathcal{N}$	33, 69	
Mutation prob	0.25				

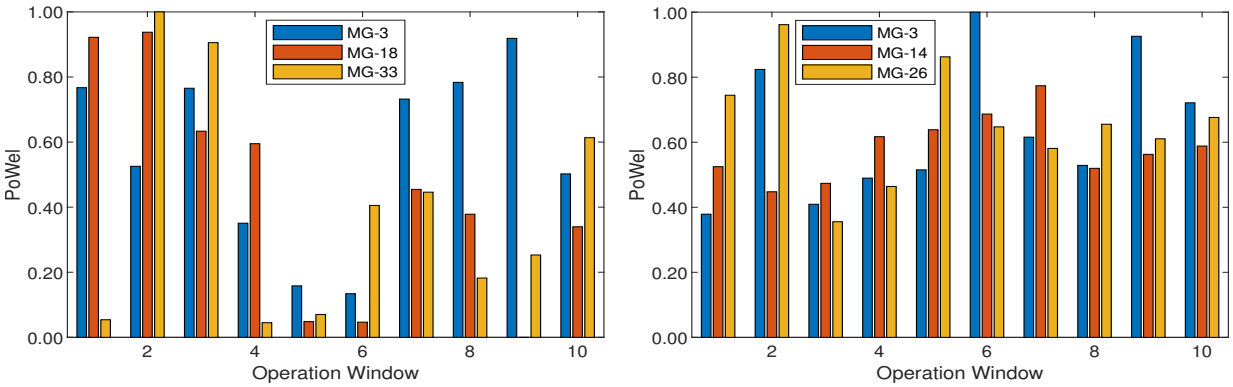

(a) 33 Bus **(b)** 69 Bus

Figure 5.4: Proof of welfare (PoWel) by three representative mining MGs across 10 operation slots in 33 and 69-bus systems.

Proof of Welfare

For generating a winning block, miners run the algorithm listed in Fig. 5.2 including its embedded evolutionary process. Since each miner starts with a random initial state, PoWel values achieved by miners vary. A miner that generates an allocation vector with the highest proof value (PoWel) wins the mining round. We analyze the PoWel values generated by three miners each from 33 and 69-bus systems over ten operation slots for this experiment. Figure 5.4 reports PoWel values generated by three representative MGs from the two networks. The results indicate that the PoWel values achieved by different

miners vary significantly. Therefore, the PoWel based mining process can effectively select the best block that meets the system objectives.

Welfare and Loss

The results in Fig. 5.5 show values of the two system objectives, i.e., welfare and power loss achieved by a proposed block. For this experiment, we analyze welfare and losses in the 33-bus system for three representative solutions selected from the two extremes and the middle of the Pareto front achieved by a miner. The two extremes relate to cases where both welfare and loss have low values as in Fig. 5.5a and vice versa as in Fig. 5.5b, whereas the middle is a tradeoff solution as in Fig. 5.5c . Next, each graph follows a table showing

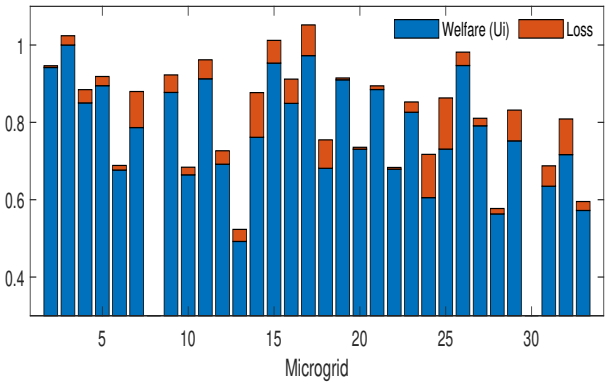

	Min	Mean	Max	Median	Std	Range
Welfare	0.1959	0.7855	1.0583	0.8009	0.2050	0.8625
Loss	2.3601e-04	0.0024	0.0070	0.0018	0.0019	0.0068

(a) Low

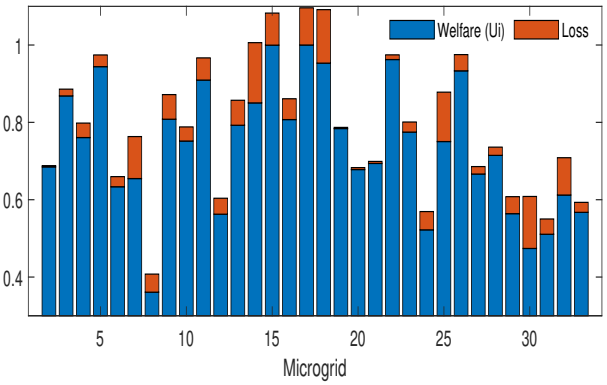

	Min	Mean	Max	Median	Std	Range
Welfare	0.3868	0.7889	1.0719	0.8051	0.1763	0.6851
Loss	1.5901e-04	0.0029	0.0083	0.0022	0.0023	0.0082

(b) mid

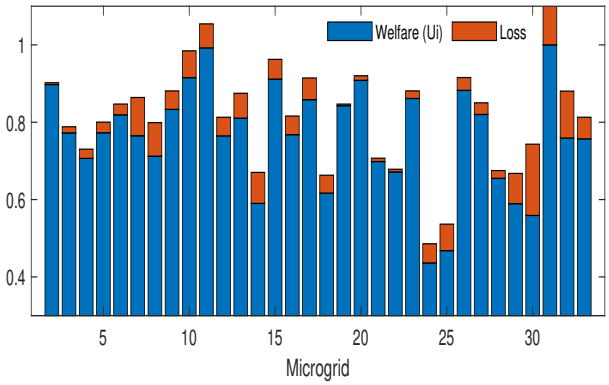

	Min	Mean	Max	Median	Std	Range
Welfare	0.4585	0.8019	1.0510	0.8094	0.1454	0.5925
Loss	2.1710e-04	0.0029	0.0098	0.0025	0.0024	0.0096

(c) High

Figure 5.5: Welfare and loss plot: Three solutions selected from two extremes and the middle of a Pareto front obtained by a miner.

important statistics for two objectives for selected solutions. For plotting, the welfare and loss values are normalized, and loss values are multiplied by 10; otherwise, relatively higher welfare values obscure loss variations.

Network Stability

This experiment analyses the impact of PoWel based winner block selection mechanism on network stability. We analyze stability index (SI) and voltage profile across each bus in 33 and 69-bus systems. We consider three representative solutions from the two extremes and the middle of the Pareto front achieved by a mining node. The stability index results are as per Fig. 5.6&5.7 whereas Fig. 5.8&5.9 show the bus voltage profile. The results show that the algorithm preserves network stability as the index in all cases is well below the threshold of unity value. Moreover, the bus voltages in both networks for all selected solutions are well within 5% of nominal voltage. Therefore, PoWel based winning block selection effectively preserves network stability by maintaining resource and voltage stability constraints compliance.

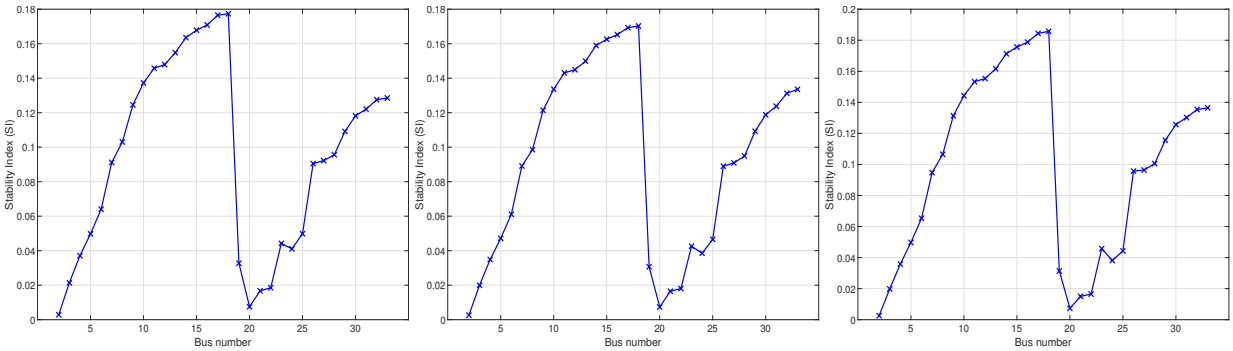

(a) Low **(b)** mid **(c)** High

Figure 5.6: Stability index for three representative solutions from two extremes and middle of a Pareto front in a IEEE-33 bus system.

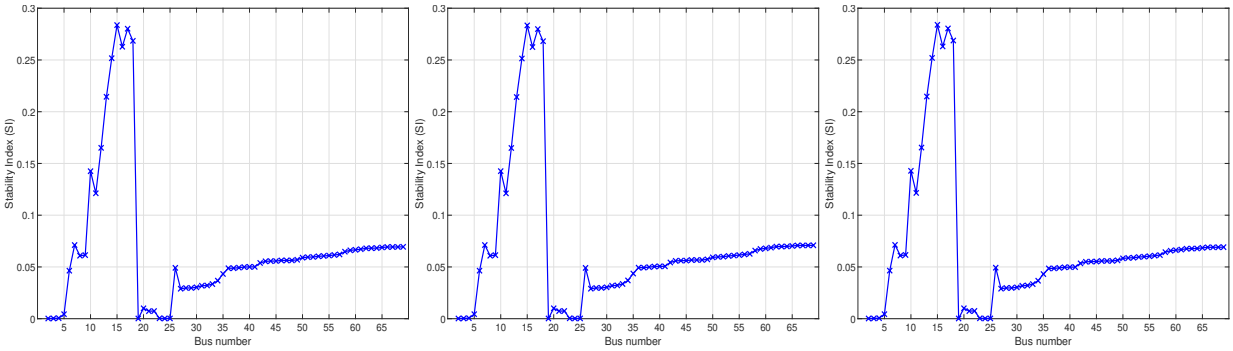

(a) Low **(b)** mid **(c)** High

Figure 5.7: Stability index for three three representative solutions from two extremes and middle of a Pareto front in a IEEE-69 bus system.

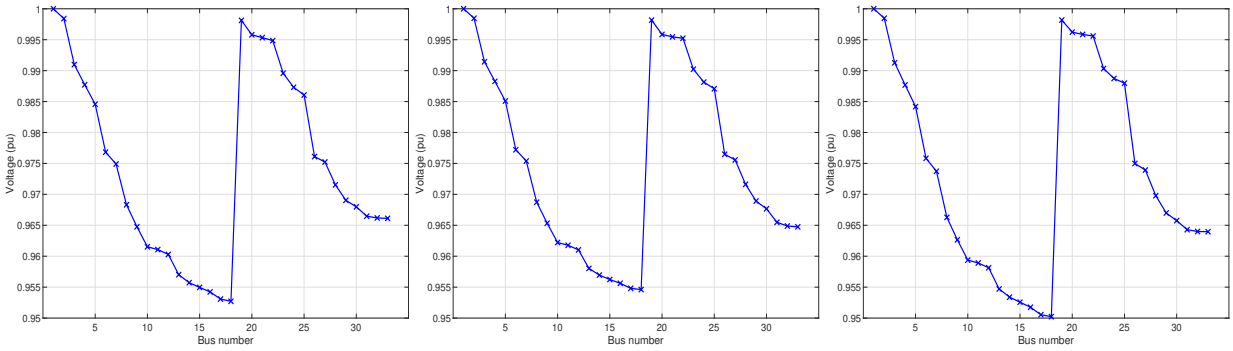

(a) Low **(b)** mid **(c)** High

Figure 5.8: Bus voltage profile for three representative solutions from two extremes and middle of a Pareto front in a IEEE-33 bus system.

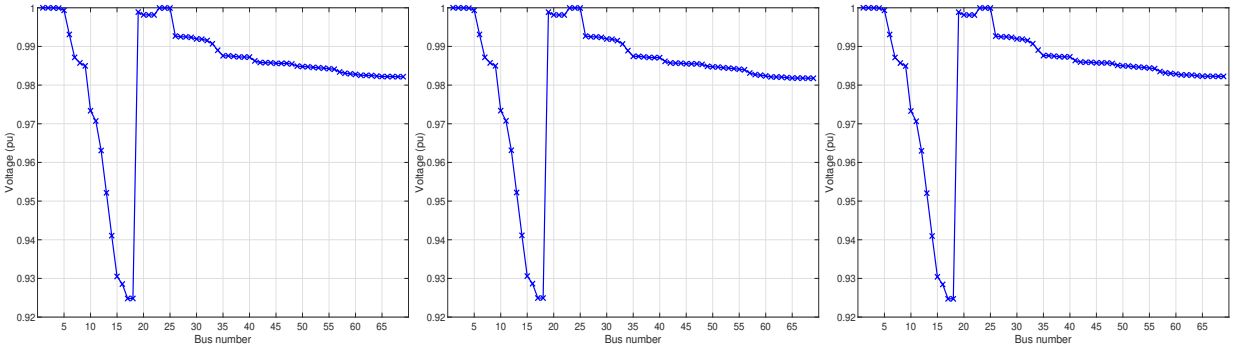

(a) Low **(b)** mid **(c)** High

Figure 5.9: Bus voltage profile for three three representative solutions from two extremes and middle of a Pareto front in a IEEE-69 bus system.

5.6 Conclusion

The chapter established the efficacy of the blockchain technology, indicating that it can effectively be utilized for service restoration using energy crowdsourced from DERs in a post-disaster distribution system. Its application in limited supply scenarios, e.g., in the aftermath of a disaster, requires optimization in its design considering the target network characteristics and system objectives. Our proposed approach utilizes distribution system features for such optimization; it fuses the resource and voltage stability constraints into the consensus mechanism to preserve distribution system stability. Moreover, our work employs miners' reputation and supply state-based consortium formulation to reduce the computational complexity and energy consumption of the blockchain framework. The security and performance analysis in IEEE-33 and 69 bus systems confirm the effectiveness of the proposed approach. The results show that PoWel based mining process effectively selects the best energy block that meets the system objectives of minimizing losses and maximizing welfare. In addition, it helps maintain the stability index and bus voltages within acceptable limits enhancing network stability. As an extension of this work, one

avenue is to analyze the impact of consortium size on the security and performance of the proposed scheme in the future.

Chapter 6

Conclusion and Future Work

This dissertation investigated the optimization of power system operations. We focused on two optimization problems from the demand management and the distribution system operations.

In the first case, we worked on the data center profit maximization. The data center profit was formulated in terms of two conflicting objectives, i.e., revenue and expense. The number of requests serviced according to the SLA determines the profit and is independent of the cost of electricity. On the other hand, the expense depends on the power consumption and the cost of energy. The focus of the research is to minimize consumption while utilizing diversity in electricity prices in a deregulated energy market. We proposed an evolutionary technique based on a higher-level heuristic to optimize data center revenue and expense objectives simultaneously. The scheme utilizes real-time variations of power prices across different geographic regions for optimal request routing and resource allocation decisions. Next, we proposed an integrative strategy by incorporating power network stability into the data center optimization. By considering the power network state during optimization, the data center can utilize lower power tariffs and help the grid integrate more renewable sources without catering to costly generation reserves. It also helps the grid to provide a more stable power supply to its users.

The second problem which we have investigated deals with the optimization of the distribution system. We proposed a framework to mitigate the effects of power blackouts through energy donation. The approach envisages a smart microgrid (MG) based smart distribution network where MGs with surplus supply donate or trade energy with the local grid, which is then used to help those in need. The objectives of the donation network controller are to maximize welfare and utilize limited resources optimally. The approach models welfare in terms of maximum coverage or minimizing unserviced load and to optimally use a limited supply, it embeds minimization of losses as the other objective. We also proposed an energy allocation scheme that allocates energy to MGs according to the criticality of load they serve, their historical contribution, or based on both. We proposed a

heuristic method based on the evolutionary optimization technique. We then extended the work by proposing a blockchain approach for energy sharing during restoration following a disaster. The scheme is designed considering the characteristics of the limited supply scenarios.

As future work, the research problems investigated in this dissertation may be extended as: First, for the work on data center optimization, we intend to enhance the system model by incorporating the deactivation of the underutilized servers to conserve energy spent on underutilized servers. Next, as an extension of the energy donation work, one avenue is to incorporate techniques for managing stability issues resulting from energy exchanges in DERs-based restoration at the local level. Finally, the analysis of the impact of consortium size on the security and performance of blockchain-based energy sharing is another interesting direction to extend the work.

Appendix A

List of Publications

1. S. Khalid and I. Ahmad, "Dual Optimization of Revenue and Expense in Geo-Distributed Data Centers using the Smart Grid," *(under review).*
2. S.Khalid and I. Ahmad, "QoS and power network stability aware simultaneous optimization of data center revenue and expenses *Sustainable Computing: Informatics and Systems*, vol. 30, p. 100 459, 2021.
3. S. Khalid, I. Ahmad, "Optimizing Energy Donation for Service Restoration in a Power Distribution System," *(under review).*
4. S. Khalid and I. Ahmad, "Energy Sharing for Service Restoration using a Consortium Blockchain Approach in a Power Distribution System," *(under review).*
5. S. Khalid, A. Ishfaq and K. Mohammad E., "An Evolutionary Approach to Optimize Data Center Profit in Smart Grid Environment," *2019 2nd International Conference on Data Intelligence and Security (ICDIS)*, 2019, pp. 89-96.
6. S. Khalid and I. Ahmad, "Service restoration using energy donation in a distribution system during crisis," in *2020 International Conference on Smart Grids and Energy Systems (SGES)*, 2020, pp. 562–567.
7. S. Khalid and I. Ahmad, "Blockchain based service restoration in a power distribution system during crisis," in *2021 IEEE Madrid PowerTech*, 2021.
8. S. Khalid and I. Ahmad, *"Optimizing Operations in IoT-Enabled Smart Grid,"* Springer Handbook on Internet of Things, S. Ziegler and A. Skarmeta, Eds., Berlin, Heidelberg (accepted).
9. S. Khalid and I. Ahmad, *"IoT for sustainable development,"* Springer Handbook on Internet of Things, S. Ziegler and A. Skarmeta, Eds., Berlin, Heidelberg (minor revision due).

Bibliography

[1] X. Fang, S. Misra, G. Xue, and D. Yang, "Smart grid — the new and improved power grid: A survey," *IEEE Communications Surveys Tutorials*, vol. 14, no. 4, pp. 944–980, Fourth 2012.

[2] U.S. Energy Information Administration - EIA, "Demand for electricity changes through the day - today in energy," [Online; accessed 02-Dec-2019]. [Online]. Available: https://www.eia.gov/todayinenergy/detail.php?id=830

[3] A. Satre-Meloy, M. Diakonova, and P. Grünewald, "Daily life and demand: an analysis of intra-day variations in residential electricity consumption with time-use data," *Energy Efficiency*, Apr 2019. [Online]. Available: https://doi.org/10.1007/s12053-019-09791-1

[4] E. P. A. (EPA), "U.S. greenhouse gas inventory and sinks (1990 -2017)," in *U.S. Greenhouse Gas Inventory and Sinks (1990 -2017*, ser. 2019. Washington, DC, USA: EPA, 2019.

[5] L. Yu, T. Jiang, and Y. Zou, "Price-sensitivity aware load balancing for geographically distributed internet data centers in smart grid environment," *IEEE Trans. Cloud Comput.*, vol. 6, no. 4, pp. 1125–1135, 2018.

[6] A. Wierman, Z. Liu, I. Liu, and H. Mohsenian-Rad, "Opportunities and challenges for data center demand response," in *International Green Computing Conference*, 2014, pp. 1–10.

[7] N. H. Tran, D. H. Tran, S. Ren, Z. Han, E. Huh, and C. S. Hong, "How geo-distributed data centers do demand response: A game-theoretic approach," *IEEE Transactions on Smart Grid*, vol. 7, no. 2, pp. 937–947, 2016.

[8] H. Hu, Y. Wen, L. Yin, and L. Qiu, "Towards cost-efficient workload scheduling for a tango between geo-distributed data center and power grid," in *2016 IEEE International Conference on Communications (ICC)*, 2016, pp. 1–7.

[9] A. Rahman, X. Liu, and F. Kong, "A survey on geographic load balancing based data center power management in the smart grid environment," *IEEE Communications Surveys Tutorials*, vol. 16, no. 1, pp. 214–233, 2014.

[10] M. M. Moghaddam, M. H. Manshaei, W. Saad, and M. Goudarzi, "On data center demand response: A cloud federation approach," *IEEE Access*, vol. 7, pp. 101 829–101 843, 2019.

[11] H. Wang, J. Huang, X. Lin, and H. Mohsenian-Rad, "Proactive demand response for data centers: A win-win solution," *IEEE Transactions on Smart Grid*, vol. 7, no. 3, pp. 1584–1596, 2016.

[12] ——, "Exploring smart grid and data center interactions for electric power load balancing," *SIGMETRICS Perform. Eval. Rev.*, vol. 41, no. 3, pp. 89–94, Jan. 2014.

[13] Y. Wang, X. Lin, and M. Pedram, "A stackelberg game-based optimization framework of the smart grid with distributed PV power generations and data centers," *IEEE Trans. Energy Convers.*, vol. 29, no. 4, pp. 978–987, Dec 2014.

[14] B. Aksanli, A. S. Akyurek, and T. Rosing, "Minimizing the effects of data centers on microgrid stability," in *2015 Sixth International Green and Sustainable Computing Conference (IGSC)*, 2015, pp. 1–9.

[15] S. Park, J. Lee, S. Bae, G. Hwang, and J. K. Choi, "Contribution-based energy-trading mechanism in microgrids for future smart grid: A game theoretic approach," *IEEE Transactions on Industrial Electronics*, vol. 63, no. 7, pp. 4255–4265, 2016.

[16] A. M. Jadhav and N. R. Patne, "Priority-based energy scheduling in a smart distributed network with multiple microgrids," *IEEE Trans. Ind. Informat.*, vol. 13, no. 6, pp. 3134–3143, 2017.

[17] E. Mengelkamp, J. Gärttner, K. Rock, S. Kessler, L. Orsini, and C. Weinhardt, "Designing microgrid energy markets: A case study: The brooklyn microgrid," *Applied Energy*, vol. 210, pp. 870–880, 2018. [Online]. Available: https://www.sciencedirect.com/science/article/pii/S030626191730805X

[18] S. Wang, A. F. Taha, J. Wang, K. Kvaternik, and A. Hahn, "Energy crowdsourcing and peer-to-peer energy trading in blockchain-enabled smart grids," *IEEE Trans. Syst., Man, Cybern. Syst.*, vol. 49, no. 8, pp. 1612–1623, 2019.

[19] Q. Yang and H. Wang, "Blockchain-empowered socially optimal transactive energy system: Framework and implementation," *IEEE Trans. Ind. Informat.*, vol. 17, no. 5, pp. 3122–3132, 2021.

[20] F. Luo, Z. Y. Dong, G. Liang, J. Murata, and Z. Xu, "A distributed electricity trading system in active distribution networks based on multi-agent coalition and blockchain," *IEEE Trans. Power Syst.*, vol. 34, no. 5, pp. 4097–4108, 2019.

[21] Q. Yang and H. Wang, "Privacy-preserving transactive energy management for iot-aided smart homes via blockchain," *IEEE Internet of Things Journal*, vol. 8, no. 14, pp. 11 463–11 475, 2021.

[22] D. Ardagna, M. Trubian, and L. Zhang, "SLA based resource allocation policies in autonomic environments," *J. Parallel Distrib. Comput.*, vol. 67, no. 3, pp. 259–270, Mar. 2007.

[23] D. Ardagna, B. Panicucci, M. Trubian, and L. Zhang, "Energy-aware autonomic resource allocation in multitier virtualized environments," *IEEE Trans. Serv. Comput.*, vol. 5, no. 1, pp. 2–19, Jan 2012.

[24] J. Mei, K. Li, A. Ouyang, and K. Li, "A profit maximization scheme with guaranteed quality of service in cloud computing," *IEEE Trans. Computers*, vol. 64, no. 11, pp. 3064–3078, Nov 2015.

[25] J. Mei, K. Li, and K. Li, "Customer-satisfaction-aware optimal multiserver configuration for profit maximization in cloud computing," *IEEE Trans. Sustain. Comput.*, vol. 2, no. 1, pp. 17–29, Jan 2017.

[26] I. Rodero, E. K. Lee, D. Pompili, M. Parashar, M. Gamell, and R. J. Figueiredo, "Towards energy-efficient reactive thermal management in instrumented datacenters," in *2010 11th IEEE/ACM Int. Conf. Grid Computing*, Oct 2010, pp. 321–328.

[27] Y. Song, Y. Sun, and W. Shi, "A two-tiered on-demand resource allocation mechanism for VM-based data centers," *IEEE Trans. Serv. Comput.*, vol. 6, no. 1, pp. 116–129, First 2013.

[28] A. Qureshi, R. Weber, H. Balakrishnan, J. Guttag, and B. Maggs, "Cutting the electric bill for internet-scale systems," *SIGCOMM Comput. Commun. Rev.*, vol. 39, no. 4, pp. 123–134, Aug. 2009.

[29] A. H. Mohsenian-Rad and A. Leon-Garcia, "Coordination of cloud computing and smart power grids," in *2010 1st IEEE Int. Conf. Smart Grid Commun.*, Oct 2010, pp. 368–372.

[30] M. Ghamkhari, A. Wierman, and H. Mohsenian-Rad, "Energy portfolio optimization of data centers," *IEEE Trans. Smart Grid*, vol. 8, no. 4, pp. 1898–1910, July 2017.

[31] M. Ghamkhari and H. Mohsenian-Rad, "Energy and performance management of green data centers: A profit maximization approach," *IEEE Trans. Smart Grid*, vol. 4, no. 2, pp. 1017–1025, June 2013.

[32] A. Kiani and N. Ansari, "Profit maximization for geographically dispersed green data centers," *IEEE Trans. Smart Grid*, vol. 9, no. 2, pp. 703–711, March 2018.

[33] L. Gu, D. Zeng, A. Barnawi, S. Guo, and I. Stojmenovic, "Optimal task placement with QoS constraints in geo-distributed data centers using DVFS," *IEEE Trans. Comput.*, vol. 64, no. 7, pp. 2049–2059, July 2015.

[34] S. Liu, S. Ren, G. Quan, M. Zhao, and S. Ren, "Profit aware load balancing for distributed cloud data centers," in *2013 IEEE 27th Int. Symp. Parallel and Distributed Processing*, May 2013, pp. 611–622.

[35] K. Kim, F. Yang, V. M. Zavala, and A. A. Chien, "Data centers as dispatchable loads to harness stranded power," *IEEE Trans. on Sustain. Energy*, vol. 8, no. 1, pp. 208–218, 2017.

[36] H. Kim, J. Lee, S. Bahrami, and V. W. S. Wong, "Direct energy trading of microgrids in distribution energy market," *IEEE Trans. Power Syst.*, vol. 35, no. 1, pp. 639–651, Jan. 2020.

[37] D. Gregoratti and J. Matamoros, "Distributed energy trading: The multiple-microgrid case," *IEEE Trans. Ind. Electron.*, vol. 62, no. 4, pp. 2551–2559, 2015.

[38] K. Rahbar, C. C. Chai, and R. Zhang, "Energy cooperation optimization in microgrids with renewable energy integration," *IEEE Trans. Smart Grid*, vol. 9, no. 2, pp. 1482–1493, Mar. 2018.

[39] C. Zhang, J. Wu, Y. Zhou, M. Cheng, and C. Long, "Peer-to-peer energy trading in a microgrid," *Applied Energy*, vol. 220, pp. 1–12, 2018.

[40] Z. Huang, T. Zhu, Y. Gu, D. Irwin, A. Mishra, and P. Shenoy, "Minimizing electricity costs by sharing energy in sustainable microgrids," in *Proc. 1st ACM Conf. Embedded Syst. for Energy-Efficient Buildings*, ser. BuildSys '14. New York, NY, USA: ACM, 2014, pp. 120–129. [Online]. Available: http://doi.acm.org/10.1145/2676061.2674063

[41] T. Zhu, Z. Huang, A. Sharma, J. Su, D. Irwin, A. Mishra, D. Menasche, and P. Shenoy, "Sharing renewable energy in smart microgrids," in *2013 ACM/IEEE Int. Conf. Cyber-Physical Syst. (ICCPS)*, April 2013, pp. 219–228.

[42] N. Liu, X. Yu, C. Wang, and J. Wang, "Energy sharing management for microgrids with PV prosumers: A stackelberg game approach," *IEEE Trans. Ind. Informat.*, vol. 13, no. 3, pp. 1088–1098, June 2017.

[43] S. Khalid and I. Ahmad, "Service restoration using energy donation in a distribution system during crisis," in *2020 International Conference on Smart Grids and Energy Systems (SGES)*, 2020, pp. 562–567.

[44] J. Guerrero, A. C. Chapman, and G. Verbič, "Decentralized p2p energy trading under network constraints in a low-voltage network," *IEEE Transactions on Smart Grid*, vol. 10, no. 5, pp. 5163–5173, 2019.

[45] S. Poudel and A. Dubey, "Critical load restoration using distributed energy resources for resilient power distribution system," *IEEE Trans. Power Syst.*, vol. 34, no. 1, pp. 52–63, 2019.

[46] Y. Xu, C. Liu, K. P. Schneider, F. K. Tuffner, and D. T. Ton, "Microgrids for service restoration to critical load in a resilient distribution system," *IEEE Trans. Smart Grid*, vol. 9, no. 1, pp. 426–437, 2018.

[47] H. Gao, Y. Chen, Y. Xu, and C. Liu, "Resilience-oriented critical load restoration using microgrids in distribution systems," *IEEE Trans. Smart Grid*, vol. 7, no. 6, pp. 2837–2848, 2016.

[48] C. Ju, S. Yao, and P. Wang, "Resilient post-disaster system reconfiguration for multiple energy service restoration," in *2017 IEEE Conf. Energy Internet and Energy System Integration (EI2)*, 2017, pp. 1–6.

[49] Y. Xu, C. Liu, Z. Wang, K. Mo, K. P. Schneider, F. K. Tuffner, and D. T. Ton, "Dgs for service restoration to critical loads in a secondary network," *IEEE Trans. Smart Grid*, vol. 10, no. 1, pp. 435–447, 2019.

[50] H. Ahmadi, A. Alsubaie, and J. R. Martí, "Distribution system restoration considering critical infrastructures interdependencies," in *2014 IEEE PES General Meeting — Conf. Expo.*, 2014, pp. 1–5.

[51] E. Masanet, A. Shehabi, N. Lei, S. Smith, and J. Koomey, "Recalibrating global data center energy-use estimates," *Science*, vol. 367, no. 6481, pp. 984–986, 2020. [Online]. Available: https://science.sciencemag.org/content/367/6481/984

[52] A. Shehabi, S. Smith, D. Sartor, R. Brown, M. Herrlin, J. Koomey, E. Masanet, N. Horner, and W. Lintner, "United states data center energy usage report," Berkeley, CA, USA, June 2016.

[53] Yale E360, "Energy hogs: Can world's huge data centers be made more efficient?" 2018, [Online; accessed 23- Oct- 2018]. [Online]. Available: https://e360.yale.edu/features/energy-hogs-can-huge-data-centers-be-made-more-efficient

[54] H. Qaiser, G. Shu, and A. Malik, "Utilization driven model for server consolidation in cloud data centers," *IEEE Access*, vol. 8, pp. 1998–2007, 2020.

[55] C. Guo, K. Xu, G. Shen, and M. Zukerman, "Temperature-aware virtual data center embedding to avoid hot spots in data centers," *IEEE Trans. Green Commun. Netw.*, vol. 5, no. 1, pp. 497–511, 2021.

[56] F. Ahmad and T. N. Vijaykumar, "Joint optimization of idle and cooling power in data centers while maintaining response time," *SIGPLAN Not.*, vol. 45, no. 3, pp. 243–256, Mar. 2010.

[57] K. Mukherjee, S. Khuller, and A. Deshpande, "Saving on cooling: The thermal scheduling problem," in *ACM SIGMETRICS Perform. Eval. Rev.*, vol. 40, no. 1. ACM, 2012, pp. 397–398.

[58] J. D. Moore, J. S. Chase, P. Ranganathan, and R. K. Sharma, "Making scheduling "cool": Temperature-aware workload placement in data centers," in *USENIX Annu. Tech. Conf., General Track*, 2005, pp. 61–75.

[59] S. Khalid, A. Ishfaq, and K. Mohammad E., "An evolutionary approach to optimize data center profit in smart grid environment," in *2019 2nd International Conference on Data Intelligence and Security (ICDIS)*, 2019, pp. 89–96.

[60] G. S. Aujla, M. Singh, N. Kumar, and A. Y. Zomaya, "Stackelberg game for energy-aware resource allocation to sustain data centers using RES," *IEEE Trans. Cloud Comput.*, vol. 7, no. 4, pp. 1109–1123, 2019.

[61] M. A. Abdelghany, H. Mohsenian-Rad, and M. Alizadeh, "Wholesale electricity pricing in the presence of geographical load balancing," in *2017 51st Asilomar Conference on Signals, Systems, and Computers*, Oct 2017, pp. 653–658.

[62] J. Camacho, Y. Zhang, M. Chen, and D. M. Chiu, "Balance your bids before your bits: The economics of geographic load-balancing," in *Proc. 5th Int. Conf. Future Energy Systems*, ser. e-Energy '14. New York, NY, USA: ACM, 2014, pp. 75–85.

[63] E. Zitzler, M. Laumanns, and L. Thiele, "SPEA2: Improving the strength pareto evolutionary algorithm," *TIK-report*, vol. 103, 2001.

[64] Z. Yang, Y. Cui, X. Wang, M. Li, and Y. Liu, "Less is more: Service profit maximization in geo-distributed clouds," *IEEE Trans. Cloud Comput.*, pp. 1–1, 2020.

[65] M. Dayarathna, Y. Wen, and R. Fan, "Data center energy consumption modeling: A survey," *IEEE Commun. Surveys Tuts.*, vol. 18, no. 1, pp. 732–794, Firstquarter 2016.

[66] S. Khalid and I. Ahmad, "QoS and power network stability aware simultaneous optimization of data center revenue and expenses," *Sustainable Computing: Informatics and Systems*, vol. 30, p. 100459, 2021. [Online]. Available: https://www.sciencedirect.com/science/article/pii/S2210537920301839

[67] S. M. Ali, M. Jawad, M. U. S. Khan, K. Bilal, J. Glower, S. C. Smith, S. U. Khan, K. Li, and A. Y. Zomaya, "An ancillary services model for data centers and power systems," *IEEE Trans. Cloud Comput.*, vol. 8, no. 4, pp. 1176–1188, 2020.

[68] A. Khosravi, L. L. H. Andrew, and R. Buyya, "Dynamic vm placement method for minimizing energy and carbon cost in geographically distributed cloud data centers," *IEEE Trans. on Sustain. Comput.*, vol. 2, no. 2, pp. 183–196, April 2017.

[69] N. Hogade, S. Pasricha, H. J. Siegel, A. A. Maciejewski, M. A. Oxley, and E. Jonardi, "Minimizing energy costs for geographically distributed heterogeneous data centers," *IEEE Trans. on Sustain. Comput.*, vol. 3, no. 4, pp. 318–331, Oct 2018.

[70] P. Vytelingum, T. D. Voice, S. D. Ramchurn, A. Rogers, and N. R. Jennings, "Agent-based micro-storage management for the smart grid," in *Proc. 9th Int. Conf. Autonomous Agents and Multiagent Systems: Volume 1 - Volume 1*, ser. AAMAS '10. Richland, SC: International Foundation for Autonomous Agents and Multiagent Systems, 2010, pp. 39–46.

[71] C. Wu, H. Mohsenian-Rad, and J. Huang, "Wind power integration via aggregator-consumer coordination: A game theoretic approach," in *2012 IEEE PES Innovative Smart Grid Technologies*, Jan 2012, pp. 1–6.

[72] S. Rivoire, P. Ranganathan, and C. Kozyrakis, "A comparison of high-level full-system power models," in *Proc. 2008 Conf. Power Aware Computing and Systems*, ser. HotPower'08. Berkeley, CA, USA: USENIX Association, 2008, pp. 3–3.

[73] Q. Tang, S. K. S. Gupta, and G. Varsamopoulos, "Energy-efficient thermal-aware task scheduling for homogeneous high-performance computing data centers: A cyber-physical approach," *IEEE Trans. Parallel Distrib. Syst.*, vol. 19, no. 11, pp. 1458–1472, Nov 2008.

[74] H. Sun, P. Stolf, and J.-M. Pierson, "Spatio-temporal thermal-aware scheduling for homogeneous high-performance computing datacenters," *Future Gener. Comput. Syst.*, vol. 71, no. C, pp. 157–170, Jun. 2017.

[75] L. A. Barroso and U. Hölzle, "The case for energy-proportional computing," *Computer*, vol. 40, no. 12, pp. 33–37, Dec 2007.

[76] D. Villela, P. Pradhan, and D. Rubenstein, "Provisioning servers in the application tier for e-commerce systems," *ACM Trans. Internet Technol.*, vol. 7, no. 1, Feb. 2007.

[77] V. Gupta, R. Nathuji, and K. Schwan, "An analysis of power reduction in datacenters using heterogeneous chip multiprocessors," *SIGMETRICS Perform. Eval. Rev.*, vol. 39, no. 3, pp. 87–91, Dec. 2011.

[78] K. Deb and D. Kalyanmoy, *Multi-Objective Optimization Using Evolutionary Algorithms*. New York, NY, USA: John Wiley & Sons, 2001.

[79] Y. G. Woldesenbet, G. G. Yen, and B. G. Tessema, "Constraint handling in multiobjective evolutionary optimization," *IEEE Trans. Evol. Comput.*, vol. 13, no. 3, pp. 514–525, June 2009.

[80] H. Singh, A. Isaacs, T. Nguyen, T. Ray, and X. Yao, "Infeasibility driven evolutionary algorithm for constrained optimization," in *in Constraint Handling in Evolutionary Optimization, ser. Studies in Computational Intelligence*. Springer, 2009, pp. 145–165.

[81] F. Herrera, M. Lozano, and J. Verdegay, "Tackling real-coded genetic algorithms: Operators and tools for behavioural analysis," *Artificial Intelligence Review*, vol. 12, no. 4, pp. 265–319, Aug. 1998.

[82] R. Agrawal and K. Deb, "Simulated binary crossover for continuous search space," *Complex Syst.*, vol. 9, no. 2, pp. 115–148, 1995.

[83] H.-S. Yoon and B.-R. Moon, "An empirical study on the synergy of multiple crossover operators," *IEEE Trans. Evol. Comput.*, vol. 6, no. 2, pp. 212–223, Apr. 2002.

[84] D. Simon, *Evolutionary optimization algorithms*. John Wiley & Sons, 2013.

[85] J. Whitney and P. Delforge, "Data center efficiency assessment," *Issue paper on NRDC (The Natural Resource Defense Council)*, 2014.

[86] European Commission., "Shaping Europe's digital future," 2020, [Online; Accessed 2-Aug-2020]. [Online]. Available: https://ec.europa.eu/info/sites/info/files/communication-shaping-europes-digital-future-feb2020_en_4.pdf

[87] C. Koronen, M. Åhman, and L. J. Nilsson, "Data centres in future european energy systems—energy efficiency, integration and policy," *Energy Efficiency*, vol. 13, no. 1, pp. 129–144, 2020.

[88] Z. Liu, M. Lin, A. Wierman, S. Low, and L. L. H. Andrew, "Greening geographical load balancing," *IEEE/ACM Trans. on Networking*, vol. 23, no. 2, pp. 657–671, 2015.

[89] D. Shirmohammadi, H. Hong, A. Semlyen, and G. Luo, "A compensation-based power flow method for weakly meshed distribution and transmission networks," *IEEE Trans. Power Syst.*, vol. 3, no. 2, pp. 753–762, 1988.

[90] S. D. Beigvand, H. Abdi, and S. N. Singh, "Voltage stability analysis in radial smart distribution grids," *IET Generation, Transmission Distribution*, vol. 11, no. 15, pp. 3722–3730, 2017.

[91] M. Chakravorty and D. Das, "Voltage stability analysis of radial distribution networks," *Int. J. of Electrical Power & Energy Syst.*, vol. 23, no. 2, pp. 129–135, 2001. [Online]. Available: http://www.sciencedirect.com/science/article/pii/S0142061500000405

[92] L. Aolaritei, S. Bolognani, and F. Dörfler, "A distributed voltage stability margin for power distribution networks," *IFAC-PapersOnLine*, vol. 50, no. 1, pp. 13 240–13 245, 2017, 20th IFAC World Congress. [Online]. Available: http://www.sciencedirect.com/science/article/pii/S2405896317325892

[93] R. Abri, E. El-Saadany, and Y. Atwa, "Optimal placement and sizing method to improve the voltage stability margin in a distribution system using distributed generation," *IEEE Trans. Power Syst.*, vol. 28, no. 1, pp. 326–334, Feb. 2013.

[94] M. Aman, G. Jasmon, H. Mokhlis, and A. Bakar, "Optimal placement and sizing of a DG based on a new power stability index and line losses," *Int. J. Electrical Power & Energy Syst.*, vol. 43, no. 1, pp. 1296–1304, 2012. [Online]. Available: http://www.sciencedirect.com/science/article/pii/S0142061512002438

[95] M. E. Baran and F. F. Wu, "Network reconfiguration in distribution systems for loss reduction and load balancing," *IEEE Trans. Power Del.*, vol. 4, no. 2, pp. 1401–1407, April 1989.

[96] PG&E, "Public safety power shutoff (PSPS)," (accessed May. 10, 2020). [Online]. Available: https://www.pge.com/en_US/safety/emergency-preparedness/natural-disaster/wildfires/public-safety-power-shutoff-faq.page

[97] F. Thomas, "Californians confront a blackout induced to prevent blazes," 2019, (accessed May. 10, 2020). [Online]. Available: https://www.nytimes.com/2019/10/10/us/pge-outage.html

[98] B. Howard, "PG&E warns of 10 years of power shut-offs. california officials don't like it," 2019, (accessed May. 10, 2020). [Online]. Available: https://www.latimes.com/california/story/2019-10-19/pg-e-ten-years-of-power-shutoffs

[99] L. Rao, R. Han, X. Ren, X. Bai, R. Zheng, H. Liu, Z. Wang, J. Li, K. Zhang, and S. Li, "Disadvantage and prosocial behavior: the effects of the wenchuan earthquake," *Evolution and Human Behavior*, vol. 32, no. 1, pp. 63–69, 2011. [Online]. Available: http://www.sciencedirect.com/science/article/pii/S1090513810000735

[100] M. I. Azim, W. Tushar, and T. K. Saha, "Coalition graph game-based P2P energy trading with local voltage management," *IEEE Transactions on Smart Grid*, pp. 1–1, 2021.

[101] S.-W. Park, K.-S. Cho, and S.-Y. Son, "Voltage management method of distribution system in P2P energy transaction environment," *IFAC-PapersOnLine*, vol. 52, no. 4, pp. 324–329, 2019, iFAC Workshop on Control of Smart Grid and Renewable Energy Systems CSGRES 2019. [Online]. Available: https://www.sciencedirect.com/science/article/pii/S2405896319305671

[102] J. Lucia and E. Schwartz, "Electricity prices and power derivatives: Evidence from the nordic power exchange," *Review of Derivatives Research*, vol. 5, no. 1, pp. 5–50, Jan. 2002. [Online]. Available: https://doi.org/10.1023/A:1013846631785

[103] H. Moulin, "Chapter 6 axiomatic cost and surplus sharing," in *Handbook of Social Choice and Welfare*, ser. Handbook of Social Choice and Welfare. Elsevier, 2002, vol. 1, pp. 289–357. [Online]. Available: http://www.sciencedirect.com/science/article/pii/S1574011002800108

[104] N. Daniels, *Resource Allocation and Priority Setting*. Springer, 04 2016, pp. 61–94.

[105] T. Alpcan and T. Basar, "A globally stable adaptive congestion control scheme for internet-style networks with delay," *IEEE/ACM Trans. Netw.*, vol. 13, no. 6, pp. 1261–1274, Dec. 2005.

[106] M. Baran and F. F. Wu, "Optimal sizing of capacitors placed on a radial distribution system," *IEEE Trans. Power Del.*, vol. 4, no. 1, pp. 735–743, 1989.

[107] H. Li, A. Bose, and V. Venkatasubramanian, "Wide-area voltage monitoring and optimization," *IEEE Trans.Smart Grid*, vol. 7, no. 2, pp. 785–793, 2016.

[108] P. Kayal and C. Chanda, "Placement of wind and solar based DGs in distribution system for power loss minimization and voltage stability improvement," *International Journal of Electrical Power & Energy Systems*, vol. 53, pp. 795–809, 2013. [Online]. Available: https://www.sciencedirect.com/science/article/pii/S0142061513002536

[109] Z. Michalewicz, D. Dasgupta, R. G. L. Riche], and M. Schoenauer, "Evolutionary algorithms for constrained engineering problems," *Comput. & Ind. Eng.*, vol. 30, no. 4, pp. 851–870, 1996. [Online]. Available: http://www.sciencedirect.com/science/article/pii/036083529600037X

[110] I. Makhdoom, M. Abolhasan, H. Abbas, and W. Ni, "Blockchain's adoption in IoT: The challenges, and a way forward," *Journal of Network and Computer Applications*, vol. 125, pp. 251–279, 2019. [Online]. Available: http://www.sciencedirect.com/science/article/pii/S1084804518303473

[111] M. Andoni, V. Robu, D. Flynn, S. Abram, D. Geach, D. Jenkins, P. McCallum, and A. Peacock, "Blockchain technology in the energy sector: A systematic review of challenges and opportunities," *Renewable and Sustainable Energy Reviews*, vol. 100, pp. 143–174, 2019. [Online]. Available: http://www.sciencedirect.com/science/article/pii/S1364032118307184

[112] J. Guerrero, A. C. Chapman, and G. Verbič, "Decentralized P2P energy trading under network constraints in a low-voltage network," *IEEE Trans. Smart Grid*, vol. 10, no. 5, pp. 5163–5173, 2019.

[113] H. Momen, A. Abessi, and S. Jadid, "Using EVs as distributed energy resources for critical load restoration in resilient power distribution systems," *IET Gener. Transm. Distrib.*, vol. 14, no. 18, pp. 3750–3761, 2020.

[114] C. Chen, J. Wang, F. Qiu, and D. Zhao, "Resilient distribution system by microgrids formation after natural disasters," *IEEE Trans. Smart Grid*, vol. 7, no. 2, pp. 958–966, 2016.

[115] C. Li, H. Yan, Z. Zhang, J. Wang, and X. Zuo, "Service restoration based on interruption loss for resilient distribution system considering distributed generations," in *2020 IEEE 4th Conference on Energy Internet and Energy System Integration (EI2)*, 2020, pp. 458–463.

[116] H. Farzin, M. Fotuhi-Firuzabad, and M. Moeini-Aghtaie, "Enhancing power system resilience through hierarchical outage management in multi-microgrids," *IEEE Trans. Smart Grid*, vol. 7, no. 6, pp. 2869–2879, 2016.

[117] Y. Xu, C.-C. Liu, Z. Wang, K. Mo, K. P. Schneider, F. K. Tuffner, and D. T. Ton, "DGs for service restoration to critical loads in a secondary network," *IEEE Trans. Smart Grid*, vol. 10, no. 1, pp. 435–447, 2019.

[118] Y. Wang, Y. Xu, J. He, C.-C. Liu, K. P. Schneider, M. Hong, and D. T. Ton, "Coordinating multiple sources for service restoration to enhance resilience of distribution systems," *IEEE Trans.Smart Grid*, vol. 10, no. 5, pp. 5781–5793, 2019.

[119] L. Che and M. Shahidehpour, "Adaptive formation of microgrids with mobile emergency resources for critical service restoration in extreme conditions," *IEEE Trans. Power Syst.*, vol. 34, no. 1, pp. 742–753, 2019.

[120] K. S. A. Sedzro, A. J. Lamadrid, and L. F. Zuluaga, "Allocation of resources using a microgrid formation approach for resilient electric grids," *IEEE Trans. Power Syst.*, vol. 33, no. 3, pp. 2633–2643, 2018.

[121] Q. Zhang, Z. Ma, Y. Zhu, and Z. Wang, "A two-level simulation-assisted sequential distribution system restoration model with frequency dynamics constraints," *IEEE Trans. Smart Grid*, pp. 1–1, 2021.

[122] Hyperledger, "Hyperledger – open source blockchain technologies," 2021, (accessed Jul. 15, 2021). [Online]. Available: https://hyperledger.org/

[123] Y. Xiao, N. Zhang, W. Lou, and T. Hou, "A survey of distributed consensus protocols for blockchain networks," *IEEE Commun. Surv. Tutor.*, vol. 22, no. 2, pp. 1432–1465, 2020.

[124] Q. Zhuang, Y. Liu, L. Chen, and Z. Ai, "Proof of reputation: A reputation-based consensus protocol for blockchain based systems," in *Proc. 2019 Int. Electronics Communication Conf.*, 2019, pp. 131–138.

[125] M. Oliveira, L. Reis, D. Medeiros, R. Carrano, S. Olabarriaga, and D. Mattos, "Blockchain reputation-based consensus: A scalable and resilient mechanism for distributed mistrusting applications," *Computer Networks*, vol. 179, p. 107367, 2020. [Online]. Available: http://www.sciencedirect.com/science/article/pii/S1389128620300360

[126] C. Liu, K. Chai, X. Zhang, and Y. Chen, "Proof-of-benefit: A blockchain-enabled EV charging scheme," in *2019 IEEE 89th Vehicular Technology Conference (VTC2019-Spring)*, 2019, pp. 1–6.

[127] S. Khalid and I. Ahmad, "Blockchain based service restoration in a power distribution system during crisis," in *2021 IEEE Madrid PowerTech*, 2021.

[128] ——, "Service restoration using energy donation in a distribution system during crisis," in *2020 Int. Conf. Smart Grids and Energy Systems (SGES)*, 2020, pp. 562–567.

[129] W. Wang, D. T. Hoang, P. Hu, Z. Xiong, D. Niyato, P. Wang, Y. Wen, and D. I. Kim, "A survey on consensus mechanisms and mining strategy management in blockchain networks," *IEEE Access*, vol. 7, pp. 22 328–22 370, 2019.

[130] Y. Xiao, N. Zhang, W. Lou, and Y. T. Hou, "A survey of distributed consensus protocols for blockchain networks," *IEEE Commun. Surv. Tutor.*, vol. 22, no. 2, pp. 1432–1465, 2020.

[131] J. Koski and R. Silvennoinen, "Norm methods and partial weighting in multicriterion optimization of structures," *International Journal for Numerical Methods in Engineering*, vol. 24, no. 6, pp. 1101–1121, 1987.

[132] U. of Cambridge, "Cambridge Bitcoin electricity consumption index," 2021, (accessed Jul. 11, 2021). [Online]. Available: https://cbeci.org/

[133] O. Jogunola, W. Wang, and B. Adebisi, "Prosumers matching and least-cost energy path optimisation for peer-to-peer energy trading," *IEEE Access*, vol. 8, pp. 95 266–95 277, 2020.

[134] S. M. H. Bamakan, A. Motavali, and A. Babaei Bondarti, "A survey of blockchain consensus algorithms performance evaluation criteria," *Expert Systems with Applications*, vol. 154, p. 113385, 2020. [Online]. Available: https://www.sciencedirect.com/science/article/pii/S0957417420302098

BIOGRAPHICAL STATEMENT

Saifullah Khalid received BE degree in Electrical Engineering in 1996 and an MS degree in Computer Science in 2013 from the National University of Sciences and Technology, Islamabad, Pakistan. He received his Ph.D. in computer engineering from the University of Texas at Arlington, Texas, in 2021. He is a recipient of outstanding dissertation award and University of Texas at Arlington summer dissertation fellowship 2021. His research interests include smart grid, blockchains, data center optimization, high-performance computing, evolutionary optimization techniques, and IoT